Title
Identifying and Understanding the Functional Significance of Cancer Stem Cells in Prostate and Pancreatic Cancer Initiation and Chemoresistance

Author
Hindoyan, Antreas Agop

Publication Date
2013

Peer reviewed|Thesis/dissertation

UNIVERSITY OF CALIFORNIA

Los Angeles

Identifying and Understanding the Functional Significance of Cancer Stem Cells in Prostate and Pancreatic Cancer Initiation and Chemoresistance

A dissertation submitted in partial satisfaction of the requirements for the degree Doctor of Philosophy in Molecular and Medical Pharmacology

by

Antreas Agop Hindoyan

2013

ABSTRACT OF THE DISSERTATION

Identifying and Understanding the Functional Significance
of Cancer Stem Cells in Prostate and Pancreatic Cancer
Initiation and Chemoresistance

by

Antreas Agop Hindoyan
Doctor of Philosophy in Molecular and Medical Pharmacology
University of California, Los Angeles, 2013
Professor Hong Wu, Chair

The functional heterogeneity of cancer phenotypes and responses to therapeutics is a huge obstacle to clinical cures and an intense area of study. A relatively new hypothesis posits the existence of a subpopulation of tumor cells, termed cancer stem cells, which are primarily responsible for tumor propagation and resistance to therapy. Identification of such cells may be important to develop targeted therapies for more effective cancer treatment. This dissertation focuses on the validation and functional study of cancer stem cells associated with human prostate and pancreatic cancers. By leveraging the fact that surgical castration leads to enrichment of stem/progenitor cells in the prostate, we idenitifed CD166 as a novel marker for prostate stem cells. We show that CD166 can further enrich and refine the established prostate

stem/progenitor cell and cancer stem cell population in both murine and human systems. While genetic deletion of CD166 would not inhibit the development of the prostate gland or the formation of prostate cancer in our genetically engineered model systems, this protein may serve as an attractive marker for identifying and targeting prostate cancer stem cells. Further attempts were made at identifying stem/progenitor populations for prostate and pancreatic cancer through various discovery and targeted approaches. We found that Lgr5, a marker of stem cells in the gut and skin, is not expressed in prostate and pancreatic epithelial tissue, but only in prostatic stroma. Novel surface markers such as CD138 were found to be highly upregulated in pancreatic tumors, but specificity for cancer stem cells was lacking. Lastly, we studied the functional role of cancer stem cells in gemcitabine therapy resistance in a human pancreatic cancer model. We found that the PI3K and ubiquitin-mediated proteosomal degradation pathways can be used to stratify gemcitabine treatment response in patient tumors. Inhibition of Skp2 expression and therapeutic treatment with PI3K inhibitors proved to be effective sensitiziers to gemcitabine treatment. Importantly, cancer stem cell content and function did not mediate gemcitabine relapse. As such, our studies reveal the cancer stem cell paradigm may be more complicated and cancer context-dependent, and must be rigorously functionally proven prior to clinical adoption.

The dissertation of Antreas Agop Hindoyan is approved.

Owen Witte

Lily Wu

William Lowry

Heather Christofk

Hong Wu, Committee Chair

University of California, Los Angeles

2013

DEDICATION

To my parents, Agop and Annie, for their sacrifice, support, and unrelenting work ethic, providing me with the opportunity to pursue my education.

To my late grandparents, Sarkis and Artin, who succumbed to prostate and pancreatic cancer respectively, and became the motivation for my current endeavors.

TABLE OF CONTENTS

LIST OF FIGURES AND TABLES

ACKNOWLEDGEMENTS

I would like to acknowledge my mentor Dr. Hong Wu, for providing me the opportunity to work and learn in such a supportive and collaborative environment. She has been a great role model for me to emulate, and I am indebted to her for my development as a scientist.

To my committee members, Owen Witte, William Lowry, Lily Wu, and Heather Christofk for their input and support.

To Dr. Steven Goodman, whose lab I was first introduced to research as an undergraduate. My two years in his lab at USC confirmed my enthusiasm for bench work and set me on my current path. I would also like to thank Dr. Randall Story, who supervised my undergraduate research project. His constant communication and support provided the impetus for my independent thinking and analytical skills.

To my collaborators, without whom none of my graduate studies would be possible. To Bahram Valamehr and Hide Tsutsui, for initial studies optimizing embryonic stem cell culture conditions. To Jing Jiao, for her humble, analytic, and industrious demeanor, whose perseverance and guidance was instrumental for completion of the studies in Chapter 2. To Dr. Timothy Donahue, who provided practical insight into the clinical relevance of my studies, as well as access to patient samples at UCLA which served as the foundation for the experiments in Chapter 4.

To all the Wu/Liu lab members, both past and present, for the tremendous scientific support as well as fond memories. To Jonathan Nakashima, who entered Hong's lab the same time I did. We have battled through classes and the rigors of graduate work, become roommates, and leaned on each other to get to this point. To Dr. Reginald Hill and Dr. David Mulholland, with whom I constantly engaged in fruitful scientific discussions, providing me with invaluable insight and direction.

To all my friends and family who have been invaluable the past five years, providing a strong support system and distraction from the frustrations of graduate life.

I would lastly like to thank the funding sources which made my training possible: R01 Supplement 3R01CA121119-02S2 from the NIH, and the Eugene V. Cota-Robles Fellowship from the UCLA Graduate Division.

VITA

Teaching Assistant, Biomedical Research 5HB, UCLA	2013
First Place Team, L.E.K. Consulting Competition	2013
Executive Board Member, Advanced Degree Consulting Club	2012-2013
Consulting Intern, Myelin Repair Foundation	2012
First Place Team, Accenture Consulting Competition	2012
Undergraduate Student Mentor, Trained and developed student research project	2011-2012
Travel Award, UCLA Department of Molecular and Medical Pharmacology	2011
Executive Board Member, Homenetmen Los Angeles Chapter	2009-2013
NIH R01 Minority Supplement Award: 3R01CA121119-02S2	2009-2012
Eugene V Cota-Robles Fellowship, UCLA Graduate Division	2007-2009
B.S. Biochemistry, University of Southern California	2007

Undergraduate Researcher, 2005-2007
University of Southern California

Trustee Scholarship, 2003-2007
University of Southern California

Publications

- **Hindoyan A**, Godavarthi S, Tran L, Li Y, Braas D, Christofk H, Donahue T, Wu H. Pathway alterations define gemcitabine relapse in a human pancreatic cancer xenograft model. (Manuscript in preparation)

- Jiao J*, **Hindoyan A***, Wang S, Goldstein A, Lawson D, Chen D, Li Y, Guo C, Zhang, B, Gleave M, Witte O, Garraway I, Wu H (2012). Identification of CD166 as a surface marker for enriching prostate stem/progenitor and cancer inititating cells. Plos One, *7*(8):e42564, 1-14.

- Donahue T, Tran L, Hill R, Li Y, Kovochich A, Calvopina J, Patel S, Wu N, **Hindoyan A**, Farrell J, Li X, Dawson D, Wu H (2012). Integrative Survival-Based Molecular Profiling of Human Pancreatic Cancer. Clinical Cancer Research, *18*: 1352-1363.

- Tsutsui H, Valamehr B, **Hindoyan A**, Qiao R, Ding X, Guo S, Witte O, Liu X, Ho CM, Wu H (2011). An optimizd small molecule inhibitor cocktail supports long-term maintenance of human embryonic stem cells. Nature Communications, *2*(167): 1-8.

*Authors contributed equally to work

Chapter 1:

Overview

I. Introduction

Cancer is the second-leading cause of death in the US, narrowly trailing only myocardial infarction in total number of victims (Hoyert 2012). It is estimated that 1.66 million new cases of cancer will be diagnosed this year resulting in about 580,000 deaths (American Cancer Society 2013). This disease is a tremendous burden on our society, which spent an estimated $77 billion dollars in direct medical costs and $124 billion on indirect mortality costs such as lost productivity in 2008 (American Cancer Society 2013). Prostate and pancreatic cancer represent two of the top four deadliest cancers, estimated to result in 29,720 and 38,460 deaths in the US this year, respectively (American Cancer Society 2013). It is therefore clear that better treatments are needed to curb the devastating toll from this parasitic, deadly disease.

One in six men living in the US will develop prostate cancer in their lifetime (Prostate Cancer Foundation 2013). Fortunately, the prostate is a hormone-responsive tissue which is dependent on Androgen Receptor (AR) signaling for cell survival and growth (Cunha 1985, Yeh 2002), and as such early stage prostate cancer is currently treated very effectively with anti-androgen therapy and surgery (Huggins 1941, Bahler 2010). However, over time certain patients develop disease recurrence and progress to a stage of castration resistant prostate cancer or CRPC (Chen 2008). Several mechanisms of tumor relapse have been suggested, including alternative activation of androgen signaling (Niraula 2012), or dependance on other signaling pathways such as the PI3K-AKT-mTOR axis (Mulholland 2011). There are currently no effective therapies for CRPC, with patients developing multiple metastases to bone and liver, eventually succumbing to disease burden (Toren 2013).

Pancreatic Cancer is the most lethal common tumor type in the US, with a median 5-year survival of only 5% (American Cancer Society 2013). The most common and malignant form of

this disease is Pancreatic Ductal Adenocarcinoma (PDAC), an epithelial tumor thought to arise from the exocrine compartment of the pancreas (Pour 2003, Stanger 2006). Reasons for the high lethality of PDAC include its uniquely aggressive biology as well as late diagnosis, due to a lack of sensitive testing and obvious symptoms (Morris 2010, Stathis 2010). At the point of diagnosis, tumors are mostly locally advanced or metastatic, with only roughly 20% of patients being candidates for surgical resection (Conlon 1996). Gemcitabine is the current standard chemotherapeutic prescribed, although it only extends survival by a few weeks in metastatic patients (Burris 1997). Even with surgical intervention, long-term survival remains poor due to disease recurrence. As such, surgery alone remains an inadequate treatment modality.

The cellular mechanisms underlying tumor initiation, progression, and therapeutic resistance are areas of avid research. Cancer has long been known to be caused by an aberrant genome, and many recent DNA sequencing efforts have yielded a lot of information regarding specific mutational events which occur in prostate and pancreatic cancer (Jones 2008, Mann 2011, Grasso 2012, Biankin 2012). Nevertheless, there remains much patient-to-patient heterogeneity, and clonal selection of specific mutational drivers may result in differential oncogenic phenotypes in a tumor (Greaves 2012). Furthermore, it is becoming increasingly appreciated that transformation of the initial mutational clone may occur in different cell types within a tissue, and that this cell-of-origin may yield different subtypes of tumors that will have a large effect on downstream genetic, epigenetic, and phenotypic characteristics (Visvader 2011). Moreover, after tumor initiation, cells within the tumor population seem to exhibit functional heterogeneity, with a small subpopulation seemingly responsible for tumor propagation (Fig 1A) and resistance (Fig 1B) (Visvader 2008). Pioneering studies in acute myeloid leukemia showed that this cancer is organized as a hierarchy of cells, reminiscent to tissue-specific stem cells and

their differentiated progeny, with leukemia stem cells on the top that drive the production of leukemic cells and the progression of the disease (Lapidot 1994). This 'cancer stem cell' paradigm has been applied to a variety of blood and solid tumor malignancies (Mimeault 2007, Visvader 2008). Therefore, prospective identification and validation of cancer stem cell populations may shed light on the biology of tumor initiation, provide prognostic value for tumor subtype stratification, as well as provide an avenue for targeted therapeutic intervention (Frank 2010, Eppert 2011).

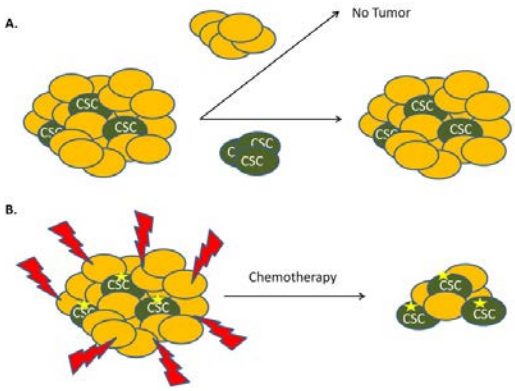

Figure 1-1: Cancer Stem Cell Paradigm. (A) Cancer Stem Cells (CSC) are a subpopulation of cells within a tumor bulk which can initiate and propagate the cancer. (B) CSCs are thought to be more resistant to chemotherapy than the rest of the tumor cell bulk.

This dissertation seeks to shed light on two fundamental questions: Is there a cell type within a tumor which is responsible for tumor initiation and progression in prostate and/or pancreatic cancer? Second, is this identified cancer stem cell preferentially resistant to treatment and the cause for disease recurrence and death? To address these questions, we begin in Chapter 2 with the identification of CD166 as a putative stem/progenitor marker of prostate cells and characterize its role in prostate tumorigenesis. In Chapter 3, we seek to identify additional novel populations of cancer stem cells in both prostate and pancreas systems using discovery and targeted approaches. In Chapter 4, we test the hypothesis that cancer stem cells play a role in chemotherapy resistance and tumor relapse in a human model of pancreatic cancer. These results have direct implications regarding the mechanisms of tumor progression and resistance, as well as for the use of targeted therapies for patient treatment.

II. References

American Cancer Society (2013). Cancer Facts and Figures 2013. Atlanta: American Cancer Society

Bahler CD, Foster RS, Bihrle R, Beck SD, Gardner TA, Sundaram CP, Masterson TA, Cheng L, Koch MO (2010). Radical prostatectomy as initial monotherapy for patients with pathologically confirmed high-grade prostate cancer. BJU Int, *105*: 1372-1376.

Biankin AV et al, International Cancer Genome Consortium (2012). Pancreatic cancer genomes reveal aberrations in axon guidance pathway genes. Nature, *491*: 399-405

Burris H, Moore MJ, Andersen J, Green MR, Rothenberg ML, Modiano MR, Cripps MC, Portenay RK, Storniolo AM, Tarassoff P, Nelson R, Dorr FA, Stephens CD, Von Hoff DD (1997). Improvements in Survival and Clinical Benefit With Gemcitabine as First-Line Therapy for Patients With Advanced Pancreas Cacner: A Randomized Trial. J Clin Oncol *15*: 2403-2413.

Chen Y, Sawyers C, Scher H (2008). Targeting the androgen receptor pathway in prostate cancer. Curr Opin pharmacol, *8*: 440-448.

Conlon KC, Klimstra DS, Brennan MF (1996). Long-term survival after curative resection for pancreatic ducatal adenocarcinoma: clinicopathologic analysis of 5-year survivors. Ann Surg, *223*: 273-279.

Cunha GR (1985). Mesenchymal-epithelial interactions during androgen-induced development of the prostate. Prog Clin Biol Res, *171*: 15-24.

Eppert K, Takenaka K, Lechman ER, Waldron L, Nilsson B, van Galen P, Metzeler KH, Poeppl A, Ling V, Beyene J, Canty AJ, Danska JS, Bohlander SK, Buske C, Minden MD, Golub TR, Jurisica I, Ebert BL, Dick JE (2011). Stem cell gene expression programs influence clinical outcome in human leukemia. Nat Med, *17*: 1086-1093.

Frank N, Schatton T, Frank M (2010). The therapeutic promise of the cancer stem cell concept. Jour Clin Invest, *120*: 41-50.

Grasso CS, Wu YM, Robinson DR, Cao X, Dhanasekaran SM, Khan AP, Quist MJ, Jing X, Lonigro RJ, Brenner JC, Asangani IA, Ateeq B, Chun SY, Siddiqui J, Sam L, Anstett M, Mehra R, Prensner JR, Palanisamy N, Ryslik GA, Vandin F, Raphael BJ, Kunju LP, Rhodes DR, Pienta KJ, Chinnaiyan AM, Tomlins SA (2012). The mutational landscape of lethal castration-resistant prostate cancer. Nature, *110*: 1110-1114.

Greaves M, Maley C (2012). Clonal evolution in cancer. Nature, *481*: 306-313.

Hoyert DL, Jiaquan X (2012). Deaths: Preliminary Data for 2011. National Vital Statistics Reports, *61*: 1-7.

Huggins C, Hodges CV (1941). Studies on Prostatic Cancer. I. The Effect of Castration, of Estrogen and of Androgen Injection on Serum Phosphatases in Metastatic Carcinoma of the Prostate. Cancer Res, *1*: 293–297.

Jones S, Zhang X, Parsons D, Lin J, Leary R, Angenendt P, Mankoo P, Carter H, Kamiyama H, Jimeno A et al, Hruban RH, Karchin, Papadopoulos N, Parmigiani G, Vogelstein B, Velculescu V, Kinzler K (2008). Core Signaling Pathways in Human Pancreatic Cancers Revealed by Global Genomic Analyses. Science, 321: 1801-1806.

Lapidot T, Sirard C, Vormoor J, Murdoch B, Hoang T, Caceres-Cortes J, Minden M, Paterson B, Caligiuri MA, Dick JE (1994). A cell initiating human acute myeloid leukaemia after transplantation into SCID mice. Nature, *367*: 645-648.

Mann K, Ward JM, Yew C, Kovochich A, Dawson D, Black MA, Bret BT, Sheetz TE, Dupuy AJ, Chang DK, Biankin AV, Waddell N, Kassahn KS, Grimmond SM, Rust AG, Adams DJ, Jenkins AN, Copeland NG (2012). Sleeping Beauty muragenesis reveals cooperating mutations and pathways in pancreatic adenocarcinoma. PNAS, *109:* 5934-5941.

Mimeault M, Hauke R, Mehta P, Batra S (2007). Recent advances in cancer stem/progenitor cell research: therapeutic implications for overcoming resistance to the most aggressive cancers. J Cell Mol Med, *11*: 981-1011.

Morris JP, Wang SC, Hebrok M (2010). KRAS, Hedgehog, Wnt and the twisted developmental biology of pancreatic ductal adenocarcinoma. Nat Rev Cancer, *10*: 683-695.

Mulholland DJ, Tran LM, Li Y, Cai H, Morim A, et al. (2011) Cell autonomous role of PTEN in regulating castration-resistant prostate cancer growth. Cancer Cell, *19*: 792-804.

Niraula S, Chi K, Joshua AM. Beyond castration-defining future directions in the hormonal treatment of prostate cancer. Horm Cancer, *3*: 3-13.

Prostate Cancer Foundation (2013). Prostate Cancer Risk Factors. Retrieved May 2, 2013, from http://www.pcf.org/site/c.leJRIROrEpH/b.5802027/k.D271/Prostate_Cancer_Risk_Factors.htm

Pour PM, Pandey KK, Batra S (2003). What is the origin of pancreatic adenocarcinoma? Molecular Cancer, *2*:13.

Stanger B and Dor Y (2006). Dissecting the Cellular Origins of Pancreatic Cancer. Cell Cycle, *5*: 43-46.

Stathis A and Moore M (2010). Advanced pancreatic carcinoma: current treatment and future challenges. Nat Rev Clin Oncol, *7*: 163-172.

Toren PJ, Gleave ME (2013). Evolving landscape and novel treatments in metastatic castrate-resistant prostate cancer. Asian J Androl, doi:10.1038/aja.2013.38.

Visvader JE (2011). Cells of origin in cancer. Nature, *469*: 314-322.

Visvader JE, Lindeman GJ (2008). Cancer stem cells in solid tumours: accumulating evidence and unresolved questions. Nat Rev Cancer, *8*: 755-768.

Yeh S, Tsai MY, Xu Q, Mu XM, Lardy H, Huang KE, Lin H, Yeh SD, Altuwaijri S, Zhou X, et al. (2002). Generation and characterization of androgen receptor knockout (ARKO) mice: an in vivo model for the study of androgen functions in selective tissues. PNAS, *99*: 13498–13503.

Chapter 2:

CD166 and Prostate Cancer

I. Introduction

Despite advances in the early detection and management of prostate cancer, castration resistant prostate cancer (CRPC) remains the second most common cause of male *mortality* in the United States (Jemal 2010). Mounting evidence suggests that a subpopulation of prostate cells can initiate prostate cancer and may be responsible for the castration resistance (Taylor 2010, Wang 2011, Goldstein 2010, Tang 2007). Therefore, these cancer initiating cells (Visvader 2011) may serve as promising cellular targets for prostate cancer and identification of this subpopulation has become the necessary step toward future effective therapy.

The origins of prostate cancer initiating cells are controversial (Maitland 2005, Moscatelli 2010). Normal prostate from human or mouse contains three different types of cells, namely luminal secretory, basal and neuroendocrine cells. Since human prostate cancer is characterized by loss of basal cells and expansion of luminal cells, several animal models posit that luminal-specific progenitors are the sources of prostate cancer initiation (Korsten 2009, Wang 2009, Kurita 2004). However, using the tissue regeneration approach, basal cells have proved to be more efficient oncogenic targets for both human and mouse prostate cancer initiation (Lawson 2010, Goldstein 2010). Interestingly, Xin's group demonstrated that adult murine prostate basal and luminal cells are self-sustained lineages that can both serve as oncogenic targets for prostate cancer initiation (Choi 2012).

PTEN plays an important role in human prostate cancer and CRPC development (Sarker 2009) and is inactivated in 20% of primary and 60% of metastatic lesions (McMenamin 1999). The murine *Pten* prostate cancer model ($Pb\text{-}Cre^{+};Pten^{L/L}$) recapitulates the disease progression seen in humans, including CRPC (Wang 2003, Wang 2006, Mulholland 2009, Mulholland 2011), and shares many signature genetic changes with human disease (Wang 2003).

Importantly, the *Pb-Cre*$^{+}$*;Pten*$^{L/L}$ model provides a unique tool for studying tumor initiating cells as the majority of luminal cells and subpopulations of basal cells have *Pten* deletion (Wang 2003, Wang 2006). Using this model, we previously demonstrated that *Pten* deletion causes an expansion of basal and transient amplifying subpopulations and subsequent tumor initiation *in vivo* (Wang 2006). We further showed Lin^{-}Sca-1^{+}CD49f^{hi} (LSC^{hi}) prostate stem/progenitor cells from the *Pten* null prostate are capable of initiating a cancerous phenotype that mimics the primary cancer in the *Pten* null prostate model (Mulholland 2009).

Here, we report the identification of a cell surface marker, CD166 or Activated Leukocyte Cell Adhesion Molecule (CD166/ALCAM) that is highly upregulated in human and murine CRPC samples. CD166 can be used to enrich for stem/progenitor sphere-forming cells from both WT and *Pten* null mutant mouse prostates. In addition, CD166 can separate LSC^{hi} mouse stem/progenitor cells into CD166^{hi} and CD166^{lo} subpopulations, with the LSC^{hi};CD166^{hi} subpopulation having much higher sphere-forming activity. We further demonstrate that CD166 can be used as an enrichment maker for isolating human prostate sphere-forming cells and tubule-forming cells.

II. Results

a. CD166 expression is upregulated in murine castrated prostatic epithelium and can be used for enriching stem/progenitor cells.

Rodent prostate contains stem-like cells that are enriched in the castrated prostate gland and can undergo more than 15 cycles of involution-regeneration in response to androgen withdrawal and replacement (Tsujimura 2002). We reasoned that castration may also lead to

upregulation or enrichment of those stem cell surface molecules that can potentially serve as marker for isolating stem/progenitor cells and for targeted drug delivery. We therefore mined publically available databases describing gene expression profiles of murine prostates at day 0 and day 3 post-castration (Wang 2007, Carver 2011). We focused on those genes that fell in the gene ontology category of 'plasma membrane' and identified CD166/ALCAM as one of only two common castration-enriched cell surface molecules (Table S1). CD166 was significantly increased (1-tail t-test <0.015) 3 days after castration as compared to intact mice. While Cxcl12 is also upregulated, we chose not to focus on this gene as it is a chemokine and not amenable for FACS-mediated stem/progenitor cell enrichment.

CD166 is a type I transmembrane protein of the Ig superfamily that mediates cell-cell interactions via heterophilic (CD166-CD6) and/or homophilic (CD166-CD166) mechanisms (Swart 2002, van Kempen 2001). We found that in the intact mice, CD166 is preferentially expressed in the stem/progenitor-enriched proximal region (Tsujimura 2002) but low in the stem/progenitor-poor distal region of the WT prostate (Figure 1A upper panels). CD166 protein levels are also up-regulated immediately following castration (Figure 1A lower panels; comparing day 0 and day 3 post- castration).

Prostate stem/progenitor cells are characterized by their ability to form spheres *in vitro* (Lawson 2007). We performed the sphere-forming assay using sorted $CD166^{hi}$ and $CD166^{lo}$ cells and found that $CD166^{hi}$ cells have significantly higher sphere-forming activity compared to $CD166^{lo}$ cells (Figure 1B, left). Since we had previously developed the LSC^{hi} enrichment scheme (Lawson 2007), which yields 10-fold enrichment of WT sphere-forming cells, we tested whether CD166 can be used for further enriching sphere-forming activity. We gated LSC^{hi} cells according to their CD166 expression and found that LSC^{hi};$CD166^{hi}$ cells have 5-fold higher

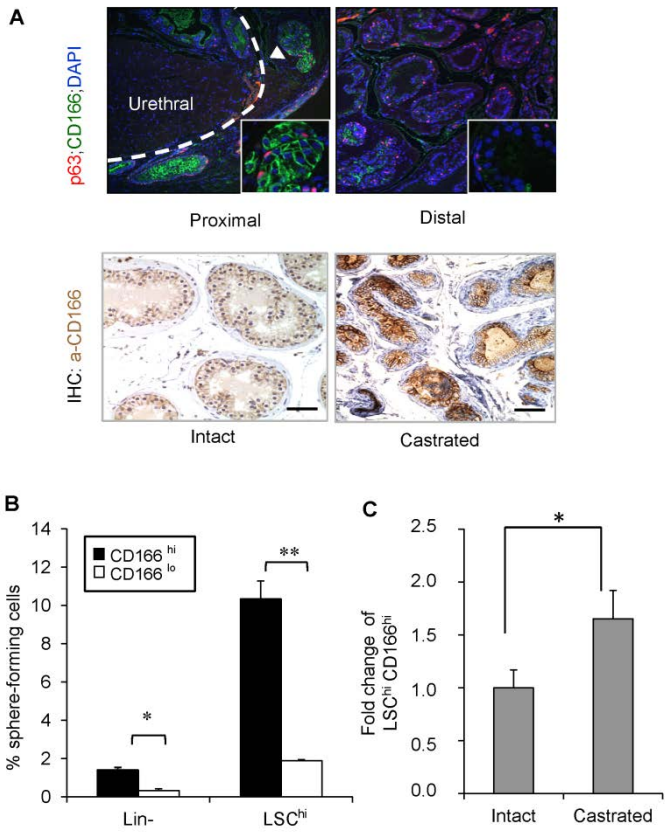

Figure 2-1: CD166 expression is upregulated in castrated prostate epithelium and CD166 can be used to enrich stem/progenitor cells in WT mice prostate. (A) Top: Comparison of p63 (red) and CD166 (green) co-IF staining between prostate proximal region and distal region. Bottom: IHC for CD166 expression from intact vs. castrated mouse prostate. Scale bar: 50 µm. (B) Lin^{-};$CD166^{hi}$, Lin^{-};$CD166^{lo}$, LSC^{hi};$CD166^{hi}$, and LSC^{hi};$CD166^{lo}$ cells were isolated by FACS from 8- to 12-week-old mice. Graph shows the percentage of sphere-forming cells, based on the spheres from each population per 2500 cells plated after 8 days of growth. Data shown as mean +/– STD (**, $p < 0.001$, n=3). (C) Fold change of LSC^{hi};$CD166^{hi}$ content based on intact WT from FACS analysis (*, $p < 0.05$, n=3).

sphere-forming activity as compared to their LSC^{hi};$CD166^{lo}$ counterpart (Figure 1B, right). Therefore, CD166 can be used as a marker to further enrich sphere forming cells within the WT prostate. Serial passaging of the spheres generated from LSC^{hi};$CD166^{hi}$ cells demonstrated that this enhanced sphere-forming activity could be maintained *in vitro* through at least three passages (Figure S1A). In contrast, less spheres were generated from LSC^{hi};$CD166^{lo}$ cells (P0-P2) and cannot undergo continuous passage due to the limited cell number. We observed no significant difference in the sphere size distribution between LSC^{hi};$CD166^{hi}$ generated spheres

and LSC^{hi};$CD166^{lo}$ generated spheres (Figure S1B and S1C). Similar to the LSC^{hi} subpopulation (Lawson 2007), castration also leads to significant enhancement of the LSC^{hi};$CD166^{hi}$ sub-population (Figure 1C).

b. $CD166^{hi}$ human prostate cells have higher sphere forming and regeneration potential.

Certain cell surface markers, such as Sca-1, are only expressed in the mouse and therefore cannot be used for isolation of human stem/progenitor cells. CD166, on the other hand, is expressed in various human organs and upregulated in human cancers, including prostate cancer (Ofori-Acquah 2008). To determine whether CD166 can be used for enriching human prostate stem/progenitors, we first examined its expression and found that CD166 is highly expressed in the developing human fetal prostate epithelium (Figure 2A, left panel) and focally expressed in the benign adult prostate, which overlaps with a subset of TROP2 and CD49f – positive cells (Figure 2, middle and right panels).

We then evaluated whether CD166 could be used as a marker for enriching human stem/progenitor cells. Benign regions of prostate tissue were collected from multiple patients who underwent radical prostatectomy and dissociated to single cells. Consistent with our previous studies (Ofori-Acquah 2008, Goldstein 2010), the percentages of $CD166^{+}$ cells vary from patient to patient (data not shown). However, the majority of sphere forming activity was identified in the $CD166^{hi}$ population (Figure 2B), similar to our findings with murine prostate cells. Data are shown from 6 representative patients.

To evaluate whether CD166 can enrich human prostate tissue regeneration capacity *in vivo*, benign human prostate cells were dissociated and sorted according to cell surface CD166 expression levels. Equal number of viable $CD166^{hi}$ and $CD166^{lo}$ cells ($2x10^{5}$) was implanted

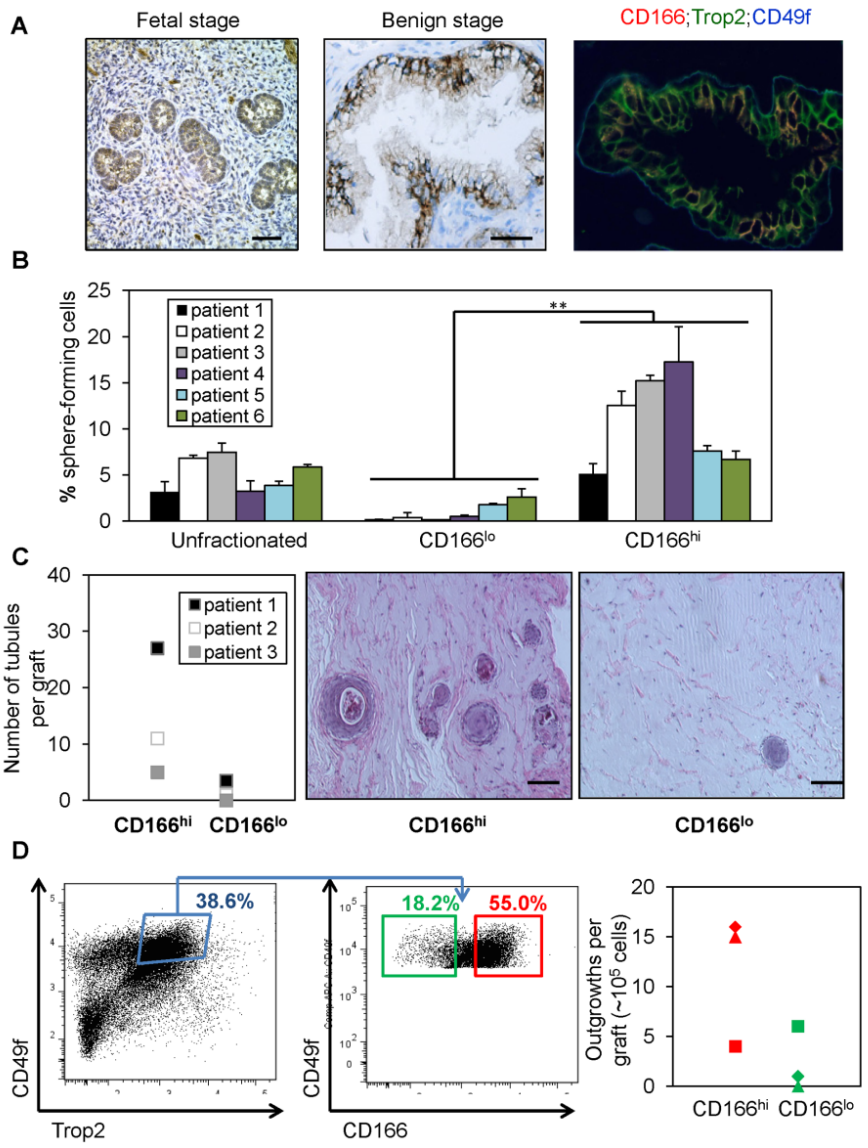

Figure 2-2: CD166^{hi} human prostate cells have higher sphere forming capacity *in vitro* and more graft outgrowth *in vivo*. (A) IHC staining of CD166 on human fetal prostate tissue and patient prostate cancer tissues. Scale bar: 50 µm. (B) Total dissociated prostate cells, CD166^{hi} and CD166^{lo} populations were isolated by FACS from 6 patient samples. Graph shows the percentage of sphere-forming cells, based on the spheres from each population per 5,000 cells plated after 7 days of culture. Data shown as mean +/− STD (**, $p < 0.001$). (C) CD166^{hi}, and CD166^{lo} populations were isolated by FACS from 3 patient samples. CD166^{hi} and CD166^{lo} cells ($2x10^5$) were implanted subcutaneously into NOD-SCID/IL2rγ null mice, in combination with $2x10^5$ rUGSM inductive mesenchymal cells. Grafts were harvested, fixed and analyzed after 8-16 weeks. Left, graph shows that CD166^{hi} human prostate cells can form more tubules in graft regeneration assay compared to CD166^{lo} human prostate cells. Right, H&E staining of representive graft. Scale bar: 100 µm. (D) Left, FACS plots show gates drawn for sorting of LTC (TROP2^{hi};CD49f^{hi}) CD166^{hi} and LTC;CD166^{lo} subpopulations from one patient. Right, representative graph shows that LTC;CD166^{hi} human prostate cells can form more tubules in graft regeneration assay compared to LTC;CD166^{lo} human prostate cells.

quantification and analyses. $CD166^{hi}$ cells have more tissue regeneration capacity as evidenced by increased number of tubule-like epithelial structures found in the grafts, which is rarely seen in the $CD166^{lo}$ grafts (Figure 2C). Further analyses showed that the tubule-like structures initiated by $CD166^{hi}$ cells contain CK5 and p63 expressing basal cells, CK8 luminal cells and AR positive cells (Figure S2).

Combination of markers TROP2 and CD49f can separate lineage-negative human prostate epithelial cells into various subpopulations, with $TROP2^{hi}$;$CD49f^{hi}$ ($Lin^{-}T^{hi}C^{hi}$ or LTC) cells possessing the highest sphere forming capability *in vitro* (Goldstein 2008). Additionally, LTC cells can develop cancer-like phenotype *in vivo* following oncogenic transformation (Goldstein 2010). We tested whether CD166 can further segregate this LTC population. FACS analysis of benign human prostate cells indicated that more than 50% of LTC stem/progenitor cells also express the CD166 surface marker (Figure 2D, left and middle panel). Furthermore, we examined if differences in regeneration potential exist between these two subpopulations. Sorted LTC;$CD166^{hi}$ and LTC;$CD166^{lo}$ cells were injected subcutaneously into NOD-SCID/IL2rγ null mice with $2x10^5$ rUGSM cells and analyzed 8-16 weeks later. Our *in vivo* data suggest that LTC;$CD166^{hi}$ cells can induce more tubule-like structures, whereas LTC;$CD166^{lo}$ cells have less regeneration capacity (Figure 2D, right panel).

c. CD166 can be used to enrich tumor sphere-forming cells in the *Pten* null prostate cancer model.

To examine whether CD166 can enrich tumor initiating cells after castration, we compared the percentage of $CD166^{hi}$ subpopulation between intact and castrated *Pten* mutant mice and observed the expansion of $CD166^{hi}$ subpopulation after castration (Figure 3A). Next,

we compared the sphere formation capabilities of LSC^{hi};$CD166^{hi}$, LSC^{hi};$CD166^{lo}$, LSC^{lo};$CD166^{hi}$, and LSC^{lo};$CD166^{lo}$ subpopulations at the pre-cancer PIN (6 weeks) and cancer stages (11 weeks). We found that the LSC^{hi};$CD166^{hi}$ subpopulation has much higher sphere-forming ability, and nearly all sphere-forming activity in the cancer stage resides in the LSC^{hi};$CD166^{hi}$ subpopulation (Figure 3B). Consistent with our previous observation that *Pten* mutant spheres are larger than WT control spheres (Mulholland 2009), both LSC^{hi};$CD166^{hi}$ and LSC^{hi};$CD166^{lo}$ subpopulations form large prostate spheres (Figure S3). Our previous study suggested that *Pten* deletion promotes the expansion of LSC^{hi} prostate stem/progenitor cells (Wang 2006, Mulholland 2009). Within the LSC^{hi} population, we observed selective expansion of LSC^{hi};$CD166^{hi}$ cells. *Pten* mutant mice have more than a 3-fold increase in the percentage of LSC^{hi};$CD166^{hi}$ subpopulation, compared to WT littermates (Figure 3C).

To further study the LSC^{hi};$CD166^{hi}$ subpopulation, we isolated RNA from LSC^{hi};$CD166^{hi}$, LSC^{hi};$CD166^{lo}$ subpopulations and the cell fraction depleted of LSC cells (non-LSC^{hi}) and compared their gene expressions by RT-PCR analysis. LSC^{hi};$CD166^{hi}$ subpopulation expresses similar levels of basal cell markers *Ck5* and *p63* as the LSC^{hi};$CD166^{lo}$ subpopulation (Figure 3D, left panel). However, LSC^{hi};$CD166^{hi}$ subpopulation expresses much higher level of luminal marker *Ck8* and *Trop2*, a new epithelial surface marker we recently identified for enriching stem cell activities in both murine and human prostates (Goldstein 2008, Goldstein 2010) (Figure 3D, right panel). Further examination of several other epithelial cell stem cells markers (Richardson 2004, Leong 2008, Wang 2009, Burger 2009, Liu 2011) showed that LSC^{hi};$CD166^{hi}$ cells have significantly higher *CD44* and *Nkx3.1* expression compared to LSC^{hi};$CD166^{lo}$ cells. Although compared to non-LSC population, LSC^{hi};$CD166^{hi}$ cells express

less *Nkx3.1*. No significant differences were found in *CD117*, and *CD133* expressions between these two populations (Figure 3D, right panel).

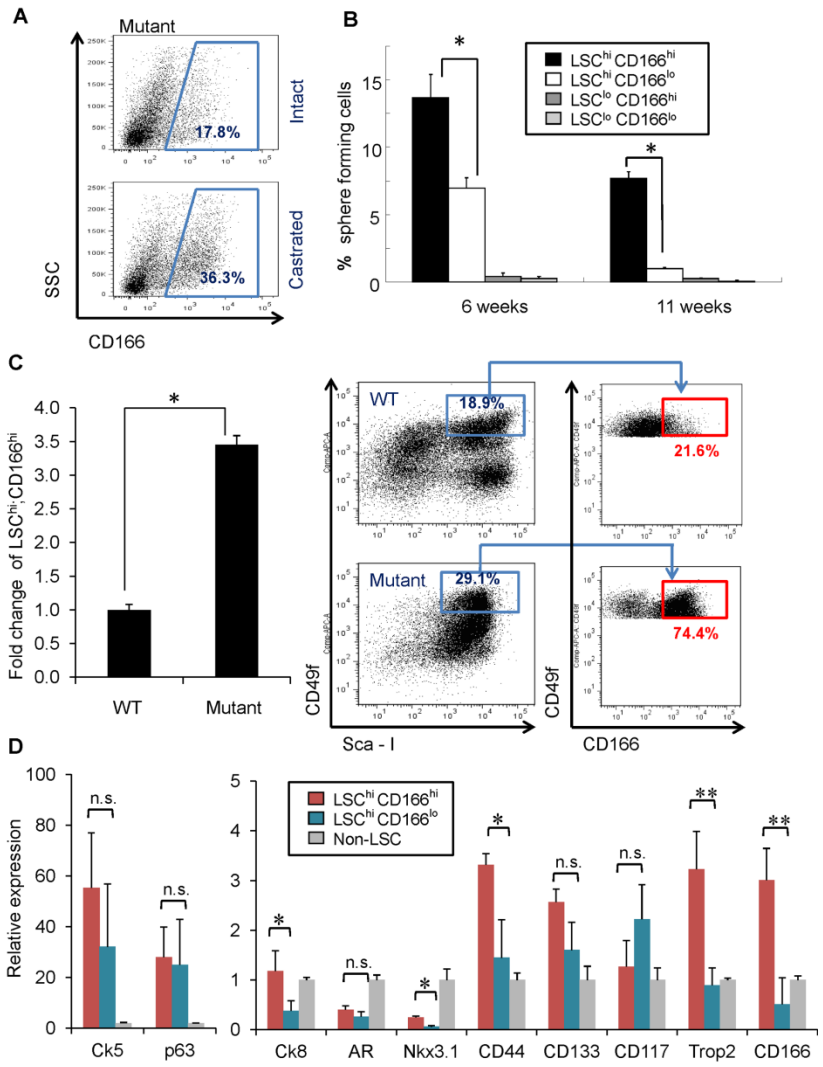

Figure 2-3: CD166 can be used to enrich tumor initiating cells in *Pten* mutant prostate. (A) FACS blots show increased Lin$^-$CD166^{hi} population after castration of *Pten* mutant mice compared to intact *Pten* mutant mice. (B) Four subpopulations (LSC^{hi}CD166^{hi}, LSC^{hi}CD166^{lo}, LSC^{lo}CD166^{hi}, LSC^{lo}CD166^{lo}) were isolated from *Pten* mutant prostate from either 6 weeks or 11 weeks old mice. Graph shows the percentage of sphere-forming cells. Data from several experiments were pooled. Data shown as mean +/− STD (*, $p < 0.05$, n=3). (C) Left: bar graph shows fold change of *Pten* mutant LSC^{hi}CD166^{hi} content compared to WT; right, FACS blots show the expansion of LSC^{hi} CD166^{hi} cells within LSC population on *Pten* mutant compared to WT. (D) RNA was isolated from non-LSC, LSC^{hi}CD166^{hi}, and LSC^{hi}CD166^{lo} fractions in duplicate experiments. RNA was synthesized into cDNA and subjected to qRT-PCR. Graph shows fold-enrichment over the non-LSC cells for each gene. Gadph was used as the reference gene (*, $p < 0.05$; **, $p < 0.01$; n.s., not significant).

d. CD166 expression is upregulated in human castration resistant prostate cancer.

Having found that CD166 can be used to enrich for human LTC cells and mouse tumor in itiating cells, we then examined the relationship between CD166 expression and human prostate cancer progression. In clinically annotated data of 218 prostate tumors (Taylor 2010), CD166 gene expression significantly correlates with increased prostate cancer aggressiveness, as indicated by Gleason score, with highest expression in metastasis samples (Figure 4A). We further surveyed CD166 expression on human prostate cancer tissue microarrays, which consist of 14 castration resistant (CRPC) metastasis samples and 98 hormone naïve primary cancer

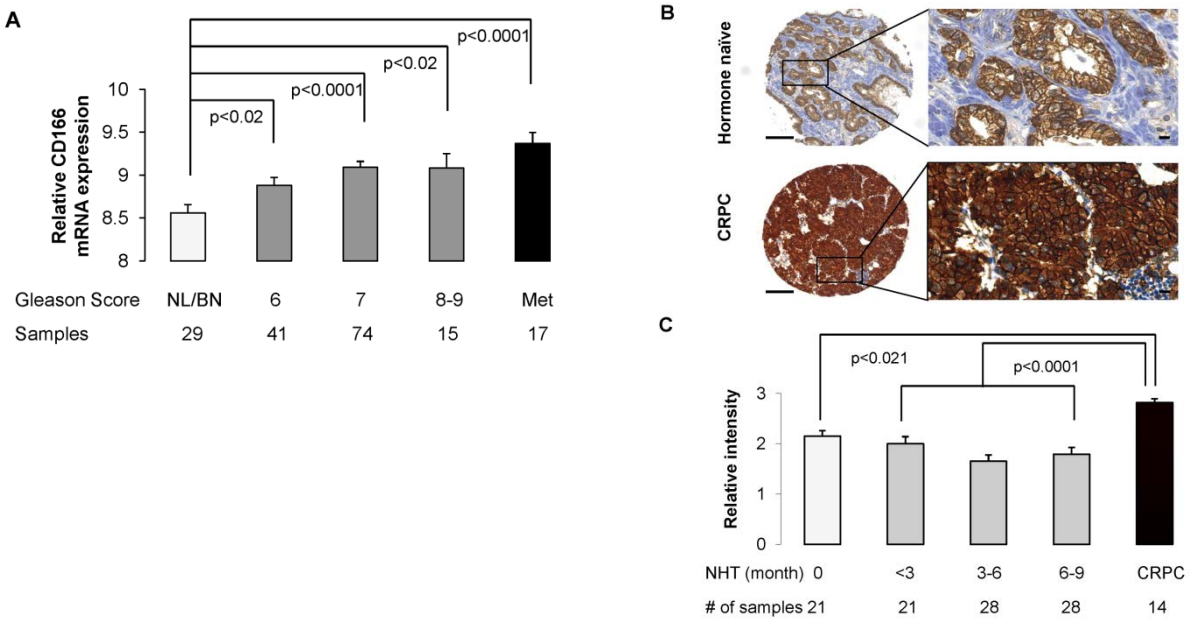

Figure 2-4: Gene expression profiling and tissue microarray (TMA) demonstrates that increased CD166 expression is correlated with high Gleason score and human castration resistant prostate cancer. (A) CD166 gene expression from 147 human prostate tumors was analyzed by comparing different Gleason score groups to normal/benign (NL/BN) prostate. (B) Representative IHC staining of CD166 expression from human prostate TMA. Top: hormone naïve primary prostate cancer; Low: castration resistant prostate cancer showing highly intensive immunostaining. Scale bar: 100 µm (left); 10 µm (right). (C) Data from 112 samples were calculated and statistical analysis of CD166 expression of human TMA conducted. NHT: neoadjuvant hormone therapy; CRPC: castrate resistant prostate cancer. Column, mean CD166 staining in NHT and CR tissues. Samples were graded from 0 to +3 representing the range from no staining to heavy staining by visual scoring. Error bar: standard error. Immunoreactivity of CD166 is significantly higher in CRPC group compared with untreated group ($p < 0.021$) or NHT with different treatment times ($p < 0.0001$).

samples from patients receiving either neoadjuvant hormone treatment (NHT) for various periods or receiving no treatment. CD166 is significantly enhanced in CRPC samples (Figure 4B for representative images). Compared to the predominant membrane localization of CD166 in hormone naïve primary cancer samples, we observed intense cytoplasmic localization of CD166 in CRPC bone metastasis samples (Figure 4B, high magnification). CD166 expression levels were scored and p values are computed by Mann-Whitney test. CD166 protein expression level is significantly higher in CRPC samples as compared with primary cancers with ($p<0.0001$) or without ($p<0.02$) NHT (Figure 4C). These data suggest that CD166 is a castration-enriched marker for both murine and human prostate cancer.

e. Loss of CD166 does not interfere with WT prostate development and prostate sphere formation.

While expressed in a wide variety of tissues, CD166 is usually restricted to subsets of cells involved in dynamic growth and/or migration, including neural development, branching organ development, hematopoiesis and immune response (Ofori-Acquah 2008). To test whether CD166 plays an intrinsic role in regulating prostate stem/progenitor cells, we analyzed *CD166* knockout mice (*CD166*$^{-/-}$). Genetic deletion of *CD166* gene was achieved by replacing its first exon with a cDNA encoding EGFP (Weiner 2004). *CD166* null mice are phenotypically normal and fertile (Weiner 2004). We examined the prostate at 8 and 20 weeks of age and found no difference in gross anatomy and histology among WT (data not shown), *CD166*$^{+/-}$ and *CD166*$^{-/-}$ mouse prostates (Figure 5A).

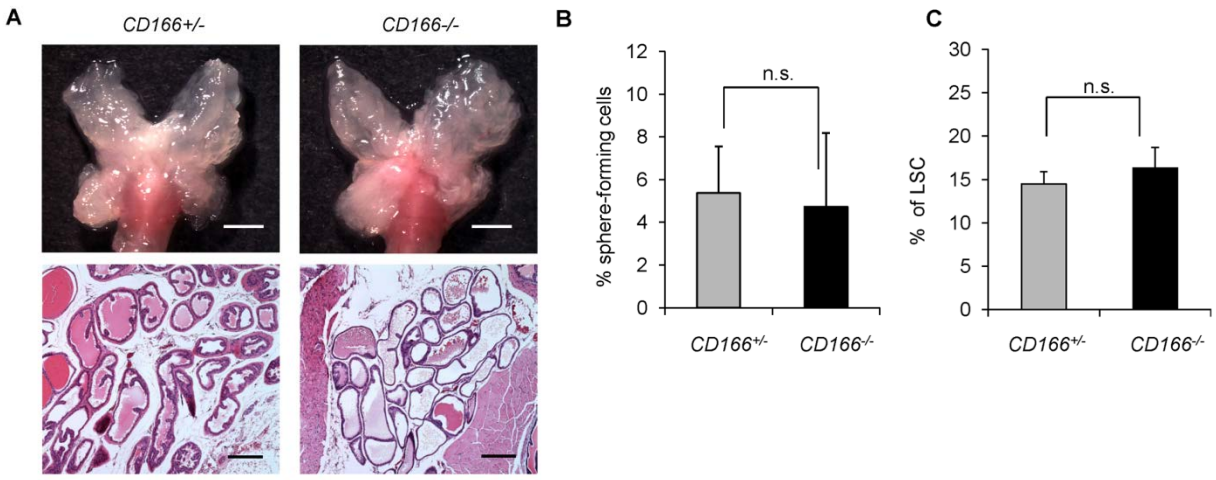

Figure 2-5: Loss of CD166 does not block WT prostate development and stem/progenitor cell function. (A) Top: The gross anatomy of the prostate of *WT* and *CD166-/-* mice at 8 weeks of age, scale bar: 2mm. Bottom: HE staining of DLP section from WT and *CD166* $^{-/-}$ mice at 8 weeks of age, scale bar: 200µm. (B) Comparison of sphere formation from total unsorted prostate cells (5000 per 12-well) between *CD166*$^{+/-}$ and *CD166*$^{-/-}$ prostates. Data represented as mean +/− STD ($p > 0.05$, n=3). (C) Comparison of LSC^{hi} content between *CD166*$^{+/-}$ and *CD166*$^{-/-}$ prostates at 8-12 weeks age ($p > 0.05$, n=5).

To further examine whether loss of CD166 has any effect on prostate stem/progenitor cells, we compared sphere formation activities of *CD166*$^{+/-}$ and *CD166*$^{-/-}$ prostate epithelium and found there is no significant difference (Figure 5B). In addition, spheres generated from *CD166*$^{-/-}$ prostate have similar size distribution compare to those from *CD166*$^{+/-}$ prostate epithelium (data not shown). Similarly, FACS analysis demonstrated that loss of CD166 does not affect LSC^{hi} content of prostates isolated from the *CD166*$^{-/-}$ mice (Figure 5C), suggesting that CD166 does not play an essential role in normal prostate gland development or prostate stem/progenitor number and function.

f. Genetic deletion of *CD166* does not block prostate cancer progression.

It has been postulated that CD166 functions as a cell surface sensor for cell density and controls the transition between local cell proliferation and tissue invasion during melanoma

progression (van Kempen 2000). To examine whether CD166 plays an essential role in prostate cancer development, especially in the tumor initiating cells, we crossed *CD166*$^{-/-}$ mice with the *Pten* conditional knockout mice (Wang 2003). Histopathologic analysis indicated that loss of CD166 did not significantly change the kinetics of prostate cancer development in *Pten* null model and all *Pb-Cre*$^{+}$*;Pten*$^{L/L}$*;CD166*$^{-/-}$ mice developed adenocarcinoma around 9 weeks of age (Figure 6A and data not shown). We observed similar levels of Ki67^{+} cells between *Pb-Cre*$^{+}$*,Pten*$^{L/L}$*,CD166*$^{+/+}$ *and Pb-Cre*$^{+}$*;Pten*$^{L/L}$*;CD166*$^{-/-}$ prostates (Figure 6A). SMA staining also demonstrated that loss of CD166 does not block prostate cancer cells from local invasion (Figure 6A, right panels).

We then compared the sphere formation between *Pb-Cre*$^{+}$*;Pten*$^{L/L}$*;CD166*$^{+/-}$ and *Pb-Cre*$^{+}$*;Pten*$^{L/L}$*;CD166*$^{-/-}$ prostates and found that loss of CD166 does not interfere with sphere-forming activity of *Pten* null epithelium (Figure 6B). Moreover, *CD166*$^{-/-}$ prostates have similar LSC^{hi} content as compared to *CD166*$^{+/-}$ *Pten* null prostates (Figure 6C). Since PI3K/AKT pathway activation is a driving force for cell proliferation and prostate cancer progression in *Pb-Cre*$^{+}$*;Pten*$^{L/L}$ prostate cancer (Wang 2003, Mulholland 2011), we then examined whether there is any alteration of AKT activation after genetic deletion of *CD166*. Western blot analysis demonstrated that *Pb-Cre*$^{+}$*;Pten*$^{L/L}$*;CD166*$^{-/-}$ prostate has no CD166 expression, but has similar P-AKT levels compared to *Pb-Cre*$^{+}$*;Pten*$^{L/L}$*;CD166*$^{+/+}$ and *Pb-Cre*$^{+}$*;Pten*$^{L/L}$*;CD166*$^{+/-}$ prostate (Figure 6D). We further confirmed that there is no negative selection against *Pten*$^{-/-}$*;CD166*$^{-/-}$ cells since equal intensity of knockin-GFP protein can be detected in all cohorts except *CD166*$^{+/+}$ mice.

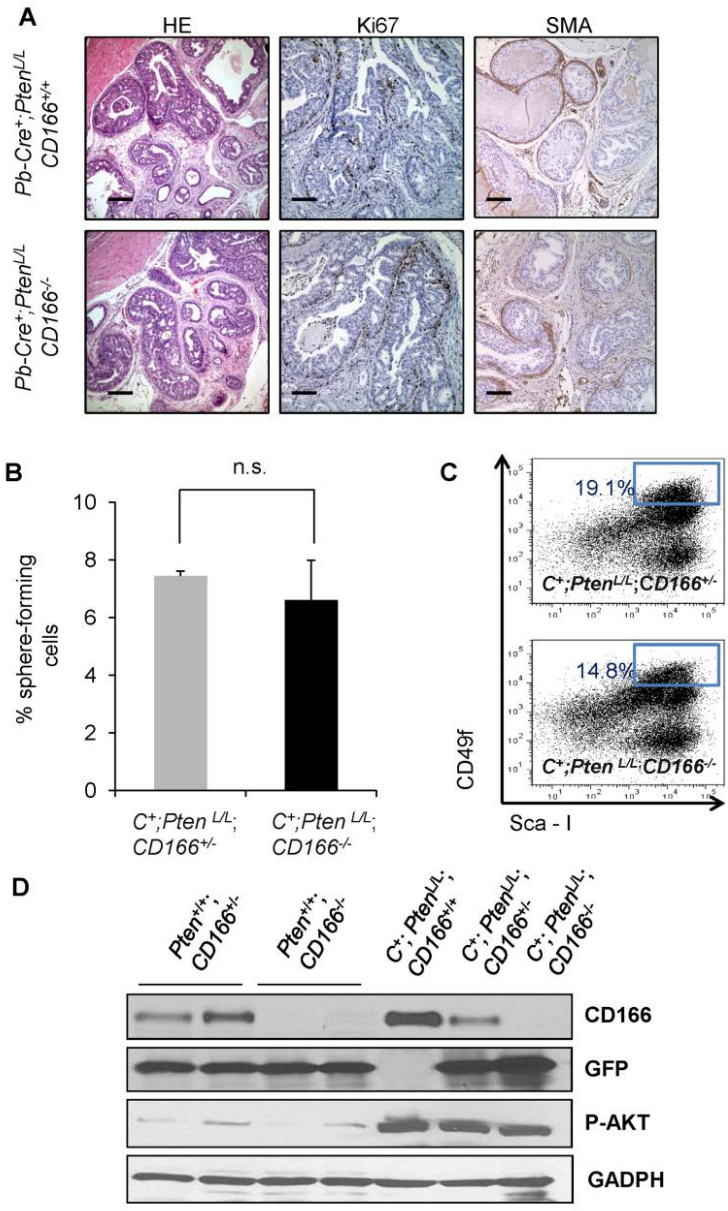

Figure 2-6: Loss of CD166 does not block prostate tumor progression and tumor initiating cell function in *Pb-Cre^{+};Pten$^{L/L}$;CD166$^{-/-}$* mice. (A) Evaluation of *CD166* deletion on prostate cancer progression (HE staining, scale bar: 200 μm), cell proliferation (Ki67 staining, scale bar: 100 μm), and prostate tumor invasion (SMA staining, scale bar: 100 μm) by comparing age matched *Pb-Cre^{+}*, *Pten$^{L/L}$*, *CD166$^{+/+}$* and *Pb-Cre^{+}*, *Pten$^{L/L}$*, *CD166$^{-/-}$* prostate tissue at 20 weeks of age. (B) Comparison of sphere formation from total unsorted prostate cells (5000 per 12-well) between *Pb-Cre^{+}*, *Pten$^{L/L}$*, *CD166$^{+/-}$* and *Pb-Cre^{+}*, *Pten$^{L/L}$*, *CD166$^{-/-}$* prostate (9 weeks of age). (C) A representative FACS blot shows LSC content between *Pb-Cre+*, *Pten$^{L/L}$*, *CD166$^{+/-}$* and *Pb-Cre^{+}*, *Pten$^{L/L}$*, *CD166$^{-/-}$*. (D) Examination of protein levels of CD166, P-AKT and GFP among different prostate tissue with indicated genotype by Western blotting. GADPH is included as an equal loading control.

Since we see significant overexpression of CD166 in human CRPC samples, we next investigated whether CD166 would influence the development of CRPC in the *Pten* null prostate cancer model. *Pb-Cre*$^{+}$*;Pten*$^{L/L}$*;CD166*$^{+/-}$ and *Pb-Cre*$^{+}$*;Pten*$^{L/L}$*;CD166*$^{-/-}$ males were castrated at 12 weeks and prostates were isolated 8 weeks later. As shown in Figure 7, deletion of CD166 does not significantly influence the formation of CRPC, as evidenced by similar pathohistology (Figure 7A), CK5/CK8 marker distribution, BrdU pulse labeling and SMA staining in both cohorts (Figure 7B). Taken together, our genetic studies indicate that CD166 has limited intrinsic function in the prostate, even in the tumor initiating cells.

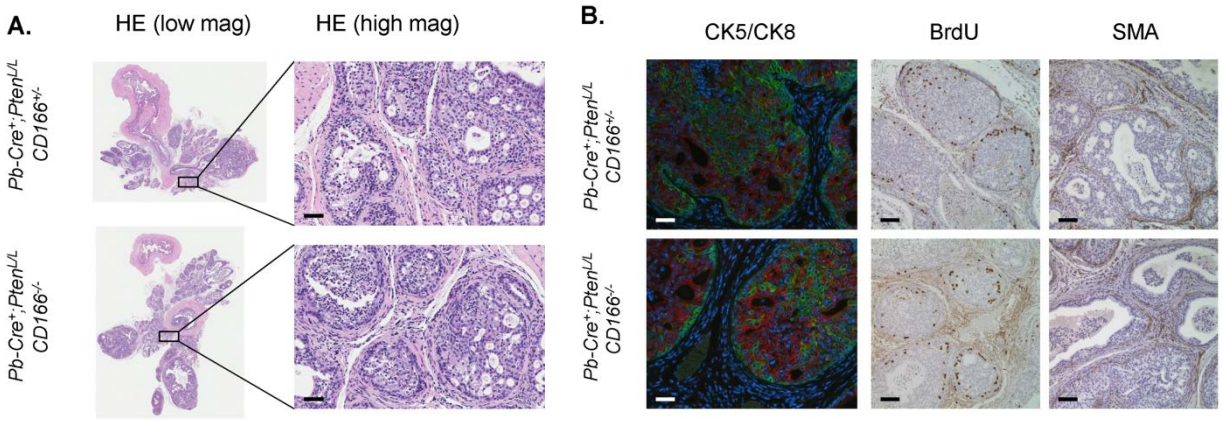

Figure 2-7: Loss of CD166 does not block castration resistant prostate tumor progression in *Pb-Cre*$^{+}$*;Pten*$^{L/L}$*;CD166*$^{-/-}$ mice. *Pb-Cre*$^{+}$, *Pten*$^{L/L}$, *CD166*$^{+/-}$ and *Pb-Cre*$^{+}$, *Pten*$^{L/L}$, *CD166*$^{-/-}$ mice were castrated at the age of 12 weeks using standard techniques. At 8 weeks post-castration, mice were intraperitoneal injected with a single dose of 100µl (1mg) of BrdU solution and sacrificed 4 hour later for analysis. Evaluation of the effects of *CD166* deletion on (A) castration resistant prostate cancer progression (HE), and (B) cell lineage composition (CK5/CK8), cell proliferation (BrdU) and prostate tumor invasion (SMA) were performed. Scale bar: 50 µm.

III. Discussion

Few surface markers are currently available for enriching both murine and human prostate tissue stem/progenitor cells and for identifying prostate cancer initiating cells. By

searching for those cell surface molecules that are upregulated in castrated murine prostate and castration resistant prostate cancers (CRPC) of murine and human origins, we identified CD166 as a surface marker for enriching both murine and human prostate tissue stem/progenitor cells based on *in vitro* sphere forming and *in vivo* tissue regeneration analyses. Importantly, upregulated CD166 expression and expansion of $CD166^{hi}$ cells correlate with *Pten* null CRPC progression as well as human CRPC development, although genetic deletion of *CD166* does not interfere with normal murine prostate development or *Pten* null prostate cancer progression. Together, our study suggests CD166 can be used as a potential surface marker for identifying castration resistant tumor cells for targeted drug delivery.

CD166 expression has been proposed as a prognostic marker for several cancers, including breast (King 2010), prostate (Kristiansen 2005), ovarian (Mezzanzanica 2008), pancreatic (Kahlert 2009), colon (Weichert 2004), oral cancers (Sawhney 2009), melanoma (van Kempen 2000) and gastric cancers (Ishigami 2011). Importantly, our microarray and TMA studies demonstrate the association of increased CD166 expression with human prostate cancer metastasis and CRPC development. Moreover, within both murine and human prostates, we show that the CD166-high expressing subpopulation encompasses prostate stem/progenitor and cancer initiating cells.

To investigate human prostate tissue stem/progenitor cell properties, we evaluated adult human prostate epithelium dissociated from benign prostate, rather than cell lines and xenografts. The advantage of this approach is to maintain the original heterogeneity in human prostate samples by avoiding the effect of long-term *in vitro* selection. However, there appears to be greater variability among patient samples in the tissue regeneration assays. This may be due to the difference in sample variability (i.e., ischemia time prior to tissue processing and cell

retrieval), individual variability in CD166 expression, and technical challenges related to the tissue regeneration assays using human prostate cells. Therefore, analysis of sufficient patient samples is essential in order to draw a valid conclusion. In the current study, 6 human samples were utilized for the *in vitro* sphere forming and another 6 samples were used for *in vivo* regeneration assays. Using this system, we have previously defined $TROP2^{hi};CD49f^{hi}$ as a cancer initiating cell (cell of origin) for human prostate cancer (Goldstein 2010). In the current study, $CD166^{hi}$ population demonstrated significantly increased sphere-forming capacity compared to the patient-matched $CD166^{lo}$ population. In addition, our study demonstrates that CD166 can not only enrich human sphere-forming cells, but also segregate $TROP2^{hi};CD49f^{hi}$ into two functionally different populations, with $TROP2^{hi};CD49f^{hi;}CD166^{hi}$ having higher regeneration capacity *in vivo*, compared to $TROP2^{hi}CD49f^{hi}CD166^{lo}$. CD166 is also highly upregulated in CRPC based on our gene expression analysis and tissue microarray study. Therefore, CD166 may enrich both human prostate tissue stem/progenitor cells and castration resistant prostate cancer cells.

LSC^{hi} subpopulation has been defined as the murine prostate tissue stem/progenitor cells and expands significantly following castration (Lawson 2010, Mulholland 2009, Lawson 2007). LSC^{hi} cells express basal markers and demonstrated robust sphere-forming activity *in vitro* and prostate regeneration capability *in vivo* (Lawson 2007). In contrast to luminal cells, LSC^{hi} cells respond efficiently to multiple oncogenic insults for prostate cancer initiation using a transplantation-based prostate regeneration assay (Lawson 2010). We and others have demonstrated that the LSC^{hi} population, isolated from *Pten* null prostate tissue, is sufficient to regenerate cancerous morphology upon transplantation that closely mimics that of primary cancers (Mulholland 2009, Liao 2010). In this study, we further separated LSC^{hi} subpopulation

into $CD166^{hi}$ and $CD166^{lo}$ subsets and found that most of sphere-forming activities are associated with the LSC^{hi};$CD166^{hi}$ cells. Importantly, this LSC^{hi};$CD166^{hi}$ population was demonstrated to have self-renewal activity as spheres from this population could be passaged at least 3 generations with a high rate of sphere formation. Moreover, LSC^{hi};$CD166^{hi}$ cells are expanded upon castration as well as *Pten* deletion in comparison to LSC^{hi};$CD166^{lo}$ cells. Therefore, CD166 can further enrich murine prostate cancer initiating cells and castration resistant cells.

The relationship of LSC^{hi};$CD166^{hi}$ cancer initiating cells described here to other cell populations is of obvious interest (De Marzo 2010). Using lineage tracing and cell type-specific Cre lines, a recent report demonstrates that both luminal cells and basal cells can initiate prostate cancer upon *Pten* deletion (Choi 2012). This new observation is not in conflict with our previous studies: we showed that *Pten* deletion mediated by *Pb-Cre* happens in both basal and luminal cells (Wang 2006). In addition, we observed significant expansion of a subset of prostate cancer cells positive for basal cell markers CK5 and p63 and luminal cell marker CK8, suggestive of transient amplifying/ intermediate cells (Wang 2006, Sato 2002). Compared to LSC^{hi};$CD166^{lo}$ cells, one of the distinguishing features of LSC^{hi};$CD166^{hi}$ cells is the higher *Trop2* expression, a cell surface marker we have used for enriching both murine and human tissue stem cells (Goldstein 2008, Goldstein 2010). TROP2 can functionally segregate mouse LSC population but there is no cytokeratin phenotypic difference between LSC^{hi};$Trop2^{hi}$ and LSC^{hi};$Trop2^{lo}$ population (Goldstein 2008). CD166, on the other hand, can enrich *Pten* null LSC^{hi} population with $CK5^{+}$/$p63^{+}$/$CK8^{+}$/AR^{-}/$TROP2^{hi}$ characteristics, suggesting that CD166 may preferentially enrich for $CK5^{+}$/$CK8^{+}$ transient amplifying/intermediate cells, which currently cannot be prospectively purified. Increased $CK5^{+}$;$CK8^{+}$ cells have been observed in the *Pten* conditional

knockout model (Wang 2006, Lu 2007) as well as *Pten*$^{-/-}$;*TP53*$^{-/-}$ prostates cancer model (Abou-Kheir 2010). A recent study also identified a subset of tumor-initiating stem-like cells in human prostate cancer cell lines and xenografts based on co-expression of the human pluripotent stem cell marker TRA-1-60, CD151 and CD166 (Rajasekhar 2011). Interestingly, this subtype of human prostate tumor initiating cells also have the AR^{-};$CK5^{+}$;$CK8^{+}$ phenotype (Rajasekhar 2011). Another characteristic of LSC^{hi};$CD166^{hi}$ cells is relatively higher CD44 expression. Since knockdown of CD44 was very effective to suppress cancer stem cell regeneration and metastasis (Liu 2011), it will be interesting to examine whether there is any functional role for CD44 in LSC^{hi};$CD166^{hi}$ tumor initiating cells.

As an adhesion molecule, CD166 can initiate homophilic (CD166-CD166) or heterophilic interaction (CD166-CD6), and play important roles in neural guidance and the immune system (Ofori-Acquah 2008). CD166 has also been suggested to play a critical role in various human cancers and as a potential therapeutic target for cancer initiating cells, similar to CD44 (Liu 2011) and CD47 (Chao 2011). A truncated CD166 variant has been shown to block melanoma metastasis by interfering with the CD166-CD166 homophilic interaction (Lunter 2005). Similarly, novel human recombinant single-chain anti-CD166 antibodies have been shown to inhibit colorectal carcinoma growth as well as breast cancer cell invasion (Wiiger 2010). Unlike subcutaneous allograft or xenograft models used in above studies, we defined the functions of CD166 in prostate cancer initiating cells and prostate cancer development in immune competent mice within the natural prostate environment. By generating the *Pb-Cre*$^{+}$;*Pten*$^{L/L}$;*CD166*$^{-/-}$ line, our study demonstrates that loss of CD166 within LSC^{hi} population does not change their ability to form spheres *in vitro* and block prostate cancer initiation and progression *in vivo*. As it is possible that other members of the Cell Adhesion Molecule (CAM)

family can compensate for the role of CD166 in murine prostate cancer development, we cannot conclude that CD166 has no *in vivo* function on prostate cancer initiation. Nevertheless, since cancer initiating cell surface markers can be used for molecular imaging (Hart 2008) and/or for internalizing a death-inducing compound for targeted therapies (Wang 2011), our work suggests that CD166 may be for a suitable surface marker for future targeted drug delivery (Roth 2007). Recently, a promising study showed substantial cytotoxic effects of the CD166 scFv-condugated drugs on three human prostate cancer cell lines (Du-145, PC3, and LNCaP) (Roth 2007). Since CD166 is highly expressed on both human and mouse tissue stem/progenitor cells, it will be interesting to examine the effect of this targeted drug delivery on their prostate sphere forming activity and prostate regeneration potential. The *Pb-Cre*$^{+}$*;Pten*$^{L/L}$*;CD166*$^{+/-}$ and *Pb-Cre*$^{+}$*;Pten*$^{L/L}$*;CD166*$^{-/-}$ mouse models generated in this study, therefore, can be used to investigate the efficiency of CD166 - mediated drug delivery to prostate cancer initiating cells *in vivo*, especially during CRPC development.

		Wang et al.		Carver et al	
GeneSymbol	Gene Name	Log2 (Cas/int)	p-value	Log2 (Cas/int)	p-value
Cxcl12	chemokine (C-X-C motif) ligand 12	0.850120125	0.004376185	0.740973333	0.000567102
Alcam/Cd166	activated leukocyte cell adhesion molecule	0.728515152	0.012644597	0.9857775	0.00585034

Table S2-1: Compared to intact prostate epithelium WT CD166 gene expression is significantly increased at day 3 post-castration.

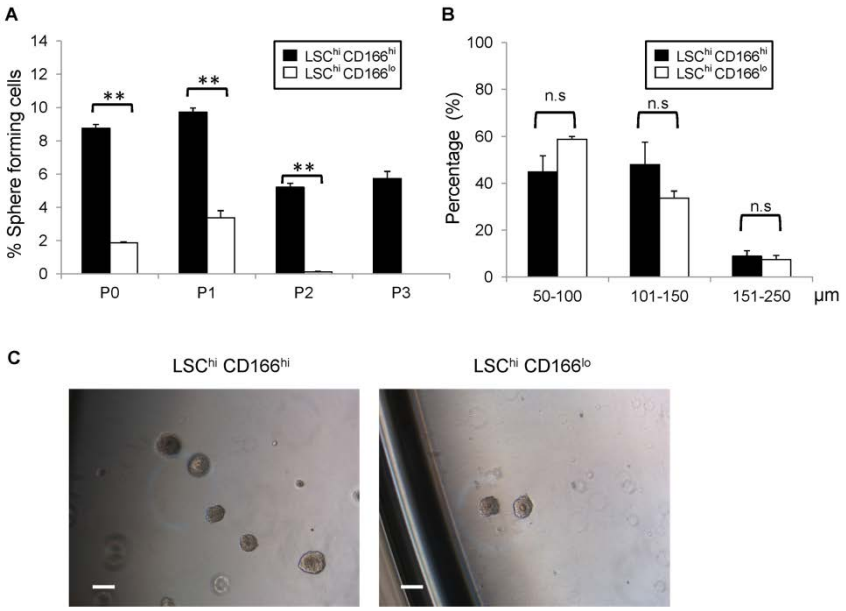

Figure S2-1: WT LSC^{hi}; CD166^{hi} prostate cells demonstrate higher self-renewal activity. (A) LSC^{hi};CD166^{hi} and LSC^{hi}; CD166^{lo} cells were isolated by FACS from 8- to 10-week-old mice and plated for sphere formation assay. Spheres from the each subpopulation (P0) were dissociated and replated for 3 successive generations (P1-P3). Graph shows the percentage of sphere-forming cells, based on the spheres from each population per 5000 cells plated after 8 days of growth. Error bars represent means and STD from triplicates of one of the two independent experiments (**, P<0.001). (B) Comparison of sphere size distribution between LSC^{hi}; CD166^{hi} and LSC^{hi}; CD166^{lo} formed spheres. n.s., not significant. (C) Representative sphere images of LSC^{hi};CD166^{hi} and LSC^{hi}; CD166^{lo} cells generated spheres. Scale bar: 100 µm.

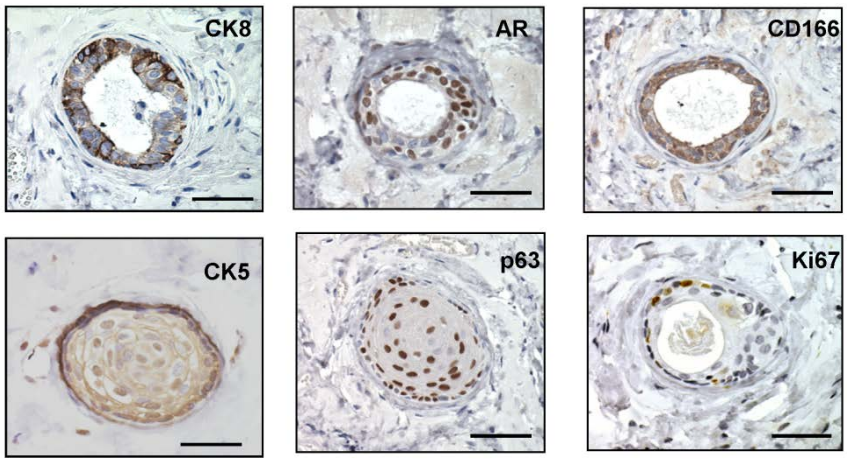

Figure S2-2: Immunohistochemical analysis of CD166^{hi} human prostate epithelium-derived graft demonstrates nuclear expression of AR and p63, CK5 and CK8 positive cells and Ki67 positive cells within tubule structure. Scale bar: 50 µm.

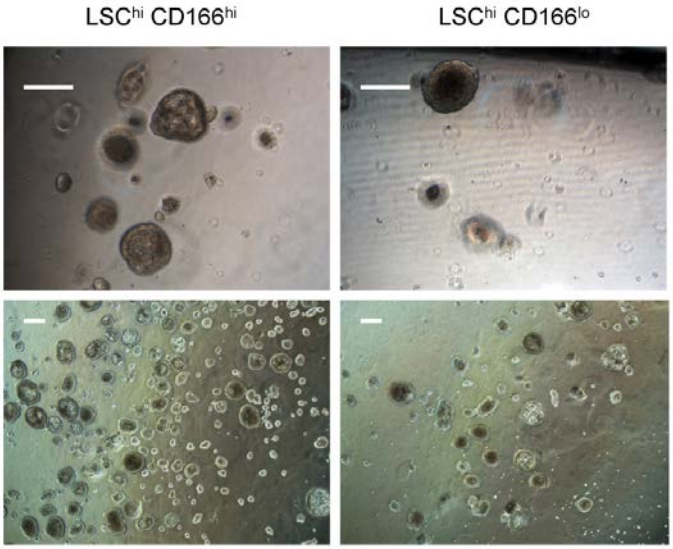

Figure S2-3: LSC^{hi};CD166^{hi} and LSC^{hi}; CD166^{lo} cells isolated from *Pten* mutant prostate form spheres with similar size distribution. Representative sphere images of LSC^{hi};CD166^{hi} and LSC^{hi}; CD166^{lo} cells generated spheres. Top: spheres maintained in matrigel. low: spheres released from matrigel after dispase treatment. Scale bar: 200 µm.

application	antibody	company
IHC/IF	CK5	PRB-160P/Covance
	CK8	MMS-162P/Covance
	P63	sc-8431/Santa Cruz
	Ki67	VP-RM04/Vector lab
	SMA	A254/Sigma Aldrich
	CD166	BAF1172/R&D systems
	CD166	VP-375/Vector Laboratories
	Trop2	BAF650/R&D systems
FACS	FITC-CD31	11-0311/ebioscience
	FITC-CD45	11-0451/eBioscience
	FITC-Ter119	11-5921/eBioscience
	APC-CD49F	313610/Biolegend
	PE-Cy7-Sca1	122514/Biolegend
	PE-CD166	12-1661/ebioscience
	PE-CD31	12-0311/ebioscience
	PE-CD45	12-0451/ebioscience
	PE-Ter119	12-5921/ebioscience

Table S2-2: Antibodies used for FACS, IHC and IF.

IV. Materials and Methods

Mouse strains. Mutant mice with prostate-specific deletion of *Pten* were generated as described previously under a mixed background (Wang 2003). The 129/C57 background CD166 knockout (*CD166*$^{-/-}$) was generously provided by the laboratory of Dr. Weiner of University of Iowa (Weiner 2004). *Pten*$^{L/L}$ mice on a 129/Balb/c background were first crossed to the *CD166* $^{-/-}$ mice to get F2 female *Pten*$^{L/L}$;*CD166*$^{-/-}$. *Pb-Cre*$^{+}$; *Pten*$^{L/L}$;*CD166*$^{-/-}$ mice were then generated by crossing female Cre^{-};*Pten*$^{L/L}$;*CD166*$^{-/-}$ with male *Pb-Cre*$^{+}$;*Pten*$^{L/L}$;*CD166*$^{+/-}$. All animal experiments were performed following Institutional Approval for Appropriate Care and use of Laboratory animals by the UCLA Institutional Animal Care and Use Committee (Chancellor's Animal Research Committee (ARC)), Animal Welfare assurance number A3196-01.

Tissue collection and FACS. The preparation of prostate epithelial cell suspensions from male mice were described previously (Mulholland 2011). Dissociated prostate cells were suspended in DMEM/10% FBS and stained with antibody for 15 min at 4 °C. Antibodies are listed in Table S2. FACS analysis was performed by using BD FACS Canto (BD Biosciences, San Jose, CA). Cell sorting was done by using BD FACS Vantage and the BD FACS Aria II.

***In Vitro* Prostate Sphere-Forming Assays.** Prostate spheres were cultured and passaged as described previously (Lukacs 2010, Xin 2007). FACS-isolated prostate cells or unsorted prostate cells were counted and suspended into a 100μL mixture of 1:1 Matrigel (BD Biosciences, San Jose, CA) and PrEGM (Lonza, Walkersville, MD). Samples were plated around the rims of wells in a 12-well plate and allowed to solidify at 37°C for 45 minutes, before 1 ml of PrEGM was

added. Sphere media was changed every three days. Spheres were counted after 8 days. To passage spheres, medium was aspirated off and matrigel was digested with 1mL Dispase solution (Invitrogen, Carlsbad, CA, 1 mg/ml, dissolved in PrEGM medium) for 30 minutes at 37°C. Spheres were collected, incubated in 1ml warm Trypsin/0.05% EDTA at 37°C for 5 minutes, passed through a 27-gauge syringe 5 times, and filtered through a 40 μm filter. Cells were counted by hemocytometer and replated.

RNA Isolation and qRT-PCR. Sorted cells were collected and spun down. RNAs from sorted cells were extracted using TRIzol® Reagent (Invitrogen, Carlsbad, CA). RNAs were reverse transcribed into cDNA with SuperScript III First-Strand Synthesis System for qRT-PCR (Invitrogen, Carlsbad, CA), and quantitative PCR was done in the iQ thermal cycler (Bio-Rad) using the iQSYBR Green Supermix (Bio-Rad) in triplicate. Primers used for study are Ck5 (F5′-ACCTTCGAAACACCAAGCAC-3′; R5′-TTGGCACACTGCTTCTTGAC-3′), Ck8 (F5′-ATCGAGATCACCACCTACCG-3′; R5′-TGAAGCCAGGGCTAGTGAGT-3′), p63 (F5'-CCCACAGACTGCAGCATTG-3'; R 5'-GAGATGAGGAGGTGAGGAGAAG-3'), AR (F5′-AACCAACCAGATTCCTTTGC-3′; R5'-ATTAGTGAAGGACCGCCAAC-3′), CD166 (F 5'-CCTAAGAGAGGAGCGGATTG-3'; R5'-CAGCCACTCCCAGAACAAAG-3'), Trop2 (F5'-AGACCAAAGCCTGCGCTGCG-3'; R 5'- AGCTGGGGTGCAGCTTGTAG-3'), Gadph (F5′-ACTGGCATGGCCTTCCG-3′; R5′-CAGGCGGCACGTCAGATC-3′), CD117 (F5-AGAAGCAGATCTCGGACAGC-3'; R5'- GACTTGGGTTTCTGCTCAGG-3'), CD133 (F5-ACCAACACCAAGAACAAGGC-3'; R5'-GGAGCTGACTTGAATTGAGG-3'), CD44 (F5-GTCAACCGTGATGGTACTCG-3'; R5'-AGTGCACAGTTGAGGCAATG-3'), *Nkx3.1* (F5'-TCCGTCTTTTGGCTCTGAGT-3'; R5'- GTGAAAGTGCACGCTGAAAA-3').

Immunofluorescence and immunohistochemistry analyses. Tissue analysis was carried out using standard techniques as described previously (Wang 2003). Sections (4μm) were stained with hematoxylin and eosin (H&E) or with specified antibodies (Table S2).

Western Blot analysis. Total protein was extracted with RIPA buffer (20 mM Tris-HCl, pH 7.5, 150 mM NaCl, 1 mM Na_2EDTA, 1 mM EGTA, 1% NP-40, 1% sodium deoxycholate) with fresh added phosphatase inhibitors (Sigma, St. Louis, MO) and protease inhibitors (Roche, Indianapolis, IN). Protein concentrations were determined by Bradford Assay kit (BioRad, Hercules, CA). Protein was separated by 4-15% gradient SDS/PAGE (BioRad, Hercules, CA) and transferred onto a PVDF membrane (Amersham Biosciences, Arlington Heights, IL). The membrane was blocked in 5% skim milk, and subsequently incubated with primary antibodies against CD166 and GADPH (Santa Cruz Biotechnology, Santa Cruz, CA), GFP (Abcam, Cambridge, MA), phospho-AKT Ser473 (Cell Signaling Technology, Beverly, MA) at 4°C overnight followed by incubation with peroxidase-conjugated goat anti-mouse IgG or goat anti-rabbit IgG (Jackson ImmunoResearch, Inc., West Grove, PA), and developed with Pierce ECL reagent (Thermal Scientific, Rockford, IL).

Human Prostate Cancer Tissue Microarray (TMA). TMA used to survey CD166 expression is composed of 112 patient samples. Written consent was obtained from the patient as well as ethics approval from University of British Columbia-British Columbia Cancer Agency Research Ethics Board (UBC BCCA REB), Vancouver, Canada. The 112 patient specimens were spotted in triplicate to create a tissue microarray with 336 cores as described previously in (Narita 2008). Scoring method was based on the intensity of the staining in each core on a 4-point scale from

none (0) to high (3). Mann-Whitney test was used to compare CD166 protein expression difference between different groups. p values <0.05 were considered significant.

Human Prostate Tissue Acquisition and Dissociation. Human prostate tissue was obtained via a research protocol that was approved by the Office for the Protection of Research Subjects at UCLA and the Greater Los Angeles VA Medical Center. Informed written consent was obtained on all participants where identifying information was included. A frozen section was prepared from an adjacent slice of prostate tissue in order to determine the location of tumor nodules. Tumor areas were encircled and dissected away from benign regions within the fresh tissue slice. Benign tissue specimens were placed on ice and brought immediately to the laboratory for mechanical and enzymatic digestion (Garraway 2010). Prostate tissue was minced into small fragments (1 mm^3) in RPMI-1640 medium supplemented with 10% FBS and went through through enzymatic digestion (12 h in 0.25% type I collagenase followed by TripLE (Invitrogen) for 5 min at 37 °C). Cell suspensions were passed through a 23-gauge needle and were filtered through 40-μm filters. Cells were plated overnight in PrEGM as described above for sphere formation assay or tissue regeneration assay.

Tissue regeneration assay. *In vivo* tissue experiments were performed in male NOD-SCID/IL2rγ null mice in accordance with protocol number 2007-189-11A, approved by the Animal Research Committee within the Office for the Protection of Research Subjects at UCLA. Cells of interest were collected from FACS sorting. $2x10^5$ viable cells were then mixed with $2x10^5$ rat urogenital sinus mesenchyme (rUGSM) and suspended in 100 μL with 50:50 matrigel:PREGM (Garraway 2008, Goldstein 2010, Goldstein 2011). Cell/Matrigel mixtures

were then injected subcutaneously into NOD-SCID/IL2rγ null mice. Animals were supplemented with a 12.5mg 90-day release testosterone pellet under the skin (Innovative Research of America, Sarasota, FL). Grafts were harvested 8-16 weeks later and subjected to further analysis.

V. References

Abou-Kheir WG, Hynes PG, Martin PL, Pierce R, Kelly K (2010). Characterizing the contribution of stem/progenitor cells to tumorigenesis in the Pten-/-TP53-/- prostate cancer model. Stem Cells, *28*: 2129-2140.

Burger PE, Gupta R, Xiong X, Ontiveros CS, Salm SN, et al. (2009). High aldehyde dehydrogenase activity: a novel functional marker of murine prostate stem/progenitor cells. Stem Cells, *27*: 2220-2228.

Carver BS, Chapinski C, Wongvipat J, Hieronymus H, Chen Y, et al. (2011). Reciprocal feedback regulation of PI3K and androgen receptor signaling in PTEN-deficient prostate cancer. Cancer Cell, *19*: 575-586.

Chao MP, Alizadeh AA, Tang C, Jan M, Weissman-Tsukamoto R, et al. (2011). Therapeutic antibody targeting of CD47 eliminates human acute lymphoblastic leukemia. Cancer Res, *71*: 1374-1384.

Choi N, Zhang B, Zhang L, Ittmann M, Xin L (2012). Adult Murine Prostate Basal and Luminal Cells Are Self-Sustained Lineages that Can Both Serve as Targets for Prostate Cancer Initiation. Cancer Cell, *21*: 253-265.

De Marzo AM, Nelson WG, Bieberich CJ, Yegnasubramanian S (2010). Prostate cancer: New answers prompt new questions regarding cell of origin. Nat Rev Urol, *7*: 650-652.

Garraway IP, Sun W, Tran CP, Perner S, Zhang B, et al. (2010). Human prostate sphere-forming cells represent a subset of basal epithelial cells capable of glandular regeneration in vivo. Prostate, *70*: 491-501.

Goldstein AS, Drake JM, Burnes DL, Finley DS, Zhang H, et al. (2011). Purification and direct transformation of epithelial progenitor cells from primary human prostate. Nat Protoc, *6*: 656-667.

Goldstein AS, Lawson DA, Cheng D, Sun W, Garraway IP, et al. (2008). Trop2 identifies a subpopulation of murine and human prostate basal cells with stem cell characteristics. Proc Natl Acad Sci, *105*: 20882-20887.

Goldstein AS, Stoyanova T, Witte ON (2010). Primitive origins of prostate cancer: in vivo evidence for prostate-regenerating cells and prostate cancer-initiating cells. Mol Oncol, *4*: 385-396.

Goldstein AS, Huang J, Guo C, Garraway IP, Witte ON (2010). Identification of a cell of origin for human prostate cancer. Science, *329*: 568-571.

Hart LS, El-Deiry WS (2008). Invincible, but not invisible: imaging approaches toward in vivo detection of cancer stem cells. J Clin Oncol, *26*: 2901-2910.

Ishigami S, Ueno S, Arigami T, Arima H, Uchikado Y, et al. (2011). Clinical implication of CD166 expression in gastric cancer. J Surg Oncol, *103*: 57-61.

Jemal A, Siegel R, Xu J, Ward E (2010). Cancer statistics, 2010. CA Cancer J Clin, *60*: 277-300.

Kahlert C, Weber H, Mogler C, Bergmann F, Schirmacher P, et al. (2009). Increased expression of ALCAM/CD166 in pancreatic cancer is an independent prognostic marker for poor survival and early tumour relapse. Br J Cancer, *101*: 457-464.

King JA, Tan F, Mbeunkui F, Chambers Z, Cantrell S, et al. (2010). Mechanisms of transcriptional regulation and prognostic significance of activated leukocyte cell adhesion molecule in cancer. Mol Cancer, *9*: 266.

Kristiansen G, Pilarsky C, Wissmann C, Kaiser S, Bruemmendorf T, et al. (2005). Expression profiling of microdissected matched prostate cancer samples reveals CD166/MEMD and CD24 as new prognostic markers for patient survival. J Pathol, *205*: 359-376.

Korsten H, Ziel-van der Made A, Ma X, van der Kwast T, Trapman J (2009). Accumulating progenitor cells in the luminal epithelial cell layer are candidate tumor initiating cells in a Pten knockout mouse prostate cancer model. PLoS One, *4*: e5662.

Kurita T, Medina RT, Mills AA, Cunha GR (2004). Role of p63 and basal cells in the prostate. Development, *131*: 4955-4964.

Lawson DA, Xin L, Lukacs RU, Cheng D, Witte ON (2007). Isolation and functional characterization of murine prostate stem cells. Proc Natl Acad Sci, *104*: 181-186.

Lawson DA, Zong Y, Memarzadeh S, Xin L, Huang J, et al. (2010). Basal epithelial stem cells are efficient targets for prostate cancer initiation. Proc Natl Acad Sci, *107*: 2610-2615.

Leong KG, Wang BE, Johnson L, Gao WQ (2008). Generation of a prostate from a single adult stem cell. Nature, *456*: 804-808.

Liao CP, Adisetiyo H, Liang M, Roy-Burman P (2010). Cancer-associated fibroblasts enhance the gland-forming capability of prostate cancer stem cells. Cancer Res, *70*: 7294-7303.

Liu C, Kelnar K, Liu B, Chen X, Calhoun-Davis T, et al. (2011). The microRNA miR-34a inhibits prostate cancer stem cells and metastasis by directly repressing CD44. Nat Med, *17*: 211-215.

Lu TL, Chang JL, Liang CC, You LR, Chen CM (2007). Tumor spectrum, tumor latency and tumor incidence of the Pten-deficient mice. PLoS One, *2*: e1237.

Lukacs RU, Goldstein AS, Lawson DA, Cheng D, Witte ON (2010). Isolation, cultivation and characterization of adult murine prostate stem cells. Nat Protoc, *5*: 702-713.

Lunter PC, van Kilsdonk JW, van Beek H, Cornelissen IM, Bergers M, et al. (2005). Activated leukocyte cell adhesion molecule (ALCAM/CD166/MEMD), a novel actor in invasive growth, controls matrix metalloproteinase activity. Cancer Res, *65*: 8801-8808.

Maitland NJ, Collins A (2005). A tumour stem cell hypothesis for the origins of prostate cancer. BJU Int, *96*: 1219-1223.

McMenamin ME, Soung P, Perera S, Kaplan I, Loda M, et al. (1999). Loss of PTEN expression in paraffin-embedded primary prostate cancer correlates with high Gleason score and advanced stage. Cancer Res, *59*: 4291-4296.

Mezzanzanica D, Fabbi M, Bagnoli M, Staurengo S, Losa M, et al. (2008). Subcellular localization of activated leukocyte cell adhesion molecule is a molecular predictor of survival in ovarian carcinoma patients. Clin Cancer Res, *14*: 1726-1733.

Moscatelli D, Wilson EL (2010). PINing down the origin of prostate cancer. Sci Transl Med, *2*: 43ps38.

Mulholland DJ, Tran LM, Li Y, Cai H, Morim A, et al. (2011). Cell autonomous role of PTEN in regulating castration-resistant prostate cancer growth. Cancer Cell, *19*: 792-804.

Mulholland DJ, Xin L, Morim A, Lawson D, Witte O, et al. (2009). Lin-Sca-1+CD49fhigh stem/progenitors are tumor-initiating cells in the Pten-null prostate cancer model. Cancer Res, *69*: 8555-8562.

Narita S, So A, Ettinger S, Hayashi N, Muramaki M, et al. (2008). GLI2 knockdown using an antisense oligonucleotide induces apoptosis and chemosensitizes cells to paclitaxel in androgen-independent prostate cancer. Clin Cancer Res, *14*: 5769-5777.

Ofori-Acquah SF, King JA (2008). Activated leukocyte cell adhesion molecule: a new paradox in cancer. Transl Res, *151*: 122-128.

Rajasekhar VK, Studer L, Gerald W, Socci ND, Scher HI (2011). Tumour-initiating stem-like cells in human prostate cancer exhibit increased NF-kappaB signalling. Nat Commun, *2*: 162.

Richardson GD, Robson CN, Lang SH, Neal DE, Maitland NJ, et al. (2004). CD133, a novel marker for human prostatic epithelial stem cells. J Cell Sci, *117*: 3539-3545.

Roth A, Drummond DC, Conrad F, Hayes ME, Kirpotin DB, et al. (2007). Anti-CD166 single chain antibody-mediated intracellular delivery of liposomal drugs to prostate cancer cells. Mol Cancer Ther, *6*: 2737-2746.

Sarker D, Reid AH, Yap TA, de Bono JS (2009). Targeting the PI3K/AKT pathway for the treatment of prostate cancer. Clin Cancer Res, *15*: 4799-4805.

Sato C, Matsuda T, Kitajima K (2002). Neuronal differentiation-dependent expression of the disialic acid epitope on CD166 and its involvement in neurite formation in Neuro2A cells. J Biol Chem, *277*: 45299-45305.

Sawhney M, Matta A, Macha MA, Kaur J, DattaGupta S, et al. (2009). Cytoplasmic accumulation of activated leukocyte cell adhesion molecule is a predictor of disease progression and reduced survival in oral cancer patients. Int J Cancer, *124*: 2098-2105.

Swart GW (2002). Activated leukocyte cell adhesion molecule (CD166/ALCAM): developmental and mechanistic aspects of cell clustering and cell migration. Eur J Cell Biol, *81*: 313-321.

Tang DG, Patrawala L, Calhoun T, Bhatia B, Choy G, et al. (2007). Prostate cancer stem/progenitor cells: identification, characterization, and implications. Mol Carcinog, *46*: 1-14.
Visvader JE (2011). Cells of origin in cancer. Nature, *469*: 314-322.

Taylor BS, Schultz N, Hieronymus H, Gopalan A, Xiao Y, et al. (2010). Integrative genomic profiling of human prostate cancer. Cancer Cell, *18*: 11-22.

Taylor RA, Toivanen R, Risbridger GP (2010). Stem cells in prostate cancer: treating the root of the problem. Endocr Relat Cancer, *17*: R273-285.

Tsujimura A, Koikawa Y, Salm S, Takao T, Coetzee S, et al. (2002). Proximal location of mouse prostate epithelial stem cells: a model of prostatic homeostasis. J Cell Biol, *157*: 1257-1265.

van Kempen LC, Nelissen JM, Degen WG, Torensma R, Weidle UH, et al. (2001). Molecular basis for the homophilic activated leukocyte cell adhesion molecule (ALCAM)-ALCAM interaction. J Biol Chem, *276*: 25783-25790.

van Kempen LC, van den Oord JJ, van Muijen GN, Weidle UH, Bloemers HP, et al. (2000). Activated leukocyte cell adhesion molecule/CD166, a marker of tumor progression in primary malignant melanoma of the skin. Am J Pathol, *156*: 769-774.

Wang ZA, Shen MM (2011). Revisiting the concept of cancer stem cells in prostate cancer. Oncogene, *30*: 1261-1271.

Wang XD, Wang BE, Soriano R, Zha J, Zhang Z, et al. (2007). Expression profiling of the mouse prostate after castration and hormone replacement: implication of H-cadherin in prostate tumorigenesis. Differentiation, *75*: 219-234.

Wang S, Gao J, Lei Q, Rozengurt N, Pritchard C, et al. (2003). Prostate-specific deletion of the murine Pten tumor suppressor gene leads to metastatic prostate cancer. Cancer Cell, *4*: 209-221.

Wang S, Garcia AJ, Wu M, Lawson DA, Witte ON, et al. (2006). Pten deletion leads to the expansion of a prostatic stem/progenitor cell subpopulation and tumor initiation. Proc Natl Acad Sci, *103*: 1480-1485.

Wang CH, Chiou SH, Chou CP, Chen YC, Huang YJ, et al. (2011). Photothermolysis of glioblastoma stem-like cells targeted by carbon nanotubes conjugated with CD133 monoclonal antibody. Nanomedicine, *7*: 69-79.

Wang X, Kruithof-de Julio M, Economides KD, Walker D, Yu H, et al. (2009). A luminal epithelial stem cell that is a cell of origin for prostate cancer. Nature, *461*: 495-500.

Weichert W, Knosel T, Bellach J, Dietel M, Kristiansen G (2004). ALCAM/CD166 is overexpressed in colorectal carcinoma and correlates with shortened patient survival. J Clin Pathol, *57*: 1160-1164.

Weiner JA, Koo SJ, Nicolas S, Fraboulet S, Pfaff SL, et al. (2004). Axon fasciculation defects and retinal dysplasias in mice lacking the immunoglobulin superfamily adhesion molecule BEN/ALCAM/SC1. Mol Cell Neurosci, *27*: 59-69.

Wiiger MT, Gehrken HB, Fodstad O, Maelandsmo GM, Andersson Y (2010). A novel human recombinant single-chain antibody targeting CD166/ALCAM inhibits cancer cell invasion in vitro and in vivo tumour growth. Cancer Immunol Immunother, *59*: 1665-1674.

Xin L, Lukacs RU, Lawson DA, Cheng D, Witte ON (2007). Self-renewal and multilineage differentiation in vitro from murine prostate stem cells. Stem Cells, *25*: 2760-2769.

Chapter 3:

Exploration of novel stem/progenitor markers in prostate and pancreas

I. Introduction

The cellular mechanisms underlying tumor heterogeneity are largely unknown and an area of intensive study. Since seminal work by John Dick and colleagues in leukemia, many recent reports have suggested that cells within a tumor population exhibit functional heterogeneity, with a small subpopulation seemingly responsible for driving tumor propagation and progression (Lapidot 1994, Visvader 2008). This 'cancer stem cell' (CSC) paradigm posits that tumors are organized in a hierarchy of cells, similar to that of stem cell biology, with CSCs positioned as self-renewing progenitors giving rise to all the remaining 'differentiated' tumor cells. CSCs have been described in a variety of blood and solid tumor malignancies (Mimeault 2007, Visvader 2008). As such, prospective identification and validation of cancer stem cell populations may lead to targeted therapeutic intervention to eliminate these cells, improving treatment outcomes (Frank 2010, Eppert 2011).

The gold-standard approach towards functional identification of these cancer stem cell populations are through limiting dilution xenotransplantation studies into immunocompromised mice (Lapidot 1994). Tumor subpopulations are dissociated to single cells, segregated based on cell surface marker expression, and transplanted into recipient mice to determine which tumor cells are capable of initiating secondary tumors. Identification of these markers has been largely informed by their expression in normal tissue development, most intensively studied in the hematopoetic lineage (Rector 2013). Cell surface markers found to specifically demarcate stem/progenitor cells in normal stem cell biology have been adapted and tested in the cancer field with some success (Mimeault 2007). It follows that specific isolation of stem cells in benign tissue is a logical first step to discover the identity of malignant cancer stem cells.

Prostate stem/progenitor cell hierarchy was introduced extensively in Chapter 2 of this document. The pancreas, however, is another endodermal organ comprised of uniquely different cell types. It has an exocrine compartment comprised of acinar cells, which produce enzymes important for digestion of food materials, as well as ductal cells that deliver this 'pancreatic juice' to the small intestine (Pan 2011). It also contains interspersed islet cells which are important for maintaining blood sugar homeostasis and regulating other endocrine functions (Pan 2011). The existence of resident tissue stem/progenitor cells in the pancreas is controversial (Habener 2004, Yalniz 2005). There have been several reports identifying cell populations with varying degrees of progenitor activity in murine fetal (Zhou 2007, Sugiyama 2007, Hori 2008, Desgraz 2009) and adult (Oshima 2007, Rovira 2010) tissues, as well as in the human system (Todorov 2005, Afrikanova 2012). Other notable papers indicate that tissue maintenance can occur through a process of de-differentiation (Zhou 2008, Xu 2008) or self-duplication (Dor 2004, Chen 2011), rather than hierarchical stem cell differentiation.

We set out to determine and further refine the identification of stem/progenitor cells within the prostate and pancreas systems. Our method will include both a discovery approach to identify novel markers based on association with stem/progenitor qualities, as well as a more targeted approach utilizing the Lgr5 gene. After testing the validity of novel progenitor populations in these tissues, we hope to leverage this information to inform identification of cancer stem cell populations after tissue transformation.

II. Results

a. Lgr5 does not mark a stem/progenitor cell in the pancreas and prostate

Lgr5 is a G-protein-coupled receptor which was first identified as a Wnt-target gene (van de Wetering 2002). It has been found to bind R-spondins to mediate Frizzled/Lrp receptor complex induction of Wnt3a and activation of the Wnt program (de Lau 2011). Lgr5 has been shown to demarcate stem cells in the gut, colon, and skin (Barker 2007, Jaks 2008), as well as serve as a cell-of-origin for intestinal cancers (Barker 2009). Given the fact that both the prostate and pancreas are of similar endodermal origin and the Wnt pathway has been implicated in their tissue homeostasis and tumorigenesis (Murtaugh 2008, Kharaishvili 2011), we set out to test the hypothesis that Lgr5+ cells may mark stem/progenitor cells in these tissues.

We utilized a previously described mouse model, wherein a GFP allele was knocked-in the Lgr5 locus (Barker 2007). As such, any mice with an Lgr5 heterozygous ($Lgr5^{+/Cre}$) genotype would have Lgr5+ cells fluoresce with GFP, amenable to visualization via FACS or microscopy.

We first checked basal Lgr5 expression in the adult prostate and pancreatic murine tissue. Gut was used as a control, which showed a clear GFP^{+} subpopulation (Fig 1A left). While no expression was observed in any pancreatic cells (Fig 1A middle), there was a clear minor population present in the prostate (Fig 1A right). This Lgr5 knock-in allele also had a tamoxifen-inducible Cre^{ERT2} element, allowing manipulation of genes floxed by the LoxP sequences in a Lgr5-specific and temporal regulated manner. We crossed $Lgr5^{+/Cre}$ mice with the *Rosa26-lacZ* reporter line, which allowed us to indelibly mark Lgr5+ cells with the LacZ gene. After 7 days of tamoxifen induction, $Lgr5^{+/Cre}$ $LacZ^{L/L}$ mice were sacrificed and organs were harvested for X-gal staining. Surprisingly, no $LacZ^{+}$ cells could be identified in the prostatic or pancreatic epithelium at this time point although LacZ+ cells were clearly present in the intestinal epithelium (Fig 1B).

To better characterize the observed prostatic Lgr5-GFP^{+} population, we performed additional FACS analysis. The $CD49^{hi}ScaI^{hi}$ (LSC+) profile has been shown to mark prostate

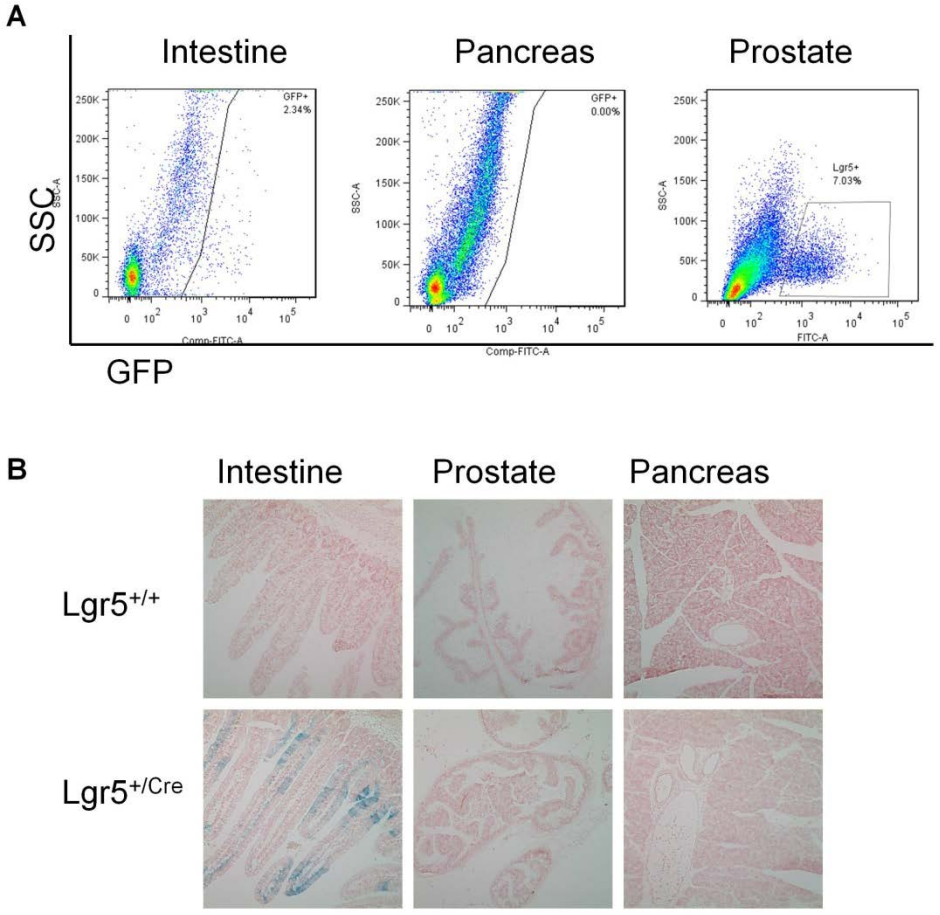

Figure 3-1: Lgr5 expression in pancreas and prostate. (A) FACS analysis of Lin$^-$;GFP+ cells from 10-week-old *Lgr5*$^{+/Cre}$ mice indicates an Lgr5+ population in the prostate but not pancreas. (B) Lineage tracing through whole mount X-gal staining after 7 days post-induction with 5mg dose of tamoxifen in *Lgr5*$^{+/Cre}$ *LacZ*$^{L/L}$ mice shows no epithelial Lgr5 expression in prostate or pancreas. Nuclear Fast Red was used as a counterstain and *Lgr5*$^{+/+}$*LacZ*$^{L/L}$ mice were used as staining controls.

.

basal stem/progenitor cells, while EpCAM^{hi}CD24^{hi} population can segregate total prostate epithelium from EpCAM^{lo}CD24^{lo} mesenchyme (Figure 2A, left panels)(Lawson 2007, Mulholland 2012). Gating on the Lgr5-GFP$^+$ population, we found that a majority of cells were found in the ScaI$^+$CD49f$^-$ and EpCAM^{lo}CD24^{lo} regions, indicating a probable stromal origin (Fig 2A). Furthermore, Lgr5 transcript levels from sorted EpCAM^{lo}CD24^{lo} mesenchymal-enriched cells were significantly higher than epithelial-enriched LSC+ and LSC- cells from the murine prostate (Fig 2B). This result was further confirmed by cytospinning FACS sorted Lgr5-GFP+

and Lgr5-GFP- prostate cells onto glass slides and staining with epithelial markers. CK5 and CK8, markers of prostate basal and luminal epithelium respectively, were significantly enriched in the Lgr5-GFP- fraction compared to Lgr5-GFP+, further supporting the notion that Lgr5+ cells are not epithelial in origin (Fig 2C).

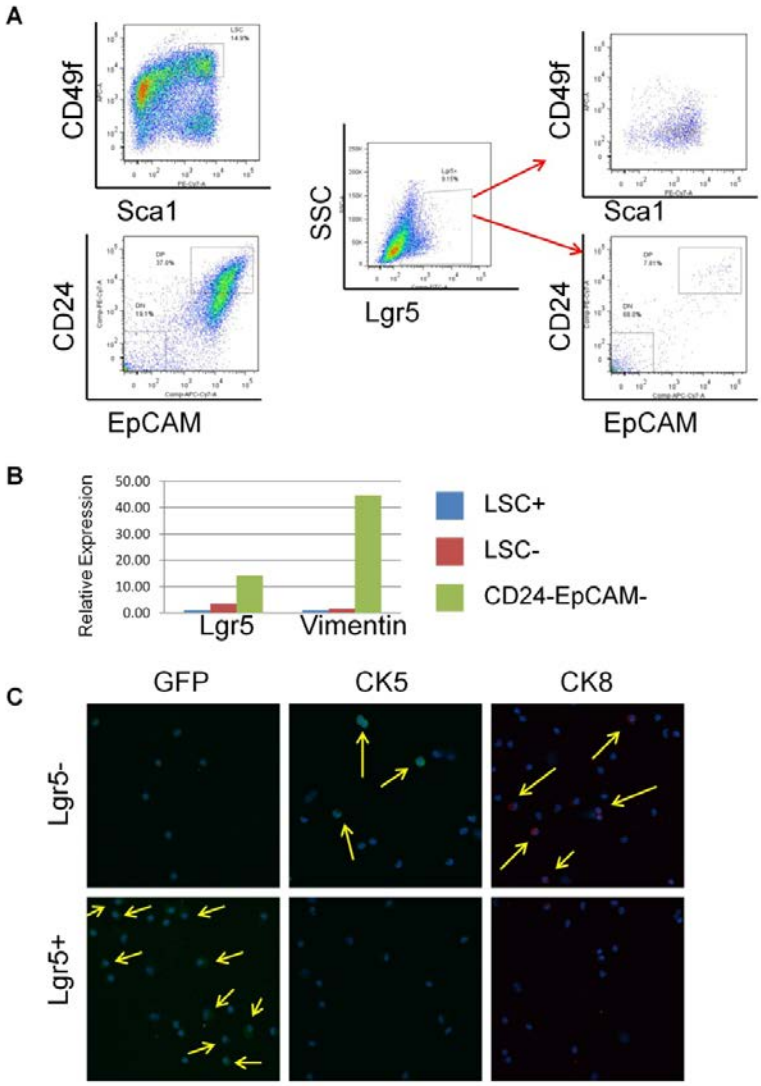

Figure 3-2: Lgr5 marks a mesenchymal population in the prostate. (A) Left: Representative FACS blots of prostate basal ($CD49f^{hi}Sca1^{hi}$), epithelial ($CD24^{hi}EpCAM^{hi}$), and mesenchymal ($CD24^{-}EpCAM^{-}$) cell types. Right: Backgating on Lin-;GFP+ cells in prostates of $Lgr5^{+/Cre}$ mice reveal most events reside in mesenchymal fraction. (B) $CD49f^{hi}Sca1^{hi}$, $CD49f^{hi}Sca1^{hi}$ and $CD24^{-}EpCAM^{-}$ populations were FACS sorted from prostate, RNA isolated and subjected to qPCR. RPL13a was used as loading control. (C) Lgr5+ and Lgr5- prostate cells from $Lgr5^{+/Cre}$ mice were FACS sorted, cytospun, and underwent immunofluorescent staining. DAPI was used to visualize nuclei. Arrows indicate positive stains.

Pancreatic epithelium typically have very little cellular turnover compared to rapidly regenerating gut and skin tissue (Kong 2011). However upon onset of pancreatitis, an inflammatory condition which results in massive cell death in pancreatic acini due to aberrant activation of digestive enzymes, there is induction of cell proliferation to repair the damage (Steer 1987). Activation of stem/progenitor activity through tissue trauma may allow easier visualization of Lgr5+ cell activity (Nygaard 2005, Xu 2008). We used two murine models of acute pancreatitis in attempt to mobilize pancreatic stem/progenitors: 1) Caerulein is a small molecule which is known to mimic acinar atrophy at high doses; 2) Ligating the pancreatic duct with surgical sutures to induce physical trauma. In both models, Lgr5+ cells were still not observed after either treatment (Fig 3A).

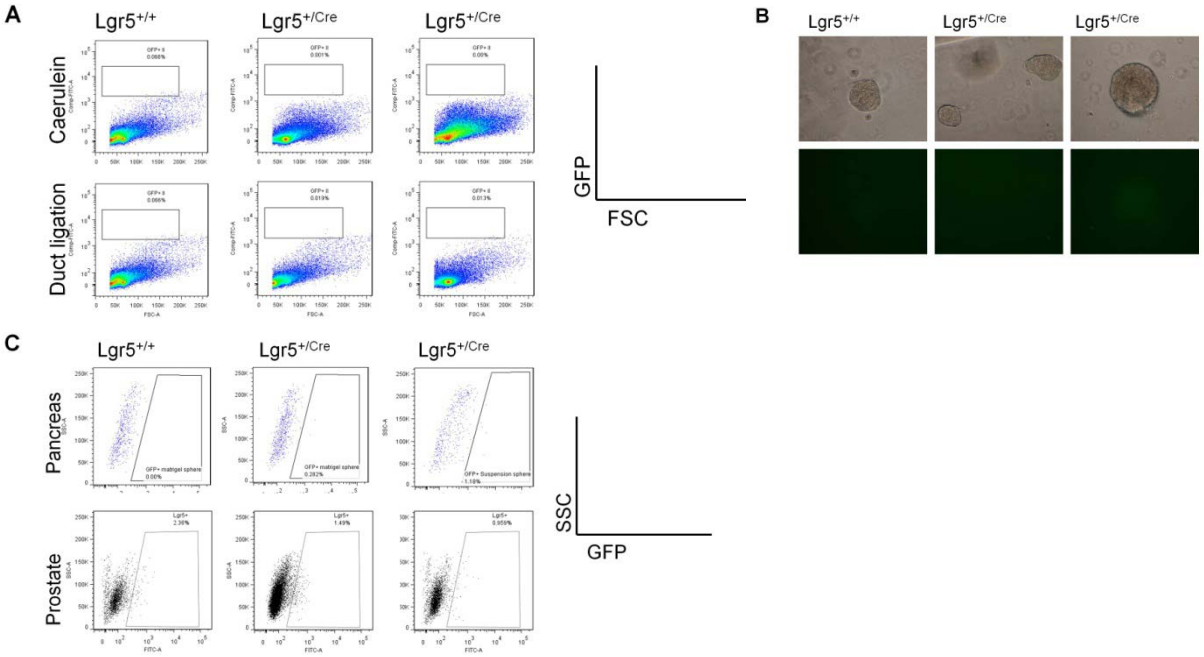

Figure 3-3: Tissue injury and *in vitro* sphere culture do not produce Lgr5+ cells. (A) *Lgr5*$^{+/Cre}$ mice were injured either with a 2-day course of 250μg/kg doses of caerulein (Top) or a 7-day latency after pancreatic duct ligation (Bottom). Lin-;GFP+ cells were analyzed with FACS. *Lgr5*$^{+/+}$ mice were used as a control, and 2 representative *Lgr5*$^{+/Cre}$ pancreata are shown. (B) Bright Field and fluorescence images of prostate spheres from *Lgr5*$^{+/+}$ and *Lgr5*$^{+/Cre}$ mice cultured for 7 days. (C) Spheres grown from *Lgr5*$^{+/Cre}$ prostate and pancreas were dissociated and FACS analysis for GFP showed no positive cells.

Both pancreatic and prostate cells can be cultured *in vitro* in special conditions known as sphere culture which selects for stem/progenitor cells (Seaberg 2004, Lawson 2007). We therefore cultured pancreas and prostate cells in the sphere forming media to test whether *in vitro* stem cell enrichment would allow us to identify Lgr5+ cells. However, no Lgr5-GFP^{+} cells could be detected by either FACS or microscopy above background levels (Fig 3B-3C).

As a final effort, we checked to see if Lgr5 is expressed during fetal pancreas and prostate development. Pregnant females were injected with tamoxifen from E8.5-E14.5, and sacrificed two days after injection. Individual pups were genotyped for Lgr5 and Y-chromosome (sex determination) and prepared for whole-mount X-gal staining. While robust LacZ expression was observed on the skin and various tissues in *Lgr5*$^{+/Cre}$*LacZ*$^{L/L}$ pups (Fig 4A), no pronounced LacZ staining compared to Lgr5$^{+/+}$ control samples was detected in the urogenital sinus or the embryonic pancreas (Fig 4B).

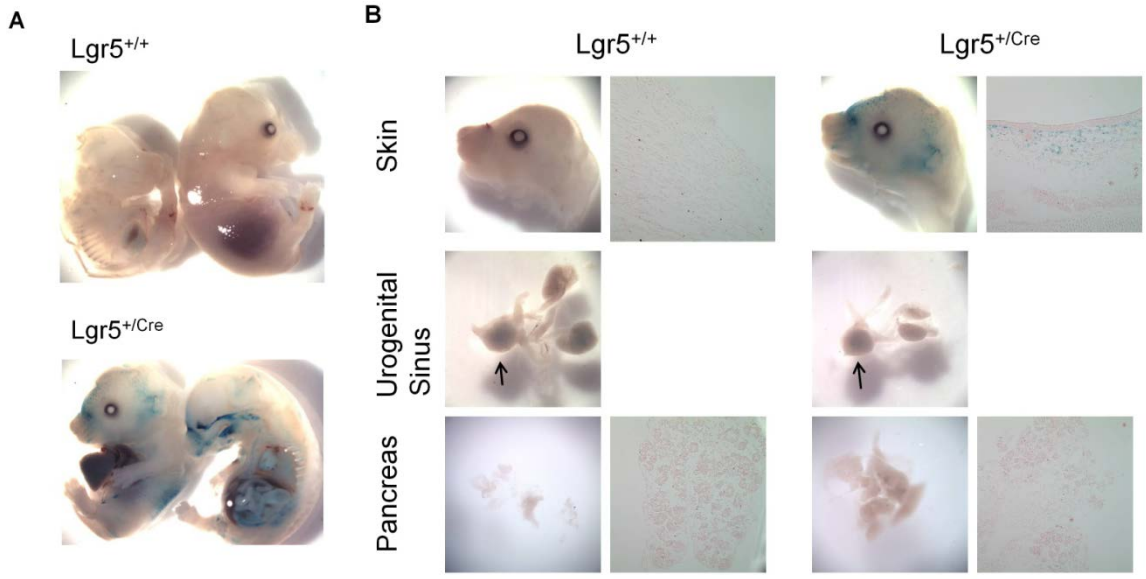

Figure 3-4: Lgr5 is not expressed in fetal pancreas or prostate epithelium. *LacZ*$^{L/L}$ females were bred with *Lgr5*$^{+/Cre}$ males. 4-5mg of tamoxifen were injected i.p. at E8.5, E10.5, E12.5, and E14.5 time points, with embryos harvested at day E16.5. Representative whole mount X-gal staining is shown on *Lgr5*$^{+/+}$ and *Lgr5*$^{+/Cre}$ embryos. (B) Zoomed gross images and tissue sections of the head, pancreas, and urogenital sinus are shown (Arrow points to UGS).

To determine if Lgr5 has a role in oncogenic transformation, *Lgr5*$^{+/Cre}$ mice were bred with previously described *Pten*$^{L/L}$ and *Kras*$^{L/+}$ allele-bearing mice (Hill 2010, Mulholland 2012). Tamoxifen administration would induce deletion of PTEN tumor suppressor and activation of oncogenic K-ras specifically in Lgr5+ cells. *Lgr5*$^{+/Cre}$*Pten*$^{L/L}$ and *Lgr5*$^{+/Cre}$*Pten*$^{L/L}$*Kras*$^{L/+}$ mice were given a bolus dose of tamoxifen and monitored for 6 months and 6 weeks, respectively. No

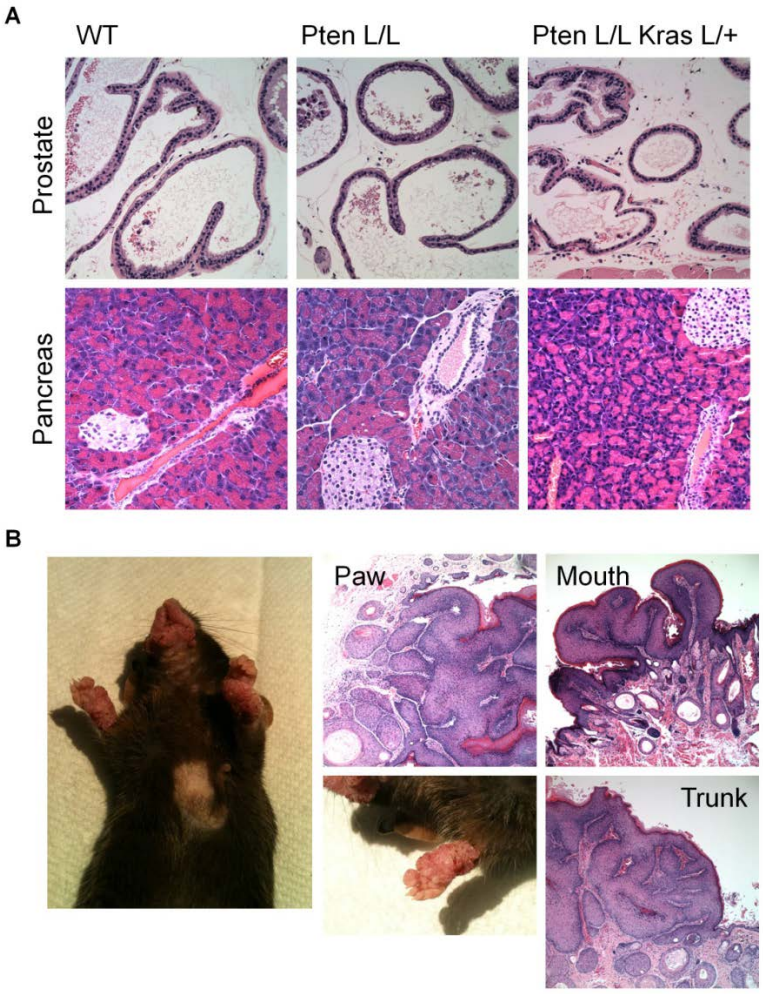

Figure 3-5: PTEN deletion and KRAS activation in Lgr5+ cells cause skin lesions, but do not induce tumor formation in the pancreas or prostate. (A) *Lgr5*$^{+/Cre}$ mice were bred with *Pten*$^{L/L}$ and *Kras*$^{L/+}$ to generate appropriate genotypes. 10-12 week old mice were then injected with 5mg of tamoxifen to induce Cre recombination in Lgr5 cells. HE of pancreas and prostate sections are shown after 6 months (*Lgr5*$^{+/Cre}$*Pten*$^{L/L}$) or 6 weeks (*Lgr5*$^{+/Cre}$*Pten*$^{L/L}$*Kras*$^{L/+}$) of tamoxifen injection. (B) Skin lesions developed on *Lgr5*$^{+/Cre}$*Pten*$^{L/L}$*Kras*$^{L/+}$ mice after six weeks post-tamoxifen on the trunk, paw, and mouth. Gross pictures and HE sections of select tumors are shown.

clear pathological phenotype was observed in either prostate or pancreas with Lgr5-CreER-mediated Pten deletion or Pten deletion and Kras activation, indicating Lgr5+ cells do not serve as a cell-of-origin for these cancer types (Fig 5A). Although no obvious skin abnormality was observed in $Lgr5^{+/Cre}Pten^{L/L}$ mice six months post Cre-mediated Pten deletion, large papilloma lesions developed rapidly in the skin of $Lgr5^{+/Cre}Pten^{L/L}Kras^{L/+}$ mice, suggesting that co-activation of the PI3K and RAS/MAPK pathway is essential for this phenotype development in Lgr5+ skin progenitor cells. The severe lesions are present in the face, paws, and trunk, which required euthanasia according to institutional protocol, precluding longer examination of this model (Fig 5B). Three pathologists from two institutions have determined these skin lesions to be benign hair follicular tumors called trichoadenomas, with extensive verrucous lesions, cysts, and parakeratosis (Shimanovich 2010).

b. Unbiased pursuit and analysis of murine pancreatic stem/progenitors

As mentioned previously, pancreatic progenitor function can be studied *in vitro* utilizing a cell culture system which promotes formation of spherical clusters of cells growing in suspension (Seaberg 2004). As a first step to identify adult tissue stem/progenitor cells, we dissociated murine pancreata to single cells, cultivated them as spheres, and passaged them *in vitro* for multiple generations to show sphere cells possessed self-renewal capacity (Fig 6A). Immunofluorescent staining of spheres revealed the presence of all three major pancreatic cell lineages, confirming the multipotent potential of sphere-forming cells (Fig 6B). Reassured that sphere cells were enriched for progenitor activity, we performed FACS analysis on a variety of cell surface markers associated with stem cells in the pancreas and other systems. Several cell surface markers were identified to be significantly upregulated in sphere cells compared to total

primary pancreatic cells (Fig 6C).

As a secondary assay to validate stem cell association with certain cell surface markers, the caerulein-induced acute pancreatitis mouse model was utilized. As previously discussed, acute pancreatic injury can induce high rates of proliferation and mobilization of stem cell function to repair and replace damaged tissue. Pancreata from mice treated with caerulein were

A

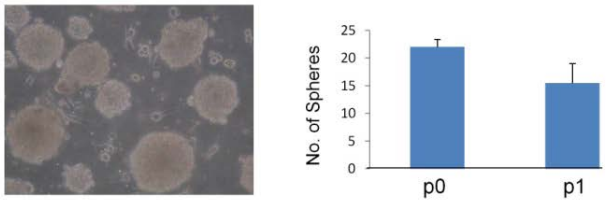

B

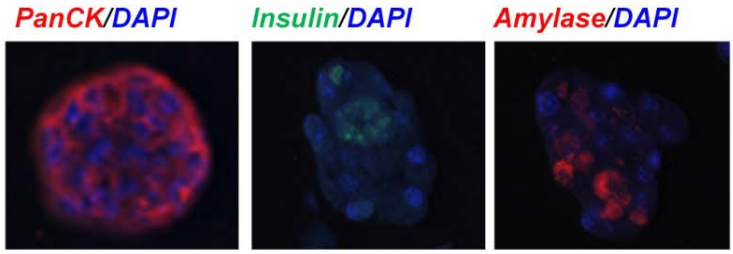

C

	WT Pancreas	Sphere Cells
CD24	84%	67%
CD44	5%	18%
CD133	7%	31%
CD49f	25%	18%
CXCR4	7%	2%
ALCAM	25%	40%
c-Kit	0.30%	0.50%
CD138	1.80%	52%
EpCAM	32%	5%
DBA	9%	21%

Figure 3-6: Pancreatic sphere cells exhibit stem cell properties and have a unique cell surface expression pattern. (A) Dissociated murine pancreatic cells grow into spherical colonies in suspension after 7 days. Graph shows quantification of sphere-forming units after seeding of 1,000 cells in a 96-well low attachment plate for the first and second passage. Data shown as mean +/− STD. (B) Immunofluorescent staining of intact spheres show regional expression of all three pancreatic lineages. DAPI is used to visualize nuclei. (C) FACS analysis tabulating average expression of cell surface markers in total viable cells isolated from the wild type pancreas and their derived sphere cells.

compared to placebo-treated mice for changes in cell populations via FACS analysis. Reassuringly, many cell-surface markers were enriched in the treatment group (Table 3-1), similarly to our observation in sphere culture conditions.

A

	PBS	Caerulein	Fold-Change
CD24	73.4	71.5	0.97
CD44	6.7	87.1	13.0
CD133	10.1	19.3	1.91
CD151	37.1	32.5	0.88
CD49f	42.3	42.4	1.0
CXCR4	7.8	20.8	2.65
ALCAM	25.8	27.7	1.07
c-Kit	1.5	29.3	19.52
CD138	0.8	2.2	2.79
EpCAM	29.4	23.1	0.79
DBA	4.8	10.3	2.17
PDGFRβ	6	9.4	1.57

Table 3-1: Cell-surface marker changes associated with induction of acute pancreatitis. (A) Mice were treated with caerulein for two consecutive days with 250μg/kg dose i.p. injections or control PBS injections (n=3). Pancreata were dissociated and FACS analysis of average cell-surface marker expression is represented (Fold-Change was calculated as Caerulein% / PBS%).

To functionally test the multipotent potential of select pancreatic subpopulations and validate stem cell identity, we sought to develop an *in vivo* assay of pancreatic regeneration. To this end, wWe first transplanted cells dissociated from fetal pancreas into the subcutaneous flank of NOD-SCID immunocompromised mice. After 8 weeks, implants were harvested and assayed for pancreatic regeneration. Strikingly, all pancreatic cell types could be regenerated from this fetal source and comfirmed with immunohistochemical analysis (Fig 7A). Encouraged by this result, we next attempted tissue regeneration utilizing adult pancreatic cells. To increase chances of success, total adult pancreatic cells were mixed with fetal pancreatic cells prior to

transplantation, which we reasoned can provide a supportive and inductive microenvironment. Adult cells were obtained from a global dsRED knock-in mouse (Vintersten 2004), which meant that any pancreatic outgrowths derived from adult, and not fetal cells, would be dsRED labeled. Despite repeated attempts, we could never detect any dsRED+ signal for adult pancreatic regenerated structures, even with robust expression in parental adult pancreatic tissue (Fig 7B).

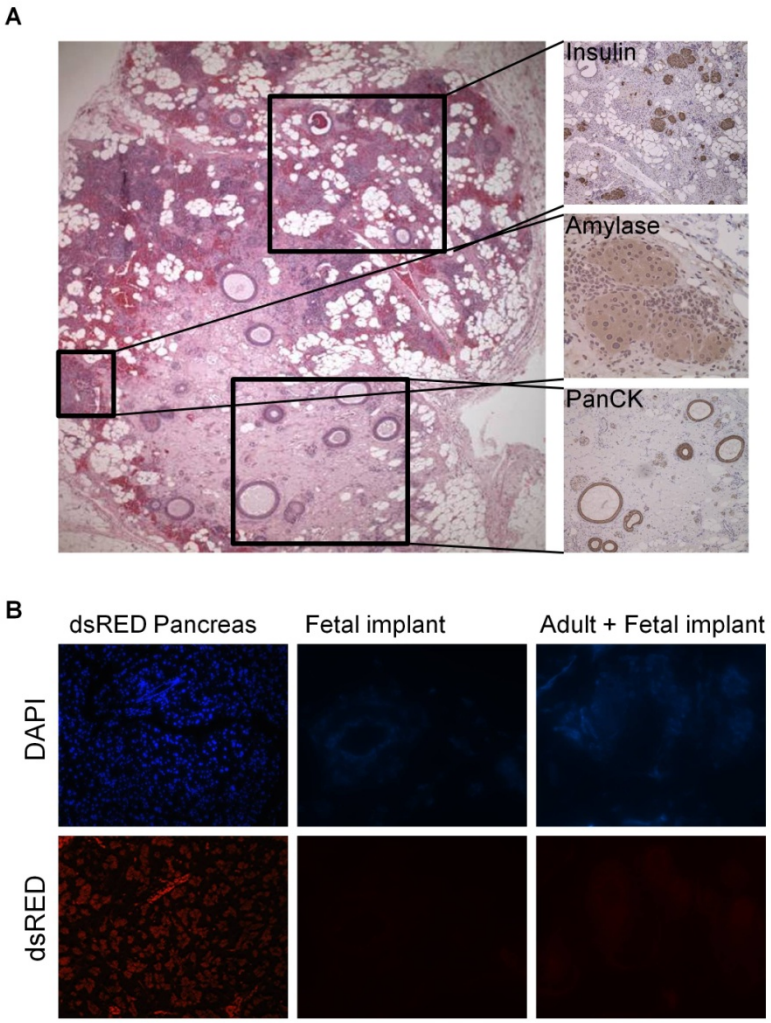

Figure 3-7: Fetal but not adult pancreatic tissue regeneration *in vivo*. (A) E12.5-E14.5 pancreatic rudiment was isolated, dissociated, and $1x10^6$ cells implanted into recipient NSG mice. Left: H&E section of a representative subcutaneous growth. Right: Immunohistochemical confirmation of three pancreatic cell lineages. (B) $1x10^6$ fetal pancreatic cells were mixed with $1x10^6$ adult dsRED pancreatic cells and implanted into NSG mice. Immunofluorescent staining showed no dsRED+ structures. Adult dsRED pancreas was used as a positive control, fetal only implants were used as a negative control, and DAPI was used to visualize nuclei.

c. Cell surface marker adaptation for identification of putative cancer stem cells

We next checked whether these identified cell surface molecules with associated stem/progenitor characteristics are also expressed on pancreatic tumors. Our lab had previously generated a novel mouse model of pancreatic cancer which closely resembles the human disease (Hill 2011). Gene expression microarray was performed on pancreatic tumors and compared to wild type cohorts. Many cell surface molecules were found to be overexpressed, including several novel markers as well as those previously associated with stem/progenitor function such as CD44 and CD133 (Supp Table S1). A panel of these hits was validated on the protein level via FACS analysis and immunohistochemistry (Fig 8).

To ensure these cell-surface markers are relavant to human PDAC, FACS analysis was performed on a panel of human pancreatic cancer xenografts. Briefly, patient tumor tissue was obtained in collaboration with the UCLA Department of Surgery and passaged in NOD-

A

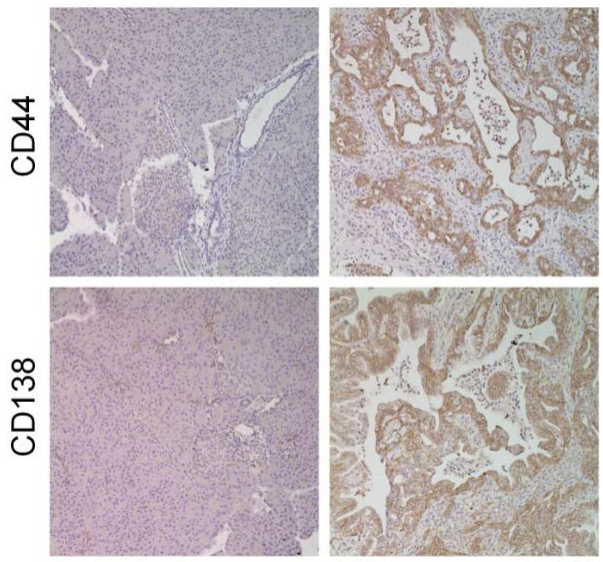

B

	WT	Pten L/L; Kras+
CD44	4.9	57.5
CD24	62.8	58.3
CD138	0.1	2.7
CD49f	58.2	16.8
CD151	72.8	44.0
CD133	7.6	13.6
CXCR4	0.4	6.2
C-Kit	0.3	20.6
CD326	30.7	45.5
DBA	36.6	75.9
CD324	9.7	12.5
ALCAM	18.7	28.9

Figure 3-8: Select markers upregulated in pancreatic cancer cells. (A) Immunohistochemical staining of Pdx1-Cre- and Pdx1-Cre+ *Pten*$^{L/L}$*Kras*$^{L/+}$ pancreatic tissue sections with CD44 and CD138 antibodies. (B) FACS analysis of select cell-surface markers in *Pdx1-Cre- and Pdx1-Cre+Pten*$^{L/L}$*Kras*$^{L/+}$ pancreas tissue.

SCID IL2γ knock-out (NSG) immunocompromised mice. We confirmed expression of many of the cell-surface markers identified in the murine model in these human samples (data not shown).

Among this array of confirmed stem cell enriched and cancer associated markers, CD138 seemed to be a good candidate as it is expressed at low levels in the normal pancreas, upregulated in tumors, and significantly overexpressed in sphere culture and inducted upon injury. CD138 is a member of the syndecan family of cell surface heparain-sulfate proteoglycans, which has been shown to bind extracellular matrix proteins to mediate a variety of biological processes including cell adhesion, migration, and proliferation (Woods 2001). CD138 has also been shown to be upregulated in pancreatic cancer and have prognostic value (Conejo 2000, Juuti 2005). To functionally determine whether CD138 demarcates a cancer stem

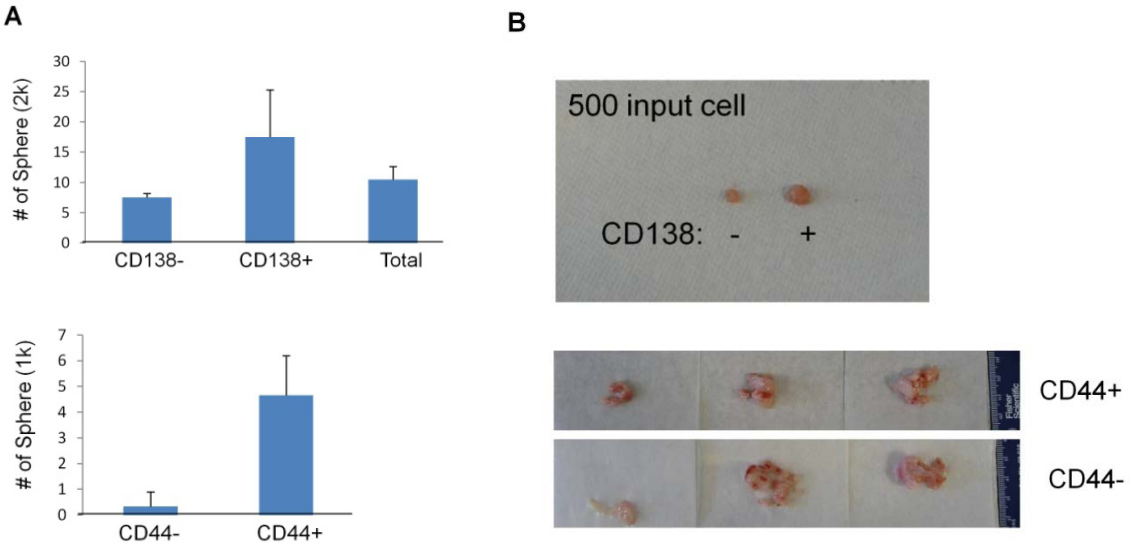

Figure 3-9: Cancer stem cell properties of pancreatic tumor subpopulations. (A) Human tumor xenografts were FACS sorted into positive and negative populations for CD138 and CD44 and then cultured *in vitro* as spheres. Graph shows quantification of sphere-forming units after seeding of 1-2,000 cells in a 96-well low attachment plate. Data shown as mean +/− STD. (B) Tumor subpopulations were FACS sorted into marker positive and negative fractions, transplanted at various doses into recipient NSG mice, and allowed to grow for 4-6 months. Examples using CD138 and CD44 are shown.

cell population, human pancreatic xenografts were FACS sorted for CD138+ and CD138- populations and seeded into *in vitro* sphere cultures, where CD138+ cells trended towards enhanced sphere-forming activity, although not statistically significant (Fig 9A). Similar validation experiments were performed with CD44, a known PDAC CSC marker (Fig 9A). However, preliminary limiting dilution xenotranplantation assays didn't segregate tumor-initiating potential by CD138 or CD44 expression, as both positive and negative cell fractions could initiate transplantable tumors at low cell doses (Fig 9B).

Given the fact that secondary tumors had arisen at such low cell dose numbers, we went on to ask what the tumor-initiating capability of total tumor epithelium was independent of positive marker selection. To that end, we identified a way of isolating and separating stromal cells from tumor cells. PDGFRβ is a receptor tyrosine kinase (Heldin 1990) highly expressed in neonatal pancreatic mesenchyme (Hori 2008). We found that in all our human PDAC tumor samples, PDGFRβ is expressed specifically in stromal cells, overlapping with the pattern of SMA expression (Fig 10A). To confirm that PDGFRβ demarcates stroma, we sorted PDGFRβ+ and PDGFRβ- cells from our xenografts and tested the expression levels of epithelial and mesenchymal associated genes. Reassuringly, PDGFRβ- cells express high levels of epithelial markers CK19 and EpCAM, as compared to PDGFRβ+ cells, which express high levels of mesenchymal marker Vimentin (Fig 10B).

In an attempt to understand the cell-autonomous behavior of these tumor xenografts, we isolated stroma-enriched PDGFRβ+ and epithelium-enriched PDGFRβ- cells and performed limiting-dilution transplantation experiments. As expected, the majority of tumor-initiating ability resides in the PDGFRβ- epithelial population (Fig 10C). Strikingly, 100 PDGFRβ- epithelial cells are sufficient for initiating transplantable tumors. This tumor-initiation potential

is comparable to the activity of positively selected CSC population transplants previously reported (Li 2007, Herman 2007, Li 2011). Tumors developed from high doses of PDGFRβ+ cell implantation are most likely due to contaminated epithelial cells from FACS sorting, as evidenced by near identical tumor histology (Fig 10D).

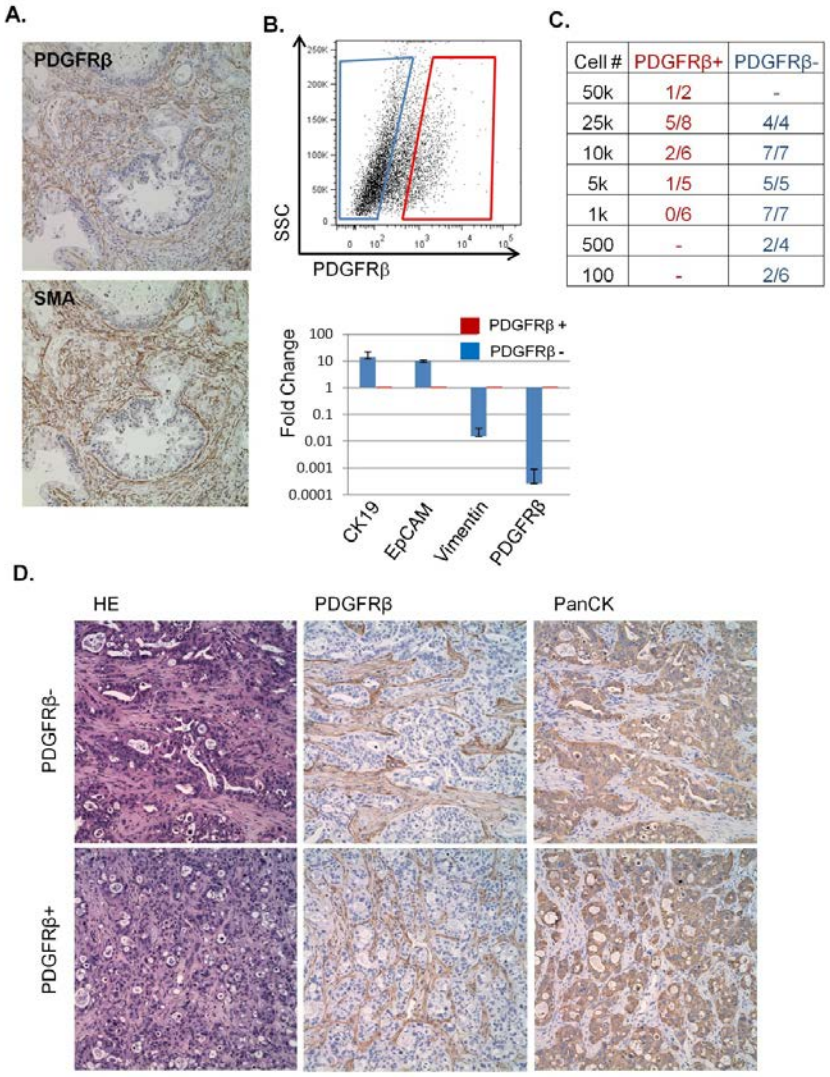

Figure 3-10: PDGFRβ marks cancer-associated fibroblasts and PDGFRβ- tumor cells have high tumor-initiating ability. (A) IHC on consecutive sections of a human tumor shows PDGFRβ staining to almost completely overlap with SMA+ stroma. (B) A human tumor xenograft was FACS sorted into PDGFRβ+ and PDGFRβ- cell populations. RNA was isolated, reverse transcribed into cDNA, and quantitative PCR performed with select genes. (C) Limiting Dilution transplantation was performed utilizing 4 independent human xenografts using PDGFRβ to segregate tumor subpopulations. Positive secondary tumors were scored with palpable masses after 4-6 months. (D) IHC on secondary tumors formed from PDGFRβ+ and PDGFRβ- cell fractions show very similar epithelial morphology.

III. Discussion

The expression of Lgr5 in prostate stroma is an interesting finding. The Wnt family of proteins is known to be expressed during murine prostate gland development, essential for bud outgrowth, duct formation and branching (Huang 2009). Stromal secreted factors have been well documented contributors to prostate cancer pathogenesis (Taylor 2008, Franco 2012). Moreover, the Wnt/β-catenin pathway can be activated in prostatic epithelium stemming from increased paracrine Wnt ligand production from the stroma, resulting in prostatic intraepithelial neoplasia lesions and tumor progression (Li 2008, Zong 2012). Given the fact that Lgr5 is a surface receptor which can mediate Wnt signaling, it will be interesting to determine what autocrine effects Wnt secretion will have on Lgr5+ stromal cells. Furthermore, due to the well-documented heterogeneity in prostate cancer stroma (Wu 2003, Kiskowski 2011, Sun 2012), interrogating the role of Lgr5+ stromal cells in mediating stroma-epithelial interactions leading to prostate cancer formation may reveal an interesting new therapeutic target.

Definitive determination of multipotent stem cells in the adult pancreas remains elusive. While restricted progenitor activity has been shown in some contexts, no single cell population has been shown to functionally derive differentiation of all three pancreatic lineages *in vivo* (Ku 2008). In our study, we identified several potential cell surface markers associated with stem/progenitor activities; however, formal functional characterization of these cell populations was not achieved due to assay system inadequacies. Perhaps with a better understanding of pancreatic developmental biology and improvements in biotechnology assay systems, this cell type may eventually be discovered. In fact, there is a large effort currently underway to understand the stem cell biology of the pancreas, with the goal of directing reprogramming and differentiation to a β cell fate as a therapeutic treatment for diabetes (Dominguez-Bendala 2012).

Alternatively, it may be the case that stem cells have not yet been formally identified because they do not exist in the pancreas, and tissue maintenance occurs through a program of de-differentiation or symmetric division (Dor 2004, Zhou 2008).

This naturally leads to the idea that a stem/progenitor hierarchy may not be as relevant in the context of pancreatic cancer as well. We observe many cell surface markers upregulated in our murine pancreatic tumor cells compared to wild type controls both on the RNA and protein levels. Moreover, many of these proteins are upregulated in sphere culture as well as activated upon pancreatic injury. However, observations in the human pancreatic xenografts revealed a striking heterogeneity of marker expression across tumor lines as well as in tumor sphere cultures of 5 independent xenografts (Supp Fig 1). Furthermore, we had initially hoped that a cell surface marker would emerge as unique in its expression pattern to merit consideration as a putative cancer stem cell. However, it seemed clear that any number of cell-surface markers identified in our screen could be rationally associated with 'stem/progenitor' characteristics in some fashion (Fig 6, 7, 10, data not shown). Previous studies linked the expression of CD133, CD44, CD24 and others as specific markers of pancreatic cancer stem cells (Li 2007, Herman 2007, Li 2011). However, these reports chose these specific markers in a biased manner based on their characterization as markers in other systems such as glioblastoma and breast cancer (Singh 2003, Al-Hajj 2003). It may be that utilization of any tumor-specific marker can enrich for tumor-initiating ability, as positive selection with such a marker would purify tumor cells from contaminating microenvironment cells such as fibroblasts and lymphocytes.

To further support this notion, we found that pure tumor cells which were specifically depleted of cancer-associated fibroblasts and immune cells had tumor-initiating potential comparable to the best known cancer stem cell populations (Fig 10C). Additionally, although

some differences in sphere forming activity were seen utilizing CD138, preliminary xenotransplantation assays did not segregate tumor-initiating ability. The fact that CD138- tumor cells still had the ability to form tumors indicates that marker phenotypic heterogeneity does not necessarily correlate with functional outcomes. It is important to note that these studies were preliminary and more exhaustive experimentation with more tumor samples are needed to draw firm conclusions. Nevertheless, it is unclear whether CD138 or any of the other cell-surface markers we have studied could specifically enrich for a cancer stem cell, or whether these markers simply enriched for total tumor cells. This raises the possibility that optimizing PDAC xenotransplantation procedures may reveal that a larger proportion of PDAC tumor cells have tumor-initiating ability than currently appreciated, similar to that observed in other systems (Quintana 2008).

A.

Gene	Fold Change	P-value
Tnfrsf12a	24.28	0.00202
Sdc1	10.89	0.00561
Ceacam1	7.18	0.00216
Cdh13	7.14	0.00434
Amot	6.61	0.03613
Plaur	6.57	0.00732
Igsf5	5.59	0.00718
Cd44	5.53	0.00148
Alcam	3.64	0.00701
Ece1	3.62	0.01337
Clec7a	3.59	0.03687
Sdc4	3.47	0.00007
Atpif1	3.39	0.00231
Fcgr2b	3.24	0.03169
Fcer1g	2.88	0.03382
Gpr126	2.86	0.03635
Agrn: agrin	2.52	0.04223
Ly6a	2.49	0.00157
Cd24a	2.10	0.00152

Supp Table S1: Genes found to be upregulated in murine pancreatic cancer model expression microarray. RNA was isolated from age-matched *WT* and *Pdx1-Cre+Pten*$^{L/+}$*Kras*$^{L/+}$ mouse pancreata (n=4) and submitted for global microarray analysis. Top hits found to be upregulated in *Pdx1-Cre+Pten*$^{L/+}$*Kras*$^{L/+}$ mice from Gene Ontology 'Cell-Surface' category is shown.

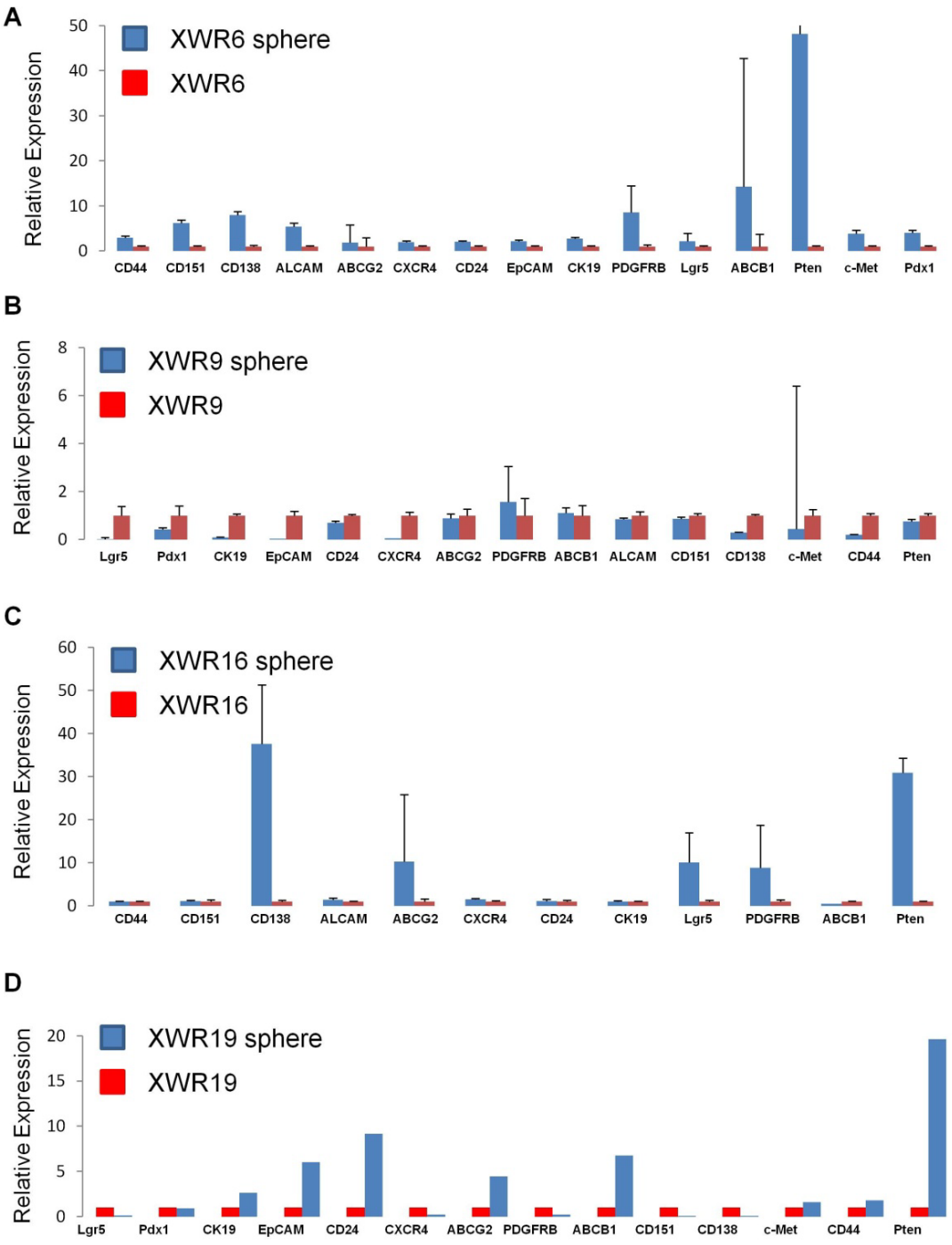

Supp Fig-1: Relative Expression of surface markers comparing total tumor cells and tumor spheres. (A-D) 4 different human xenografts were dissociated to single cells. Some cells were kept for RNA isolation. The remaining cells were used to grow spheres *in vitro*. After 7-10 days, RNA was isolated from sphere cells. cDNA was generated for quantitative PCR analysis for a panel of genes. PCR was run in duplicate or triplicate, and data for each graph is normalized to total cells for each xenograft.

IV. Materials and Methods

Mouse strains. Mice with IRES-Cre^{ERT2} and eGFP insertion at the Lgr5 promoter on the C57BL/6 background were generated as described previously (Barker 2007). These *Lgr5*$^{+/Cre}$ mice were bred with *Rosa26-LacZ* mice on a mixed background to generate *Lgr5*$^{+/Cre}$*LacZ*$^{L/L}$ mice. *Pten*$^{L/L}$ and *Kras*$^{L/+}$ mice were also bred to *Lgr5*$^{+/Cre}$ mice to generate *Lgr5*$^{+/Cre}$*Pten*$^{L/L}$ and *Lgr5*$^{+/Cre}$*Pten*$^{L/L}$*Kras*$^{L/+}$ mice. Murine pancreatic tumors were generated using the *Pdx1-Cre* mouse bred with *Pten*$^{L/L}$ and *Kras*$^{L/+}$ alleles as previously described (Hill 2010). All animal experiments were performed following Institutional Approval for Appropriate Care and use of Laboratory animals by the UCLA Institutional Animal Care and Use Committee (Chancellor's Animal Research Committee).

Isolation and engraftment of primary PDAC. Human pancreatic ductal adenocarcinoma tissue was obtained via a research protocol that was approved by the UCLA Institutional Review Board. Informed written consent was obtained by all participants. A piece of cancer tissue was dissected away from the total surgically resected specimen following pancreatectomy. PDAC tissue specimens were brought immediately to the laboratory and minced into small fragments (1 mm^3) with razor blades in PBS, dipped into a 1:1 mix of Matrigel (Becton Dickinson) and DMEM:F12 (Invitrogen), and surgically implanted into the subcutaneous flanks of recipient NOD:SCID IL2γ knock-out (NSG) mice.

Single cell dissociation. Tissues were harvested and minced into small pieces, washed with PBS, then went through enzymatic digestion at 37 °C with constant agitation: 1) murine prostate – 2

hrs in 1mg/mL Type I collagenase (Invitrogen); 2) murine pancreas – 20-30 min in 1mg/mL Type IV collagenase (Invitrogen); 3) pancreatic tumors: for 2.5-3 hr in 1 mg/mL Type IV collagenase. Digestion media was supplemented with 3mM $CaCl_2$, 0.1mg/mL DNAse I (Roche), Soybean Trypsin Inhibitor (Calbiochem), and 10mM HEPES (Invitrogen) in HBSS (Invitrogen). Cell suspensions were washed in DMEM:F12 media with 10% FBS containing DNAse I and Soybean Trypsin Inhibitor, then triturated through consecutive 18-gauge and 23-gauge needles and were passed through 40-μm filters. Cells were then xenotransplanted, FACS analyzed, or frozen for future study.

FACS sorting and analysis. Dissociated tumor cells were suspended in HBSS/2% FBS and stained with antibodies for 15 min at 4 °C. Primary antibodies include ScaI (Biolegend), CD49f (Biolegend), Ter119 (Biolegend), CD31 (Biolegend), CD45 (Biolegend), EpCAM (eBioscience), CD24 (eBioscience), CD44 (Biolegend), CD138 (BD Bioscience), CD133 (eBioscience), CD151 (R&D Systems), CXCR4 (eBioscience), CD166 (eBioscience), c-Kit (eBioscience), DBA (Vector), anti-mouse PDGFRβ (Biolegend), anti-human CD166 (R&D Systems), anti-human PDGFRβ (Biolegend). GFP fluorescence was measured endogenously. Cell sorting was performed using BD FACS Aria in the UCLA Jonsson Comprehensive Cancer Center and Center for AIDS Research Flow Cytometry Core Facility. FACS analysis was performed with BD FACS LSRII (BD Biosciences).

Immunohistochemistry. Antigen retrieval was performed on formalin-fixed, paraffin-embedded tissue by heating the slides at 95°C in citrate buffer (pH 6.0) for 15 minutes. Stains were visualized with Vectastain ABC Elite Kit (Vector Labs). Sections (4μm) were stained with

hematoxylin and eosin (H&E) or with specific antibodies against PDGFRβ (1:100, Cell Signaling), SMA (1:1000, Sigma), and PanCK (1:1000, Sigma). Staining was visualized with an Olympus BX60 microscope using PictureFrame software.

Immunofluorescence analysis. Sorted cell were cytospun on glass slides (Shandon) at 800rpm for 5 minutes and fixed with cold methanol for 10 minutes. The following primary antibodies were used: GFP (Aves Labs), CK5 (Covance), CK8 (Covance). DAPI Anti-Fade reagent (Invitrogen) was used to mark nuclei. Staining was visualized with an Olympus BX60 fluorescent microscope using PictureFrame software.

Lineage Tracing. Mice were injected i.p. with 4-hydroxytamoxifen (Sigma) to induce LacZ expression in appropriate genetic strains. After 24 hours, select tissues were harvested, fixed 90-120 minutes with 2% PFA/0.2% Glutaraldehyde , washed with PBS, and incubated with X-gal Working Solution for 1-4 hours (5mM Potassium Ferricyanide Crystalline (Sigma), 5mM Potassium Ferricyanide Trihydrate (Sigma), 2mM Magnesium Chloride (Sigma), 0.01% Sodium Deoxycholate (Sigma), 0.02% NP-40 (Sigma), 0.1% 5-bromo-4-chloro-3-indolyl-ß-D-galactoside (Boehringer Mannheim) in PBS). Tissues were then rinsed, processed into 10um sections, and counterstained with Nuclear Fast Red. Alternatively, tissues were flash frozen in OCT (Sakura) and cryosectioned at 5-10um onto glass slides. Sections were then fixed with cold 2% PFA/0.2% Glutaraldehyde for 10 min, washed with PBS, and incubated with X-gal Working Solution overnight at 37°C. Sections were then rinsed and counterstained.

RNA Isolation and qRT-PCR. Cells were collected, spun down, and RNA extracted using TRIzol® Reagent (Invitrogen). RNA was reverse transcribed into cDNA with SuperScript III First-Strand Synthesis System for qRT-PCR (Invitrogen), and quantitative PCR was done in the iQ thermal cycler (BioRad) using the iQSYBR Green Supermix (BioRad) in triplicate. Mouse primers used were: Lgr5 (F5′- GTGCATTCTCCCTTGCTGAG-3′; R5′-TGCACAGCCATTTGAGAGAG-3′), Vimentin (F5′- CGGCTGCGAGAGAAATTGC-3′; R5′-CCACTTTCCGTTCAAGGTCAAG-3′), RPL13a (F5′- TACGCTGTGAAGGCATCAAC-3′; R5′- ATCCCATCCAACACCTTGAG-3′). Human primers used were: Ck19 (F5′-ATGGCCGAGCAGAACCGGAA-3′; R5′- CCATGAGCCGCTGGTACTCC-3′), EpCAM (F5′-CGCAGCTCAGGAAGAATGTG-3′; R5′-TGAAGTACACTGGCATTGACG-3′), Vimentin (F5’-TCTGGATTCACTCCCTCTGG -3’; R5’-GCAGAAAGGCACTTGAAAGC -3’), PDGFRβ (F5′- GTGAACGCAGTGCAGACTGT-3′; R5'- AGGTGTAGGTCCCCGAGTCT-3′), RPL13a (F5'-CATCGTGGCTAAACAGGTACTG-3'; R5'- GCACGACCTTGAGGGCAGCC-3'). CD138 (F5’-GGAGCAGGACTTCACCTTTG-3’; R5’-CTCCCAGCACCTCTTTCCT-3’), Lgr5 (F5'- CAGCGTCTTCACCTCCTACCT-3'; R5'- CCTTGGGAATGTATGTCAGAGC-3'), Pdx1 (F5'- TCCACCTTGGGACCTGTTTAGAG-3'; R5'-GGACTCACTGTATTCCACTGGCATC-3'), CD24 (F5'- GGCACTGCTCCTACCCACGCAG-3'; R5'- GCCACATTGGACTTCCAGACGCC-3'), CXCR4 (F5'-ATCATCTTCTTAACTGGCATTGTG-3'; R5'- GCTGTAGAGGTTGACTGTGTAG-3'), CD133 (F5'- CCGCAGGAGTGAATCTTT-3'; R5'- AGGACTCGTTGCTGGTGA-3'), ABCG2 (F5'- CACCTTATTGGCCTCAGGAA-3'; R5'- CCTGCTTGGAAGGCTCTATG-3'), ABCB1 (F5'- AAGCTTAGTACCAAAGAGGCTCTG-3'; R5'-GGCTAGAAACAATAGTGAAAACAA-3'), CD166 (F5'- TAGCAGGAATGCAACTGTGG-

3'; R5'- CGCAGACATAGTTTCCAG-3'), CD151 (F5'- ACAGCCTACATCCTGGTGGT-3'; R5'- TTCTCCTTGAGCTCCGTGTT-3'), E-Cadherin (F5'- GACTCGTAACGACGTTGCAC-3'; R5'- AGGAGTTCAGGGAGCTCAGAC-3'), CD266 (F5'- TGCTTTCTGGCTTTTTGGTC-3'; R5'- AGGCTCCCTTTCTGTTCTGG-3'), CD87 (F5'- GAGCTGGTGGAGAAAAGCTG-3'; R5'- CATGTCTGATGAGCCACAGG-3'), Synd4 (F5'- TTGAGAGAACGGAGGTCCTG-3'; R5'- GCTAAAGTCCAAGCCAGTGC-3'), CD49f (F5'- GCTCGAGGTTATGGAACAGC-3'; R5'- AGATCCCAGCGAGAATAGCC-3').

Pancreatitis Induction. 10-12 week old mice were injected with 250μg/kg caerulein (Sigma) in the intraperitoneum either chronically 5 times a week for two weeks, or acutely for two days. Alternatively, pancreatic ducts were physically ligated for 7 days. Briefly, mice were anesthetized and the left abdominal flank shaved and sterilized with ethanol. A 1cm incision was made and pancreas exteriorized. Surgical sutures were wrapped around the pancreatic tail and tied. The pancreas was then internalized and the incision closed with surgical staples.

In vitro **prostate sphere assay.** Prostate spheres were cultured and passaged as described previously (Lukacs 2010, Xin 2007). Cells were counted and suspended into a 100μL mixture of 1:1 Matrigel (BD Biosciences) and PrEGM (Lonza). Samples were plated around the rims of wells in a 12-well plate and allowed to solidify at 37°C for 45 minutes, before 1 mL of PrEGM was added. Sphere media was changed every three days. Spheres were counted after 8 days.

In vitro **pancreatic sphere assay.** Pancreatic cells were grown as previously described (Seaberg 2004). Briefly, single cells were plated at a density of 50,000 cells/mL in low-attachment plates

(Corning). Spheres were grown in DMEM:F12 media supplemented with N-2, B27, Glutamax, 20ng/mL EGF (Invitrogen), and 20ng/mL bFGF (R&D Systems).

***In vivo* pancreatic regeneration.** Fetal pancreatic rudiment was harvested from E12-E16 embryos as previously described (Burke 2010). Cells were gently dissociated utilizing 0.1 mg/mL Collagenase IV (Invitrogen) for 5 min at 37°C then briefly triturated with a 27-guage needle. 1 $x10^6$ cells were mixed 1:1 in Sphere Media and Matrigel and injected subcutaneously into recipient NSG mice. Implants were harvested 8-12 weeks later. Alternatively, adult pancreatic cells isolated from β-actin dsRED [Tg(ACTB-DsRed.MST)1Nagy/J] were used and mixed 1:1 with fetal cells.

Microarray gene expression analysis. The gene expression was investigated by Affymetrix Mouse 430 2.0 Array by the UCLA Microarray Core. Microarray data are available at the National Center for Biotechnology Information Gene Expression Omnibus (GSE38988). The mRNA expression data from CEL files was normalized using dChip software. For each gene, its expression in each genotype group was represented by the geometric average of the biological replicated samples (n=4). The log ratio between a pair of two genotypes was then calculated.

Limiting Dilution experiments. Tumor cells were FACS sorted into PDGFRβ+ and PDGFRβ- populations, excluding lineage markers CD31, Ter119, and CD45. Single cells were mixed 1:1 into Matrigel:DMEM:F12 and implanted into subcutananeous flanks of NSG mice at varying cell doses and monitored for 4-6 months. Palpable tumors were scored for tumor initiation.

V. References

Afrikanova I, Kayali A, Lopez A, Hayek A (2012). Is stage-specific embryonic antigen 4 a marker for human ductal stem/progenitor cells? Biores Open Access, 1(4): 184-191.

Al-Hajj M, Wicha MS, Benito-Hernandez A, Morrison SJ, Clarke MF (2003). Prospective identification of tumorigenic breast cancer cells. PNAS, *100*: 3983-3988.

Barker N, Ridgway RA, van Es JH, van de Wetering M, Begthel H, van den Born M, Danenberg E, Clarke AR, Sansom OJ, Clevers H (2009). Crypt stem cells as the cells-of-origin of intestinal cancer. Nature, *457*: 608-611.

Barker N, van Es JH, Kuipers J, Kujala P, van den Born M, Cozijnsen M, Haegebarth A, Korving J, Begthel H, Peters PJ, Clevers H (2007). Identification of stem cells in small intestine and colon by marker gene Lgr5. Nature, *449*: 1003-1007.

Burke ZD, Li WC, Slack JM, Tosh D (2010). Isolation and culture of embryonic pancreas and liver. Methods Mol Biol, *633*: 91-99.

Chen H, Gu X, Liu Y, Wang J, Wirt S, Bottino R, Schorle H, Sage J, Kim S (2011). PDGF signaling controls age-dependent proliferation in pancreatic B-cells. Nature, *478*: 349-355.

Conejo JR, Kleeff J, Koliopanos A, Matsuda K, Zhu ZW, Goecke H, Bicheng N, Zimmermann A, Korc M, Friess H, Büchler MW (2000). Syndecan-1 expression is up-regulated in pancreatic but not in other gastrointestinal cancers. Int J Cancer, *88*: 12-20.

Desgraz R, Herrera P (2009). Pancreatic neurogenin 3-expressing cells are unipotent islet precursors. Development, *136*: 3567-3574.

de Lau W, Barker N, Low TY, Koo BK, Li VS, Teunissen H, Kujala P, Haegebarth A, Peters PJ, van de Wetering M, Stange DE, van Es JE, Guardavaccaro D, Schasfoort RB, Mohri Y, Nishimori K, Mohammed S, Heck AJ, Clevers H (2011). Lgr5 homologues associate withWnt receptors and mediate R-spondin signaling. Nature, *476*: 293-297.

Dominguez-Bendala J, Ricordi C (2012). Present and future cell therapies for pancreatic beta cell replenishment. World J Gastroenterol, *18*: 6876-6884.

Dor Y, Brown J, Martinez OI, Melton DA (2004). Adult panrceatic beta-cells are formed by self-duplication rather than stem-cell differentiation. Nature, *429*: 41-46.

Eppert K, Takenaka K, Lechman ER, Waldron L, Nilsson B, van Galen P, Metzeler KH, Poeppl A, Ling V, Beyene J, Canty AJ, Danska JS, Bohlander SK, Buske C, Minden MD, Golub TR, Jurisica I, Ebert BL, Dick JE (2011). Stem cell gene expression programs influence clinical outcome in human leukemia. Nat Med, *17*: 1086-1093.

Franco OE, Hayward SW (2012). Targeting the tumor stroma as a novel therapeutic approach for prostate cancer. Adv Pharmacol, *65*: 267-313.

Frank N, Schatton T, Frank M (2010). The therapeutic promise of the cancer stem cell concept. Jour Clin Invest, *120*: 41-50.

Habener JF (2004). A perspective on pancreatic stem/progenitor cells. Ped Diabetes, 5: 29-37.

Heldin CH, Westermark B (1990). Signal Transduction by the receptors for platelet-derived growth factor. J Cell Sci, *96*: 193-196.

Hori Y, Fukomoto M, Kuroda Y (2008). Enrichment of Putative Pancreatic Progenitor Cells From Mice by Sorting for Prominin1 (CD133) and PDGFRβ. Stem Cells, *26*: 2912-2920.

Huang L, Pu Y, Hu WY, Birch L, Luccio-Camelo D, Yamaguchi T, Prins GS (2009). The role of Wnt5a in prostate gland development. Dev Biol, *328*: 189-199.

Jaks V, Barker N, Kasper M, van Es JH, Snippert HJ, Clevers H, Toftgård R (2008). Lgr5 marks cycling, yet long-lived, hair follicle stem cells. Nat Genet, *40*: 1291-1299.

Juuti A, Nordling S, Lundin J, Louhimo J, Haglund C (2005). Syndecan-1 Expression – A Novel Prognostic Marker in Pancreatic Cancer. Oncology, *68*: 97-106.

Kharaishvili G, Simkova D, Makharoblidze E, Trtkova K, Kolar Z, Bouchal J (2011). Wnt signaling in prostate development and carcinogenesis. Biomed Pap Med Fac Univ Palacky Olomouc Czech Repub, 155: 11-18.

Kiskowski MA, Jackson RS 2nd, Banerjee J, Li X, Kang M, Iturregui JM, Franco OE, Hayward SW, Bhowmick NA (2011). Role for stromal heterogeneity in prostate tumorigenesis. Cancer Research, *71*: 3459-3470.

Kong B, Michalski C, Erkan M, Friess H, Kleeff J (2011). From tissue turnover to the cell of origin for pancreatic cancer. Nat Rev Gastroenterol Hepatol, *8*: 467-472.

Ku HT (2008). Minireview: pancreatic progenitor cells – recent studies. Endocrinology, *149*: 4312-4316.

Lapidot T, Sirard C, Vormoor J, Murdoch B, Hoang T, Caceres-Cortes J, Minden M, Paterson B, Caligiuri MA, Dick JE (1994). A cell initiating human acute myeloid leukaemia after transplantation into SCID mice. Nature, *367*: 645-648.

Lawson DA, Xin L, Lukacs RU, Cheng D, Witte O (2007). Isolation and functional characterization of murine prostate stem cells. PNAS, 104: 181-186.

Li X, Placencio V, Iturregui JM, Uwamariya C, Sharif-Afshar AR, Koyama T, Hayward SW, Bhowmick NA (2008). Prostate tumor progression is mediated by a paracrine TGF-beta/Wnt3a signaling axis. Oncogene, *27*: 118-130.

Lukacs RU, Goldstein AS, Lawson DA, Cheng D, Witte ON (2010) Isolation, cultivation and characterization of adult murine prostate stem cells. Nat Protoc, *5*: 702-713.

Mimeault M, Hauke R, Mehta P, Batra S (2007). Recent advances in cancer stem/progenitor cell research: therapeutic implications for overcoming resistance to the most aggressive cancers. J Cell Mol Med, *11*: 981-1011.

Mulholland DJ, Kobayashi N, Ruscetti M, Zhi A, Tran LM, Huang J, Gleave M, Wu H (2012). Pten loss and RAS/MAPK activation cooperate to promote EMT and metastasis initiated from prostate cancer stem/progenitor cells. Cancer Research, *72*: 1878-89.

Murtaugh LC (2008). The what, where, when and how of Wnt/β-catenin signaling in pancreas development. Organogenesis, *4*: 81-86.

Nygaard J, Cameron E, Garay M, Starkey T, Gianani R, Jensen J (2005). Recapitulation of Elements of Embryonic Development in Adult Mouse Pancreatic Regeneration. Gastroenterology, *128*: 728-741.

Oshima Y, Suzukia A, Kawashimo K, Ishikawa M, Ohkohchi N, Taniguchi H (2007). Isolation of Mouse Pancreatic Ductal Progenitor Cells Expressing CD133 and c-Met by Flow Cytometric Cell Sorting. Gastroenterology, *132*: 720-732.

Pan FC, Wright C (2011). Pancreas organogenesis: From Bud to Plexus to Gland. Developmental Dynamics, 240: *530*-565.

Rector K, Liu Y, Van Zant G (2013). Comprehensive hematopoietic stem cell isolation methods. Methods Mol Biol, *976*: 1-15.

Reginald Hill, Joseph Hargan Calvopina, Christine Kim, Ying Wang, David W. Dawson, Timothy R. Donahue, Sarah Dry, Hong Wu (2010). PTEN Loss Accelerates *K-RAS*^{G12D}-Induced Pancreatic Cancer Development. Cancer Res, *70*: 7114-7124.

Rovira M, Scot S, Liss A, Jensen J, Thayer S, Leach S (2010). Isolation and characterization of centroacinar/terminal ductal progenitor cells in adult mouse pancreas. PNAS, *107*: 75-80.

Seaberg RM, Smukler SR, Kieffer TJ, Enikolopov G, Asghar Z, Wheeler MB, Korbutt G, van der Kooy D (2004). Clonal identification of multipotent precursors from adult mouse pancreas that generate neural and pancreatic lineages. Nat Biotechnol, *22*: 1115-1124.

Shimanovich I, Krahl D, Rose C (2010). Trichoadenoma of Nikolowski is a distinct neoplasm within the spectrum of follicular tumors. J Am Acad Dermatol, *62*: 277-283.

Singh SK, Clarke ID, Terasaki M, Bonn VE, Hawkins C, Squire J, Dirks PB (2003). Identification of a cancer stem cell in human brain tumors. Cancer Research, *63*: 5821-5828.

Steer M, Meldolesi J (1987). The Cell Biology of Experimental Pancreatitis. NEJM, *316*:144-50.

Sun Y, Campisi J, Higano C, Beer TM, Porter P, Coleman I, True L, Nelson PS (2012). Treatment-induced damage to the tumor microenvironment promotes prostate cancer therapy resistance through WNT16B. Nat Med, *18*: 1359-68.

Sugiyama T, Rodriguez RT, McLean GW, Kim SK (2007). Conserved markers of fetal pancreatic epithelium permit prospective isolation of islet progenitor cells by FACS. PNAS, *104*: 175-180.

Taylor RA, Risbridger GP (2008). Prostatic tumor stroma: a key player in cancer progression. Curr Cancer Drug Targets, *8*: 490-497.

Todorov I, Nair I, Ferreri K, Rawson J, Kuroda A, Pascual M, Omori K, Valiente L, Orr C, Al-Abdullah I, Riggs A, Kandeel F, Mullen Y (2005). Multipotent progenitor cells isolated from adult human pancreatic tissue. Transplant Proc, *37*: 3420-1.

van de Wetering M, Sancho E, Verweij C, de Lau W, Oving I, Hurlstone A, van der Horn K, Batlle E, Coudreuse D, Haramis AP, Tjon-Pon-Fong M, Moerer P, van den Born M, Soete G, Pals S, Eilers M, Medema R, Clevers H. (2002). The β-catenin/TCF-4 complex imposes a crypt progenitor phenotype on colorectal cancer cells. Cell, *111*: 241–250.

Vintersten K, Monetti C, Gertsenstein M, Zhang P, Laszlo L, Biechele S, Nagy A (2004). Mouse in red: red fluorescent protein expression in mouse ES cells, embryos, and adult animals. Genesis, *40*: 241-246.

Visvader JE, Lindeman GJ (2008). Cancer stem cells in solid tumours: accumulating evidence and unresolved questions. Nat Rev Cancer, *8*: 755-768.

Woods A (2001). Syndecans: transmembrane modulators of adhesion and matrix assembly. J Clin Invest, *107*: 935-941.

Wu X, Jin C, Wang F, Yu C, McKeehan WL (2003). Stromal cell heterogeneity in fibroblast growth factor-mediated stromal-epithelial cell cross-talk in premalignant prostate tumors. Cancer Research, 63: 4936-4944.

Xin L, Lukacs RU, Lawson DA, Cheng D, Witte ON (2007) Self-renewal and multilineage differentiation in vitro from murine prostate stem cells. Stem Cells, *25*: 2760-2769.

Xu X, D'Hoker J, Stange G, Bonne S, De Leu N, Xiao X, Casteele M, Mellitzer G, Ling Z, Pipeleers D, Bouwens L, Scharfmann R, Gradwohl G, Heimberg H (2008). β Cells Can Be Generated from Endogenous Progenitors in Injured Adult Mouse Pancreas. Cell, *132*: 197-207.

Yalniz M, Pour P (2005). Are There Any Stem Cells in the Pancreas? Pancreas, *31*: 108-118.

Zong Y, Huang J, Sankarasharma D, Morikawa T, Fukayama M, Epstein JI, Chada KK, Witte ON (2012). Stromal epigenetic dysregulation is sufficient to initiate mouse prostate cancer via paracrine Wnt signaling. PNAS, *109*: 3395-3404.

Zhou Q, Brown J, Kanarek A, Rajagopal J, Melton DA (2008). In vivo reprogramming of adult pancreatic exocrine cells to beta-cells. Nature, *455*: 627-632.
Zhou Q, Law A, Rajagopal J, Anderson W, Gray P, Melton D (2007). A Multipotent Progenitor Domain Guides Pancreatic Organogenesis. Developmental Cell, *13*: 103-114.

Chapter 4:

Gemcitabine Sensitivity and Relapse in Pancreatic Cancer

I. Introduction

Pancreatic Cancer is the fourth leading cause of cancer-related mortality in the US, with a 5-year median survival of 5% (American Cancer Society 2013). Pancreatic Ductal Adenocarcinoma (PDAC) is the most common and malignant form of this disease, due to a uniquely aggressive tumor biology (Morris 2010, Stathis 2010). At the point of diagnosis, most PDAC patients have locally advanced or metastatic disease which precludes surgery (Conlon 1996). Roughly 20% of patients are candidates for surgical resection, however long-term survival remains poor due to disease recurrence. The chemotherapeutic gemcitabine has been the standard-of-care treatment for 15 years, shown to improve survival in metastatic pancreatic cancer patients, albeit by only a few weeks (Burris 1997). Gemcitabine is a nucleoside analog of deoxycitidine which can be inserted into newly synthesized nucleic acid during DNA replication and terminate further elongation, leading to cellular apoptosis and tumor growth inhibition (Fukunaga 2004). Additionally, gemcitabine can bind and inhibit the enzyme Ribonucleotide Reductase, halting production of necessary deoxyribonucleotide pools for DNA synthesis and thus further blocking cell cycle progression (Fukunaga 2004).

In 2007, a European study sought to understand whether gemcitabine administration in the post-operative adjuvant setting can increase survival in patients with resectable PDAC (Oettle et al 2007). This group found that disease-free survival was doubled in patients receiving adjuvant gemcitabine compared to controls (13.7 months vs 6.9 months). The utility of gemcitabine was confirmed in subsequent studies, rendering adjuvant chemotherapy post-operatively a standard treatment course at many centers (O'Reilly 2010, Sultana 2012). Despite the survival benefit, a majority of patients are refractory to treatment, relapse quickly and

succumb to disease (Sohn 2000). Therefore, determining mechanisms of PDAC resistance to gemcitabine is an important step to improve survival outcomes.

Here we have modeled the clinically heterogeneous response to gemcitabine treatment using murine xenograft models of patient-derived human PDAC samples. We have treated seven human xenograft lines *in vivo* with gemcitabine and found that two tumor lines completely responded throughout the treatment course, whereas five tumor lines relapsed immediately after drug withdrawal. We go on to show that the cause of this differential response is not a result of commonly hypothesized mechanisms of gemcitabine resistance, including dCK pathway levels and activity, microenvironmental factors, as well as cancer stem cell content and function. We performed global gene expression microarray analysis on these tumors and identified several pathway alterations which segregated response and relapse groups, including the Skp2-ubiquitin and PI3K pathway. We further validate that functionally targeting these pathways can increase gemcitabine sensitivity in patient-derived PDAC tumors *in vivo*.

II. Results

a. Gemcitabine sensitivity and relapse can be modeled in a human PDAC xenograft system

In an effort to understand the complex heterogeneity of human PDAC biology leading to differential response to gemcitabine treatment, we created a bank of 27 human PDAC xenografts from 45 surgically resected PDAC patient samples in collaboration with the UCLA Department of Surgery in accordance with institutional policy and approval. These patients had not undergone any neoadjuvant treatment, and PDAC specimens were obtained less than 3 hours after surgical resection and implanted into NOD-SCID IL2γ knock-out (NSG)

immunocompromised mice (see Materials and Methods). Individual patient tumor lines were passaged *in vivo*, propagated, and banked for future study. Relevant patient clinical data on select xenografts and their associated pathology can be found in Supplementary Table 1.

To model drug response, each patient tumor line was implanted subcutaneously and orthotopically into the same NSG mice and allowed to grow. Our unpublished results suggest that the growth rates of subcutaneous and orthotopic tumors from the same line are comparable. Therefore, we decided to use subcutaneous tumor to model the treatment responses because of its feasibility in continuous monitoring. Subcutaneous tumors were allowed to grow to about 5mm in diameter. Tumor bearing NSG mice were then randomly separated into two cohorts with 5-10 mice per cohort, including 1) control group (PBS treated); 2) GEM treatment group (100mg/kg gemcitabine twice weekly for 3-4 weeks). Group 2 was then further separated into two subgroups, one with continuous treatment and the other with treatment release; both subgroups were monitored for up to a month and the slopes of their tumor growth were calculated as shown in Fig 1A and Sup Fig 1. This treatment scheme was chosen to model the kinetics of administration of a round of gemcitabine in the clinic (Oettle 2007).

Seven patient xenograft lines were tested, yielding two unique response groups. The first group included 2 xenograft lines we hereafter term ‘Sensitive’, which shrank throughout the treatment course as observed by the negative growth slope (Fig 1A top; Supp Fig 1A). Interestingly, even after withdrawal of gemcitabine, tumors did not grow back even after a month of drug release (Fig 1A top). Histologically, whereas these tumors were highly proliferative in PBS-treated mice, tumor epithelia seemed to almost completely stop cycling after three weeks of gemcitabine treatment as seen by Ki67 staining (Fig 1B, top panels; Fig 1C, left panel). The second group included five xenograft lines, which we hereafter term ‘Relapseable’. These

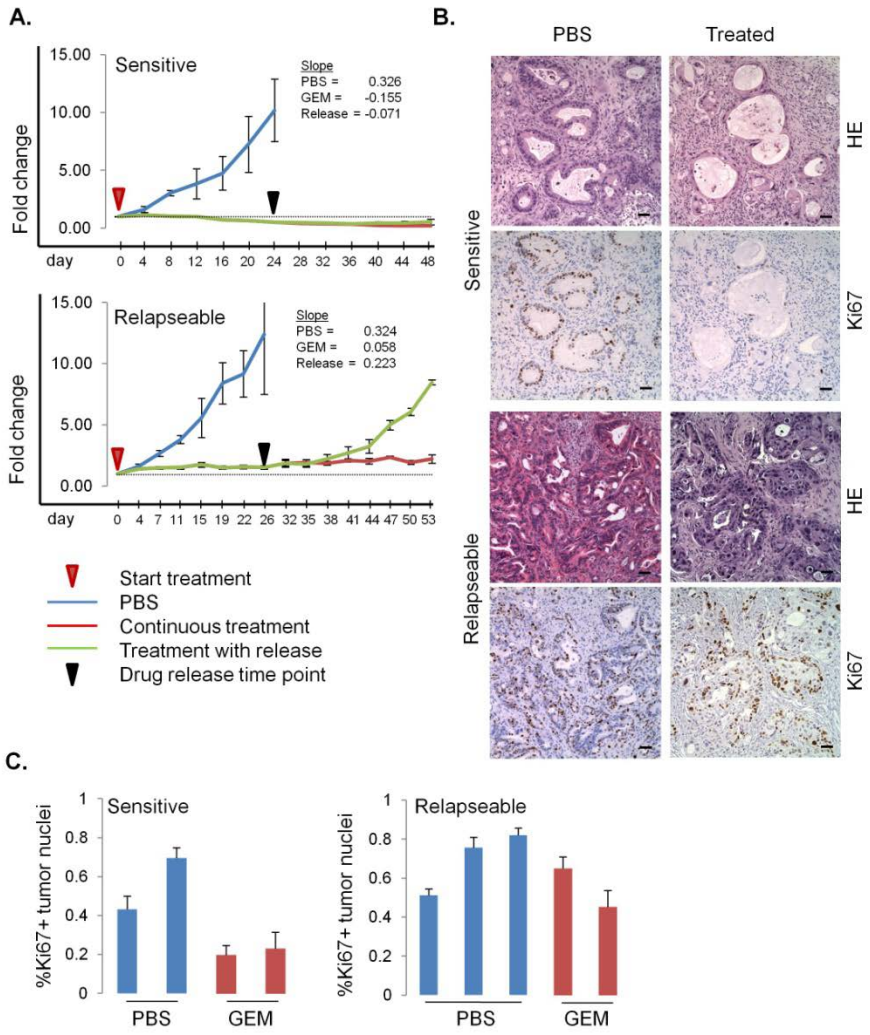

Figure 4-1: Human pancreatic xenografts can be segregated by response to gemcitabine treatment *in vivo*. (A) Graphs of *in vivo* tumor growth kinetics for two xenografts following gemcitabine treatment. Mice were treated with 100mg/kg gemcitabine i.p. starting day 0 (red arrow) twice weekly. Some mice were released from drug after 3-4 weeks (black arrow). Tumors were measured and plotted relative to day 0 tumor volume. Logarithmic tumor growth slopes are displayed for each treatment course. (B) H&E and immunohistochemical staining for Ki67 were performed on PBS and gemcitabine treated tumors (scale: 50μm). (C) Quantitation of Ki67+ tumor nuclei is represented for both xenografts, showing a significant decrease for the Sensitive, but not Relapseable, tumor after gemcitabine treatment.

tumors grew slowly throughout the treatment course as measured by the slightly positive growth slope, albeit at a much slower pace than PBS-treated controls (Fig 1A bottom; Supp Fig 1A). As soon as treatment was halted, tumors relapsed immediately and started to grow at a pace similar to untreated control groups (Fig 1A bottom; Supp Fig 1A). Strikingly, although there was a

significant growth difference between PBS and Gemcitabine treated tumors, a large percentage of tumor cells were still highly proliferative after three weeks of treatment as shown by Ki67 staining (Fig 1B bottom panels; Fig 1C, right panel). Taken together, the responses of our xenograft models seemed to correlate well with the clinical data from Oettle et al, which calculated that 22.5% of patients receiving post-operative gemcitabine survived at least 5 years. This ratio of responders is similar to 28.6% (2/7) of our patient samples which were sensitive to gemcitabine treatment.

b. Gemcitabine sensitivity is not due to differences in nucleoside salvage pathway activity

Gemcitabine is a prodrug which needs to get internalized and metabolized prior to being bioactive. The primary mechanism of its activation is through the deoxyribonucleoside salvage pathway (Shu 2010). The rate-limiting enzyme in this pathway is deoxycytidine kinase (dCK), which phosphorylates gemcitabine into a diphosphate, eventually leading to triphosphorylation and incorporation into DNA (Staub 2006). Other positive regulators include the hENT1/2 and hCNT1/2 transporters which mediate gemcitabine uptake into the cell (Garcia-Manteiga 2003), as well as ribonucleotide reductase (RRM1/2), which is important to generate the deoxyribonucleotide precursors needed for DNA synthesis (Duxbury 2004). Cytidine deaminase (CDA) is an essential gene in the pathway known to negatively affect gemcitabine efficacy, actively deaminating gemcitabine into deoxyuridine (Eda 1998). Expression levels of these genes are known to correlate with gemcitabine efficacy in patient tumors (Fujita 2010).

To determine whether the activity of nucleoside salvage pathway is a potential mechanism for the differential gemcitabine responses, we first performed global gene expression microarray analysis on untreated tumor xenografts, and found that ‘Sensitive’ and ‘Relapseable’

tumor cohorts indeed clustered together (Sup Figure 2A). Surprisingly, none of the nucleoside salvage pathway associated genes were differentially expressed in the 'Sensitive' and 'Relapseable' groups (Fig 2A). As further confirmation, we checked protein expression levels for

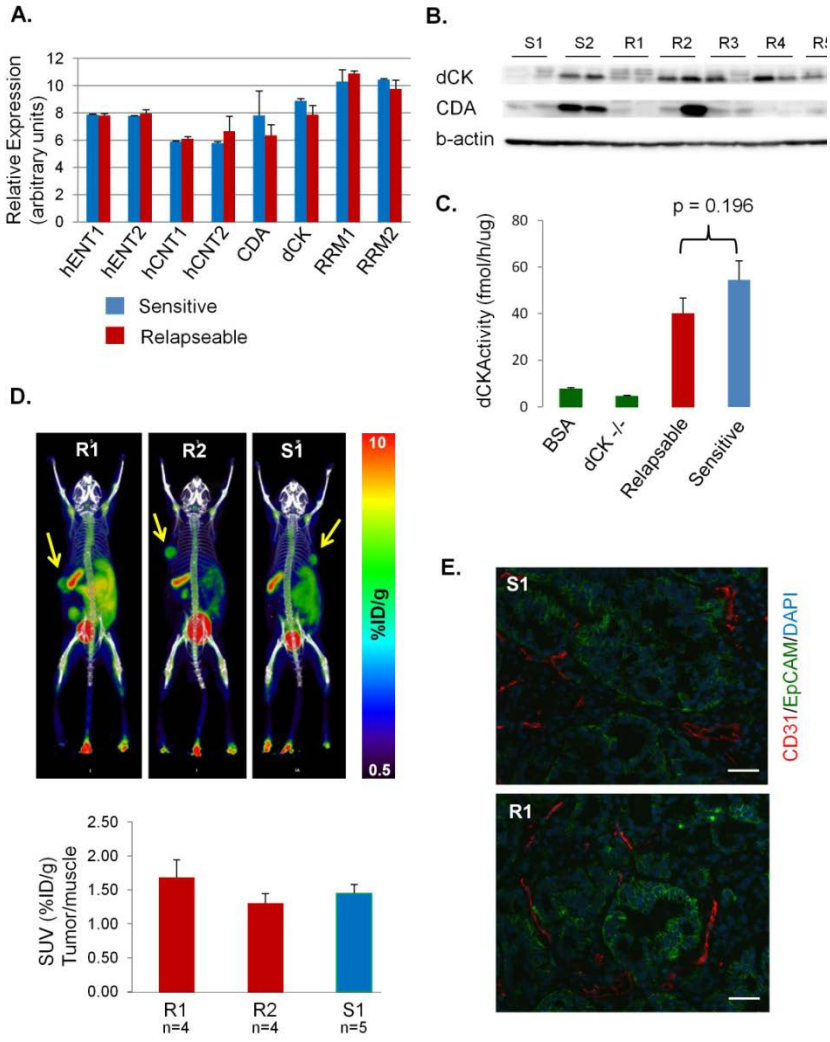

Figure 4-2: Nucleoside salvage pathway activity is similar among xenograft cohorts. (A) Gene expression microarray analysis was performed on all 7 human pancreatic xenografts. Probe signal expression for genes involved in the nucleoside salvage pathway were averaged for 'Sensitive' and 'Relapseable' tumors and displayed, showing no significant difference between them. (B) Protein levels of dCK and CDA for each xenograft was examined in duplicate by Western blotting. β-actin was used as a loading control. (C) dCK protein activity for both tumor cohorts was measured *in vitro* mixing whole cell protein extracts with radioactive dCK substrates. Phosphorylated product was quantified, using BSA-only and dCK-/- cell line as negative controls. (D) PET/CT scan images of tumor-bearing mice were performed 1hr after 200uCi of ^{18F}FAC probe was injected intravenously. Tumors are indicated by arrows and probe SUV quantitation is shown using muscle as a control. (E) Immunofluorescent staining of frozen xenograft tissue with CD31 and EpCAM antibodies showing representative areas of similar blood vessel architecture (scale: 50μm).

dCK and CDA via Western blot analysis for each tumor and did not see any trend indicating a $dCK^{hi}CDA^{low}$ pattern expected for gemcitabine sensitivity (Fig 2B, upper panels). As dCK is an essential rate-limiting step in the pathway, we reasoned that its enzymatic activity might predict gemcitabine efficacy. To this end, we employed an *in vitro* dCK assay on whole-cell lysates from frozen xenograft tissue and found no significant difference of dCK activities between the 'Sensitive' and 'Relapseable' groups (Fig 2B, lower panel).

To corroborate our *in silico* and *in vitro* observations, we measured dCK pathway activity *in vivo* in our xenograft models, utilizing the specific PET imaging probe 1-(2'-deoxy-2'-^{18}F-fluoro-β-D-arabinofuranoxyl)cytosine, or ^{18}F-FAC. Previous studies have shown that the intensity of ^{18}F-FAC signal is directly correlated with dCK activity, and ^{18}F-FAC can be used for imaging cancers *in vivo* (Radu 2008; Braas 2012). We went on to image two releapseable and one sensitive xenograft lines, and found there is no significant difference in probe uptake between the different response groups (Fig 2D). Additional imaging with the PET probe ^{18}F-fluorodeoxyglucose (^{18}F-FDG) showed there was no significant difference in overall glucose metabolism between the response groups either (Supp. Fig 2B).

It has been suggested that gemcitabine efficacy in pancreatic cancer is reduced due to poor perfusion and hypovascularity (Olive 2009, Provenzano 2012). It is therefore important to note that there are no differences in either ^{18}F-FAC or ^{18}F-FDG PET probes perfusion to the tumor sites between response groups. We co-stained xenografted tumors with CD31, an endothelial marker, and EpCAM, an epithelial cell marker, and found no significant differences in the size and density of vascularities between the response groups (Fig 2E), further supporting the notion that the differential responses to gemcitabine in our PDAC xenograft models are not

due to the differences in the availability of the drug, or the enzymatic activities required to activate the prodrug.

c. Cancer epithelium, not its associated stromal cells, is intrinsically responsible for gemcitabine resistance

It has been increasingly appreciated that cells of the tumor microenvironment have a profound effect on tumor initiation, progression, and response to therapies (Hanahan 2011). One major constituent of the tumor milieu in PDAC are the cancer-associated stromal cells. In addition to acting as a physical barrier for drug delivery, these stromal cells can secrete paracrine factors, such as pro-survival and anti-apoptosis signals, as well as growth factors for tumor cell growth (Hwang 2008, Farrow 2008, Bachem 2008, Neesse 2011), invasion (Ohuchida 2004, O'Connell 2011) and chemoprotection (Muerkoster 2004, Mantoni 2011, Sun 2012). They also have immunosuppressive effects, preventing anti-tumor immunity from occurring (Kraman 2010).

In order to understand whether gemcitabine relapse in our xenograft model is a cancer cell autonomous effect or mediated by tumor-associated stromal cells, we first identified a way to separate stromal cells from tumor cells. PDGFRβ is a receptor tyrosine kinase (Heldin 1990) highly expressed in neonatal pancreatic mesenchyme (Hori 2008). We found that in all our human PDAC tumor samples, PDGFRβ is expressed specifically in stromal cells (Fig 3A, left panel), overlapping with the pattern of SMA expression (Supp. Fig 3A). To confirm that PDGFRβ demarcates stroma, we sorted PDGFRβ+ and PDGFRβ- cells from our xenografts (Fig 3A, middle panel) and tested the expression levels of epithelial and mesenchymal associated genes. Reassuringly, PDGFRβ- cells express high levels of epithelial markers CK19 and

EpCAM, as compared to PDGFRβ+ cells, which express high levels of mesenchymal marker Vimentin (Fig 3A, right panel).

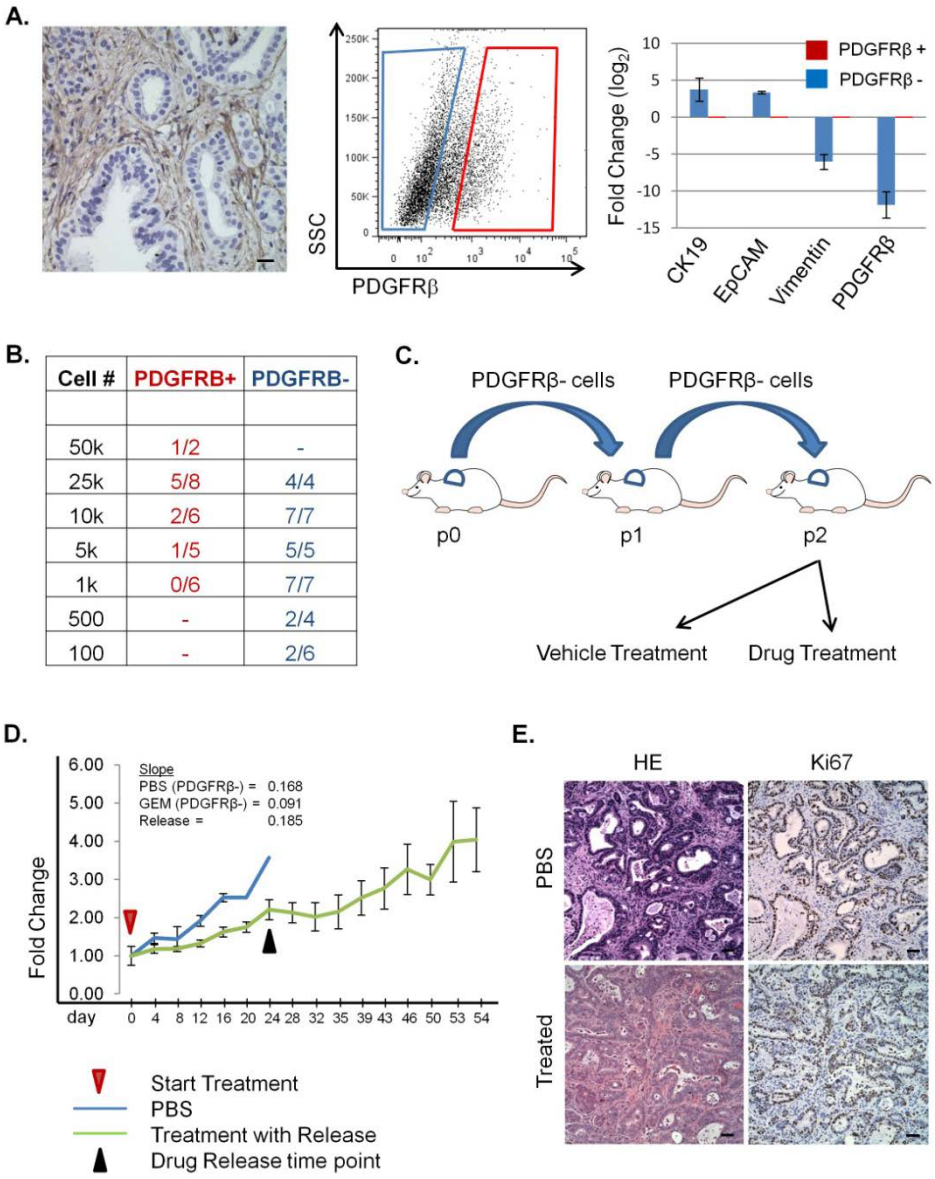

Cell #	PDGFRB+	PDGFRB-
50k	1/2	-
25k	5/8	4/4
10k	2/6	7/7
5k	1/5	5/5
1k	0/6	7/7
500	-	2/4
100	-	2/6

Figure 4-3: Depletion of PDGFRβ+ fibroblasts does not inhibit gemcitabine relapse. (A) Left: Immunohistochemical staining of human tumor with PDGFRβ shows expression in fibroblasts (scale: 50μm). Right: Cells were FACS sorted from a xenograft with PDGFRβ, RNA isolated, and qPCR analysis performed showing mesenchymal nature of PDGFRβ+ cells. (B) Limiting dilution xenotransplantation analysis shows tumor-initiating potential in the PDGFRβ- fraction. (C) Human xenografts were depleted of human fibrobalsts through serial sorts of PDGFRβ- cells *in vivo* and then treated with gemcitabine. (D) Tumors were treated for three weeks and then released from drug (Black Arrow), with logarithmic growth slopes displayed for each treatment course. (E) H&E and Ki67 staining was performed on PBS and gemcitabine treated tumors (scale: 50μm).

In an attempt to understand the cell-autonomous behavior of these tumor xenografts, we first isolated stroma-enriched PDGFRβ+ and epithelium-enriched PDGFRβ- cells and performed limiting-dilution transplantation experiments. As expected, the majority of tumor-initiating ability resides in the PDGFRβ- epithelial population (Fig 3B, left). Importantly, 100 PDGFRβ- epithelial cells are sufficient for initiating transplantable tumors (see below). Tumors developed from high doses of PDGFRβ+ cell implantation are most likely due to contaminated epithelial cells from FACS sorting, as evidenced by near identical tumor histology (Supp Fig 3B).

To test the tumor cell-autonomous effects of gemcitabine resistance and relapse, we first went through two rounds of sorting PDGFRβ- cells from a relapseable xenograft line and passaging in NSG mice, to ensure depletion of cancer-associated stroma (Fig 3C). We then subjected the resulting PDGFRβ- cell-derived xenografts to the same gemcitabine *in vivo* treatment scheme and found that these epithelial only xenograft behaved similarly to the parental xenograft with both epithelial and stroma (Fig 3D). Importantly, after gemcitabine release, PDGFRβ- cell-derived tumors relapsed quickly, growing at a pace similar to vehicle controls (Fig 3D) and are highly proliferative (Fig 3E). Taken together, these results indicate that cancer cells, not cancer-associated stromal cells, are the key determinants for chemoresistance and relapse in our model systems.

d. Cancer stem cell content and function is not altered by gemcitabine treatment

Increasing evidence suggests that specific tumor subpopulations, termed cancer stem cells (CSC), exist within human cancers (Dalerba 2007). CSCs exhibit properties of self-renewal and multi-lineage differentiation and are responsible for continuous tumor growth and therapeutic resistance (Mimeault 2007). Several groups have identified CSC populations in

PDAC, utilizing markers such as CD133, ALDH, CD44, CD24, EpCAM, and c-Met to prospectively isolate and test their function (Li 2007, Herman 2007, Kim 2011, Li 2011). It is thought that cancer stem cells are resistant to many chemotherapeutics, either through upregulation of drug efflux pumps, relative quiescence, upregulation of developmental pathways or other pro-survival mechanisms (Mimeault 2007, Lee 2008, Chen 2012). Therefore, we sought to examine the content and function of the putative cancer stem cell populations, based on previous published cell surface markers, within our tumor xenografts as a possible mechanism for differential gemcitabine sensitivity.

One possibility was that CSC populations represented a higher percentage of total tumor cells in our 'Relapseable' group as compared to the 'Sensitive' group. We reasoned that more CSCs might result in more intrinsically chemoresistant cells at the baseline level, leading to quicker relapse. To test this hypothesis, we performed FACS analysis using a panel of previously published PDAC CSC markers on all seven xenografts (Fig 4A). In addition to known CSC markers in PDAC, we also tested a panel of novel cell surface proteins our group previously identified to be upregulated in a mouse model of PDAC and human PDACs (Supp Table 2A) (Hill 2012; Donahue et al 2012 and our unpublished observation). To ensure that tumor cells were being specifically measured, we first excluded hematopoietic-derived, endothelial and stromal cells by negative selection to enrich epithelial cells, then gated on CSC marker positive cells (Supp Fig 4A). Intriguingly, the 'relapseable' group is not associated with higher percentages of CSC marker-positive cells, either using single or combinations of markers (Supp Table 2A). Additional immunofluorescence staining to co-localize CSC marker CD24 and CD44 expression confirmed that the distributions of double-positive cells are not restricted to a particular tumor region or as a small subpopulation of cells (Supp Fig 4B-C).

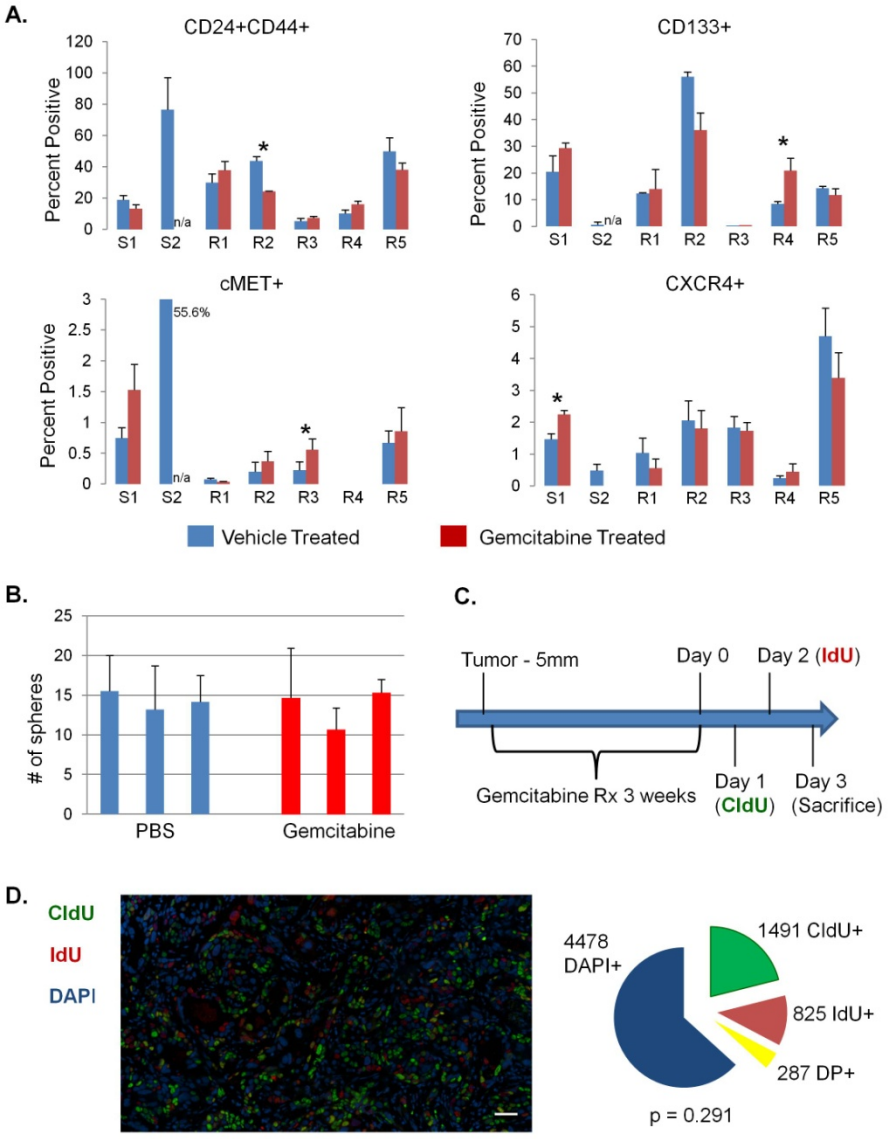

Figure 4-4: Cancer stem cell content or functional activation is not selected for after gemcitabine treatment. (A) Bar graphs representing cell population percentages from FACS analysis of cell-surface marker expression for xenograft tumors after PBS (blue) and gemcitabine (red) treatment. Stars indicate statistically significant differences in expression. (B) PBS and gemcitabine treated xenografts were dissociated to single cells, depleted of immune and fibroblast cells, and plated *in vitro* for sphere-forming analysis in triplicate. 2,000 cells were cultured for 10 days in suspension and spheres larger than 50um counted. (C) Diagram of pulse-chase experiment timeline. (D) Immunofluorescent staining of xenograft with CldU (green), IdU (red), and DAPI (blue) (scale: 50μm). Quantitation of positive tumor cells are displayed in the pie chart, with no significant enrichment of double positive cells as calculated by Fisher Exact Test.

We then postulated that if CSCs were indeed selectively chemoresistant, these cells would preferentially survive and be enriched after gemcitabine treatment. We treated xenograft

lines *in vivo* for 3-4 weeks and submitted tumors to the same negative selection before FACS analysis for CSC marker positive cells. It is important to note that the amount of stromal cells varied considerably before and after treatment, rendering exclusion of these cells essential for this comparative analysis (Supp Fig 4D). Surprisingly, virtually all marker-positive populations tested remained at similar percentages to vehicle controls (Fig 4A and Supp Table 2B). Statistically significant increases or decreases were observed in few select instances (marked with *). However, these changes are not consistent and cannot be used to stratify sensitive and relapsable groups.

While established FACS markers are good surrogates for CSC content, functional test of stem/progenitor activity is needed to formally exclude the contribution of CSCs from gemcitabine relapse. To this end, we employed an established *in vitro* sphere assay as a read-out of CSC activity. xenograft lines were either vehicle or gemcitabine treated *in vivo* for three weeks. Tumors were harvested, dissociated into single cells, then depleted PDGFRβ+, CD31+, Ter119+, and CD45+ cells. The resulting tumor cells were then plated for sphere forming activities. We found no difference in sphere-forming potential in tumor cells before and after gemcitabine treatment, indicating no functional gain in CSC content or activity after gencitabine treatment (Fig 4B).

If a specific subpopulation within a tumor is responsible for tumor relapse, such as a CSC compartment, those cells should be preferentially resistant and be the “parents” of those repopulating tumor cells after treatment. Alternatively, if no distinct subpopulation is responsible for the regrowth of the cancer, we would expect the remaining cells in the xenograft to proliferate stochastically after drug withdrawal. To visualize proliferating tumor cells *in vivo* in an unbiased manner, a pulse-chase strategy was employed utilizing two nucleoside analogs

chloro-deoxyuridine (CldU) and iodo-deoxyuridine (IdU) (Fig 4C). As shown by previous studies utilizing a similar strategy (Chen 2012), if a unique chemoresistant cell population is responsible for tumor relapse, they most likely proliferate after drug withdrawal and incorporate the first nucleoside analog pulse. After this first cell division, the chemoresistant repopulating cell will continue to divide and incorporate the second analog pulse. It follows that these cells should retain both pulse labels at a significantly higher frequency than expected by chance. However if many of the remaining tumor cells divide stochastically after drug withdrawal, retention of both pulses should be essentially random.

A 'Relapseable' xenograft line was pulsed on consecutive days after the last dose of gemcitabine administration. Small Intestines from the same animals were used as controls, as the stem/progenitors responsible for intestine growth and maintenance have been well defined (King 2013). As expected, CldU+IdU+ cells are concentrated in the stem cell enriched crypt region, with CIdU+ cells from the first pulse having differentiated and migrated to the upper part of microvilli without further proliferation (Supp Fig 5A). In the xenograft, we observed that 25.1% of tumor cells stained for CldU on day 1 after treatment and 15.1% on day 2 with IdU, with only 4% cells were double positive for CldU and IdU (Fig 4D). Double positive cells which were not adjacent to a proliferating cell were counted as single positive, as this indicates these tumor cells had likely not cycled twice (Supp Fig 5B). There was no regional restriction of double positive cells in the tumors, with expression interspersed throughout the tissue. Moreover, after statistical analysis utilizing Fisher Exact Test, it was determined that the percentage of double positive cells was not significantly different than expected from pure chance. The same result was obtained with a 'Sensitive' xenograft line (Supp Fig 5C). This suggests that the tumor cells remaining after drug treatment behave similarly and contribute equally to tumor relapse.

e. Gene expression microarray reveals unique gemcitabine sensitivity signature

To understand global pathway differences that might explain phenotypic differences to gemcitabine treatment, gene expression microarray analysis was performed as previously described (Supp Fig 2A and Supp Table 4). We found a total of 890 differentially regulated genes between the 'Sensitive' and 'Relapseable' groups (196 up, 694 down in 'Relapseable'). Additionally, we performed gene set enrichment analysis utilizing the KEGG reference database to identify those pathways that were most significantly different between these two groups. Among the top upregulated pathways in the 'Relapseable' group is the 'FC Epsilon RI signaling' pathway, which is comprised of major mediators of both the PI3K and MAPK signaling cascade (Fig 5A, left panel). Both PTEN and p85β, important negative regulators of the PI3K pathway, were significantly downregulated by 2.1 and 1.8-fold respectively in the 'Relapseable' group. Another highly significant hit was the 'Ubiquitin mediated proteolysis' pathway, which is downregulated in the 'Sensitive' group (Fig 5A, right panel). Among the key regulators of the Ubiquitin mediated proteolysis pathway is SKP2, which was found to be significantly upregulated by 1.6-fold in the 'Relapseable' group.

Skp2 is an F-box protein comprising part of an E3 ubiquitin ligase, which tightly regulates cell cycle entry and progression through targeted degradation of checkpoint proteins such as p27, p21, and cyclins (Nakayama 2004, Hu and Aplin 2008). It has been well-established that overexpression of Skp2 leads to aberrant proliferation and can be oncogenic in breast, prostate, and other tissues (Chan 2010, Wang 2012, Shim 2003). Skp2 has a variety of other validated target substrates outside of cell cycle control, including proteins involved in gene transcription, DNA repair, and various signal transduction pathways (Frescas 2008). Interestingly, Skp2 has been recently shown to directly ubiquitinate and activate AKT by

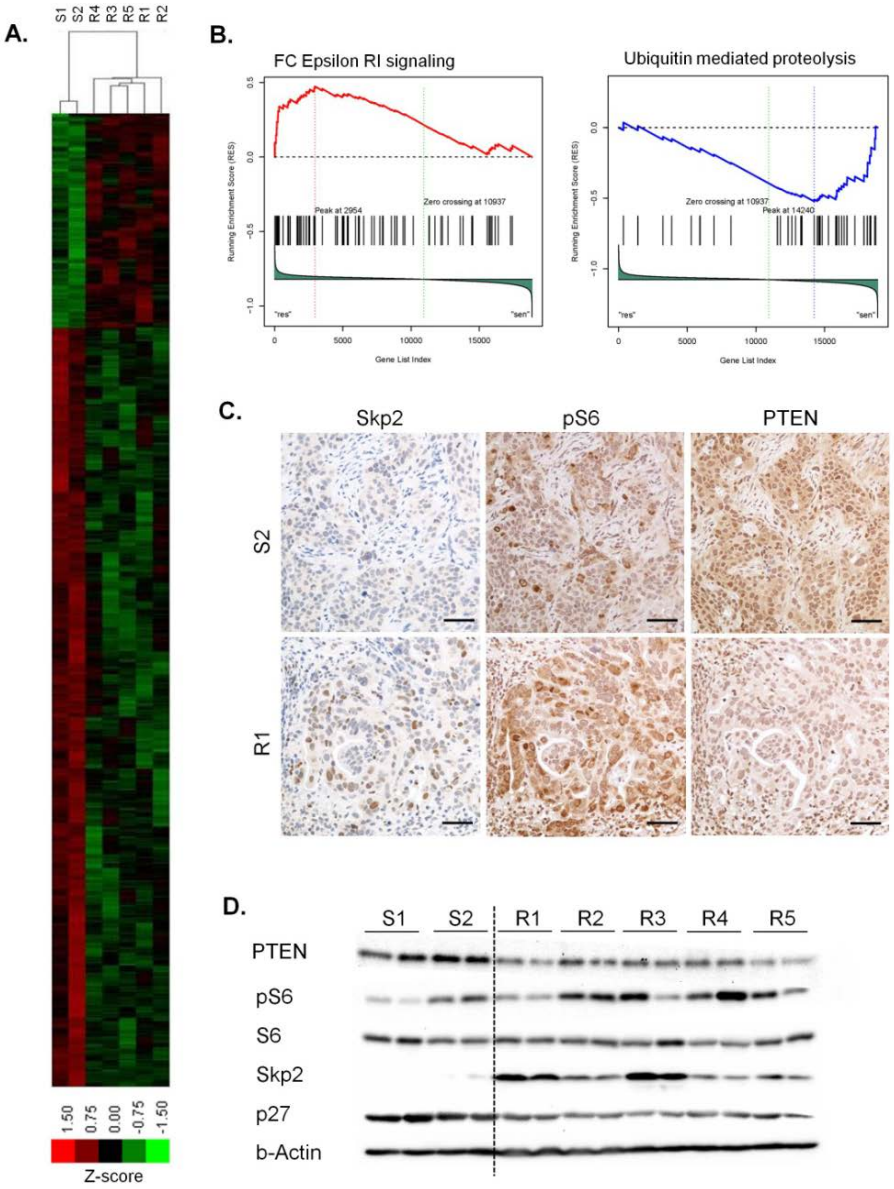

Figure 4-5: Specific gene signature segregates Sensitive and Relpaseable xenograft cohorts. (A) Heatmap of differentially expressed genes between two groups determined through >1.5 probe intensity fold-change and significant p-value ($p<0.05$). (B) Graphs showing gene set enrichment analysis identifying significantly altered pathways utilizing KEGG database. Immunohistochemical staining (C) and Western blot analysis (D) of Skp2, pS6, S6, PTEN, and p27 on xenograft tissues to validate differential expression on protein level. β-Actin was used as a loading control (scale: 50μm).

recruiting it to the cell membrane (Chan 2012). Reciprocally, AKT interacts with and phosphorylate Skp2 (Gao 2009, Lin 2009). Moreover, the PI3K pathway has been shown to directly control Skp2 levels (van Duijn 2006, Reichert 2007, Jonason 2007).

In addition to their roles in tumorigenesis, both of these pathways have been implicated in PDAC chemoresistance. Deletion of FKBP5, a negative regulator of AKT, was shown to result in AKT activation and increased resistance to gemcitabine and other chemotherapeutics in pancreatic cancer cell lines (Pei 2009). Skp2 deletion induces hypersensitivity of pancreatic cancer cells to TRAIL-induced apoptosis (Schuler 2011). Furthermore, upregulation of Skp2 and PI3K pathway is correlated with poor survival in PDAC patients (Einama 2006, Donahue 2012). Taken together, the PI3K-Skp2 axis is an attractive target to test in our gemcitabine relapse model.

We validated the differential expression of these genes on the protein level through immunohistochemistry and Western blot analysis (Fig 5B and 5C). 'Sensitive' xenograft lines in general exhibited higher PTEN and lower P-S6 levels as well as lower SKP2 and higher p27 levels as compared to 'Relapseable' xenograft lines, suggesting that these two pathways may collaboratively regulate gemcitibine sensitivity.

f. SKP2 and PI3K pathway are integral in PDAC gemcitabine relapse

To confirm the importance of SKP2 in mediating gemcitabine sensitivity, we first dowregulated its expression utilizing two sets of siRNAs on the MiaPaca2 and AsPC1 PDAC cell lines to choose the most effective siRNA (date not shown). Efficient knockdown was observed after 24 hours and maintained until day 6 (Fig 6A). Concomitant upregulation of p27 confirmed the efficient functional inhibition of SKP2-associated activity. Strikingly, a significant attenuation of P-AKT and P-S6 were observed, confirming Skp2 interaction with the PI3K pathway (Fig 6A). SKP2 has been shown to mediate the DNA repair of double-stranded breaks through recruitment of ATM (Wu 2012). Skp2 knock-down also lead to an increase in γH2AX

(Fig 6A), indicating an increase in DNA damage possibly through decreased repair. We next tested the effect of Skp2 inhibition on tumor cell growth in the presence of gemcitabine. We found that Skp2 inhibition sensitized MiaPaca2 cells to gemcitabine treatment, resulting in significantly increased cell death in the dual treatment (Fig 6B).

There are few selective small molecule inhibitors to Skp2. MLN4924 is a NEDD8-activating enzyme inhibitor which affects multiple subtypes of the cullin-RING ubiquitin ligase family (Soucy 2009). Wu et al recently described identification of several novel compounds to specifically inhibit Skp2, although these are not yet publically available and need to be validated (Wu 2012). Given our data indicating the importance of the PI3K pathway in 'Relapseable' xenografts, as well as our observed (Fig 6A) and previously described interaction of the Skp2-PI3K pathway, we reasoned we can indirectly target Skp2 degradation while simultaneously inhibiting the PI3K pathway.

PKI-587 is a recent dual PI3K/mTOR kinase inhibitor developed by Pfizer, showing anti-tumor efficacy in a panel of cancer cell lines *in vitro* and *in vivo* (Mallon 2011). We treated PDAC cells *in vitro* with PKI-587 and observed efficient downregulation of both pAKT and pS6 (Fig 6C and Supp Fig 6A). Importantly, there was also a dose-dependent decrease in Skp2 protein levels, confirming PI3K control of Skp2 expression. Similar to siRNA knockdown, we found that PKI-587 dual treatment with gemcitabine lead to significantly increased tumor cell death compared to either drug alone (Fig 6D).

To confirm this observation *in vivo*, we treated a 'Relapseable' tumor xenograft with gemcitabine, PKI-587, or both over a 2.5-week time course. We found that the dual treatment is significantly more effective at shrinking the tumor than either drug alone (Fig 6E). Western blot analysis indicated that PKI-587 treated tumors showed dramatic downregulation of pS6, however

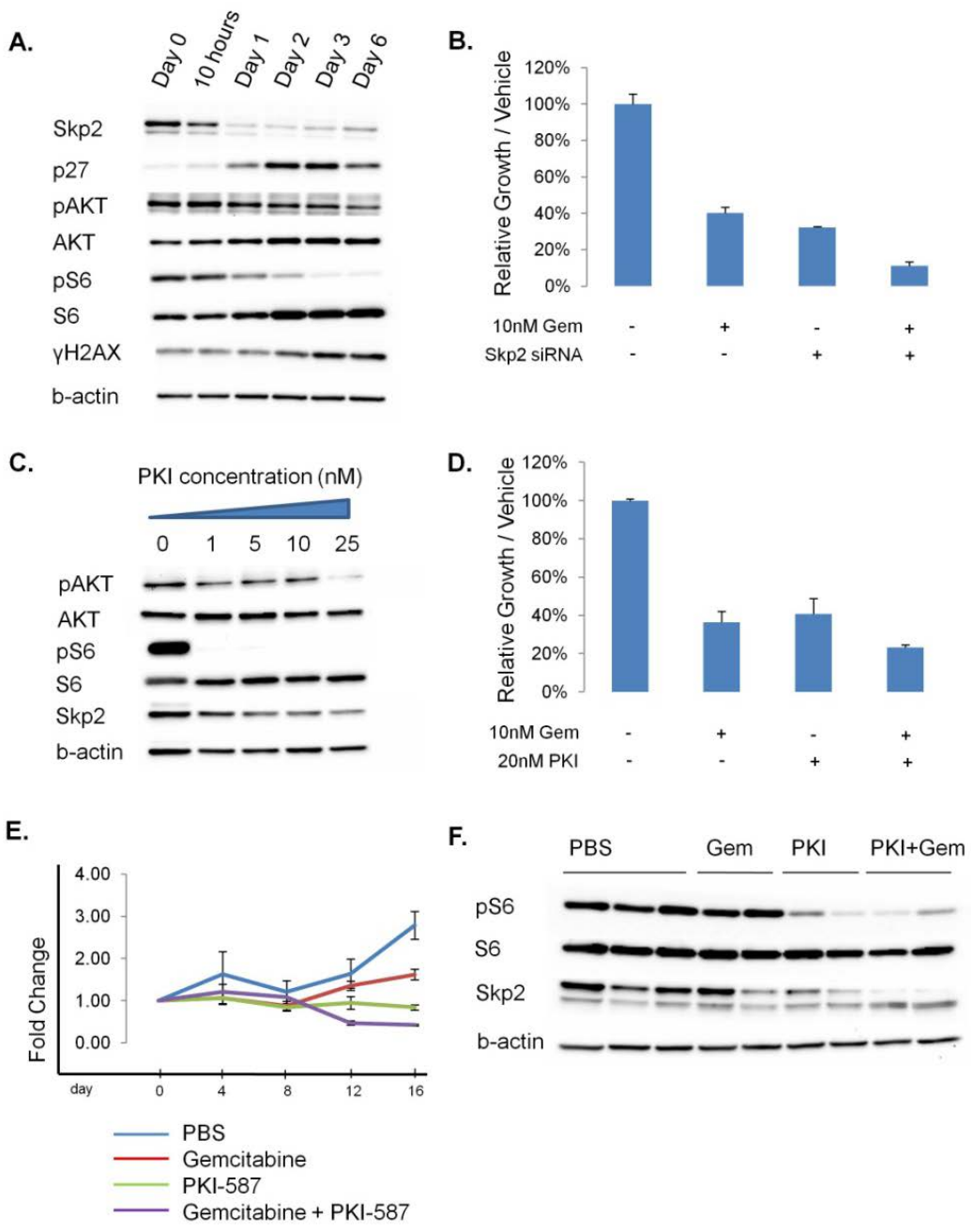

Figure 4-6: Targeting Skp2 and PI3K pathways increase gemcitabine sensitivity *in vitro* and *in vivo*. (A) Time course of specific RNAi inhibition of Skp2 in MiaPaca2 cells. Protein levels were examined by Western blot using β-actin as loading control. (B) Graph of MiaPaca2 cell line proliferation over a 72-hour time course with gemcitabine, Skp2 siRNA, or dual treatment with MTT assay. (C) MiaPaca2 cells were cultured for 24 hours with an increasing concentration of PKI-587. Western blot analysis confirmed inhibition of the AKT and mTOR pathways, as well as inhibition of Skp2. (D) Graph of MiaPaca2 cell line proliferation over a 72-hour time course with gemcitabine, PKI-587, or dual treatment with MTT assay. (E) A Relapseable xenograft was treated *in vivo* for 16 days twice weekly i.p. with gemcitabine, PKI-587, or both and tumor growth was measured, resulting in significant tumor shrinkage in the dual treatment. (F) Western blot analysis confirmed inhibition of Skp2 and pS6 in PKI-treated tumors.

pAKT was not significantly decreased (Fig 6F). Importantly, Skp2 expression was effectively inhibited with the PKI-587 treatment, with almost complete knock-down in the dual treatment. Immunohistochemical analysis revealed similar patterns, additionally indicating decreased proliferation in dual treated tumors (Supp Fig 6B). Interestingly, remaining Ki67+ tumor cells in dual treated tumors also maintained Skp2 and pS6 staining as seen in consecutive sections, indicating that if complete shutdown of these pathways is achieved, an even greater anti-tumor effect may be expected (Supp Fig 6B arrows).

III. Discussion

5-year survival rates for pancreatic cancer have not appreciably improved over the past three decades (American Cancer Society 2013). Despite dozens of attempts with a variety of small molecule interventions, painfully few clinical trials have successfully extended overall patient survival for this disease, and gemcitabine remains the standard chemotherapeutic treatment modality for pancreatic cancer patients (Burris 1997, Moore 2007, Conroy 2011). Therefore, understanding the mechanisms of intrinsic PDAC resisistance to chemotherapies is an area of great interest and intensive research.

Many of the genetic alterations required for tumor initiation and progression of pancreatic cancer have been well documented (Jones 2008, Mann 2011, Biankin 2012). In addition to the impressive variety of lesions which may lead to differential patient response to treatment belies a further layer of complexity due to substantial intra-tumoral clonal heterogeneity, both within a primary tumor as well as in relation to disseminated metastases (Campbell 2011, Yachida 2011). In order to capture the complexity of human disease, we chose to model PDAC utilizing low-passage human xenografts grown in NSG mice in place of genetically engineered mouse models

or cancer cell lines. While there are drawbacks in a foreign, compromised microenvironment and lack of natural tumor initiation and progression, we felt the most important aspect of studying mechanisms of intrinsic chemotherapy resistance was to maintain the integrity of patient genetic diversity and testing sensitivity with clear functional readouts in a relevant *in vivo* model mimicking a treatment schedule patients receive. There have been numerous studies attempting to elucidate gemcitibine resistance mechanisms, including in pancreatic cell lines (Akada 2005, Shah 2007, Hong 2009), subtype classifications (Collisson 2012) or correlations from clinical patient histories (Fujita 2010, Garrido-Laguna 2011). We feel our functional *in vivo* model is more representative of clinical anti-tumor gemcitabine efficacy, which correlates well with matched patient survival outcomes.

Major known therapeutic determinants of clinical gemcitabine efficacy include nucleoside salvage pathway activity, sufficient drug delivery to tumor cells, and pro-survival signals both from tumor cells and the microenvironment (Wang 2011, Hung 2012). In this set of seven human PDAC xenografts, these common mechanisms do not explain our phenotypically differential results. We show on the transcriptional, translational, and pathway levels that gemcitabine metabolism is very similar across all xenograft lines tested. Further, after stripping away cancer-associated fibroblasts from tumor cells utilizing the stromal-specific marker PDGFRβ, we show that *in vivo* gemcitabine relapse functions independently of the presence of supporting tumor-derived mesenchymal cells. While murine fibroblasts from the subcutaneous space do infiltrate tumor epithelium and may secrete paracrine signals after stromal depletion, these cells would presumably be present in ‘Sensitive’ xenograft lines as well, and as such cannot explain the differential gemcitabine response.

A relatively new paradigm in cancer biology which has been applied to PDAC posits the existence of a hierarchy of cancer cells, whereby tumor growth is driven by cancer stem cells, and while chemotherapy may eliminate more 'differentiated' tumor bulk, CSCs are resistant and are the cause of tumor relapse (Bhagwandin 2009). As a corollary, much excitement has surrounded the potential clinical implications, with active research focusing on identifying these CSCs and understanding how best to therapeutically target them to increase patient survival (Frank 2010). Several groups have identified CSC markers and cell populations in PDAC which are resistant to gemcitabine treatment, and that targeting specific pathways upregulated in these CSCs may improve gemcitabine efficacy (Herman 2007, Li 2011, Jimeno 2009). However, these reports are still in their preliminary stages and quite controversial, with no clinical relevance observed to date (Adams 2008, Shipitsin 2008, Lewis 2008). To test the hypothesis that CSCs are selectively resistant to gemcitabine in PDAC and responsible for tumor relapse, we first performed exhaustive FACS analysis on our xenograft lines before and after treatment, but saw no significant consistent enrichment of any marker population. Moreover we performed functional *in vitro* sphere forming analysis of treated xenografts, and saw no elevation of sphere-forming activity. Lastly, we conducted an unbiased pulse-chase assay to see if there is a specifc subpopulation of cells within the tumor which continues to proliferate after gemcitabine treatment, and found that all the remaining tumor cells cycle stochastically. Taken together, this data indicates that all the tumor cells within a xenograft line behave similarly in response to chemotherapy, and there is no one specific tumor subpopulation or cancer stem cell selected for and functionally responsible for gemcitabine relapse in this model. It will be interesting to see if future studies in transgenic animal models of PDAC interrogating mechanisms of recurrence will yield similar results.

There are several reasons for the discrepancies of our findings compared with other groups. First, the primary tissue used in this study come from different patients than previously described xenografts, so although they are all derived from pathologically confirmed PDAC samples, it is formally possible that inherent patient heterogeneity may induce differential CSC content, identity, and behavior. In fact, it is becoming increasingly evident that patient-to-patient expression of CSC markers are dramatically different (Rosen 2009). Second, our FACS analysis was meticulous to specifically exclude all immune and stromal constituents and focused on marker expression of tumor cells only. In fact, these microenvironmental cells often comprised a sizeable portion of the tumor milieu and expressed many CSC proteins to high levels, which can confound the analysis if not considered (data not shown). Moreover, depletion of these cells and xenotransplation of total unselected PDGFRβ- tumor epithelium resulted in tumor initiation in 2/6 of transplants at our lowest dose of 100 cells. This tumor-initiation potential is comparable to the activity of positively selected CSC population transplants previously reported (Li 2007, Herman 2007, Li 2011). This raises the possibility that optimizing PDAC xenotransplantation procedures may reveal that a larger proportion of PDAC tumor cells have tumor-initiating ability than currently appreciated, similar to that observed in other systems (Quintana 2008).

Clinical realities indicate that effective responses to therapy are often restricted to subsets of patients. One cause of this stratification of patient response has been suggested to be a result of underlying molecular genetic differences among tumors of similar pathology (Kalia 2013). The ability to determine the effectiveness of therapies for specific tumor molecular subtypes will represent a giant step forward in rational cancer treatment strategies and lead to an era of ‘personalized’ medicine (Dietel 2013). Large-scale efforts are underway to identify genetic loci that can sensitize cells to specific therapeutic treatments (Whitehurst 2007, Garnett 2012,

Barretina 2012). In this study, we have identified a gene signature that is predictive of gemcitabine resistance and relapse of human patient-derived PDAC xenografts, which may provide prognositic information that can guide clinical treatment options. Specifically, the PI3K and Skp2 pathways are important mediators of this gemcitabine resistance, and targeted inhibition of both can significantly improve anti-tumor efficacy compared to chemotherapy-alone both *in vitro* and *in vivo*.

The PI3K-Skp2 axis signals into multiple feedback loops which may act in synergy to provide the anti-apoptotic and pro-growth signals needed for tumor cells to survive gemcitabine treatment (Hafsi 2012). Decreased PTEN expression has been shown to induce Skp2 overexpression (Mamillapalli 2001), which can then feedback to the PI3K pathway via ubiquitination of AKT and recruitment to the cell membrane for activation (Chan 2012). Moreover, both PTEN and AKT have been shown to modulate the APC-CDH1 complex, which targets Skp2 for degradation and as such determines Skp2 stability and expression (Gao 2009, Song 2011). Skp2 can also directly target and degrade the tumor suppressor FOXO1, which is implicated in tumor homeostasis-inducing growth arrest and apoptosis (Huang 2005, Zhang 2011). Additionally, Skp2 overexpression can force progression through the cell cycle despite DNA damage through bypassing checkpoint controls (Bashir 2004, Lobrich 2007), driving aberrant cell proliferation and genomic instability (Lord 2012). Interestingly, Skp2 has been recently shown to activate DNA repair through its recruitment of ATM to regions of double stranded breaks (Wu 2012), which may lead to a greater ability for tumor cells to sustain gemcitabine-induced genetic damage. As such, Skp2 represents a potential biomarker which may predict poor clinical gemcitabine efficacy and eventual tumor relapse. We provide rationale for

the therapeutic use of PI3K inhibitors in conjuction with gemcitabine for PDAC patients overexpressing Skp2, which may delay tumor recurrance and increase overall survival.

A.

Tumor	Age	Tumor size	Pathology Primary	Xenograft	T Stage	Lymph Node Positive	Lymph Node Examined	Margins	Lymphovascular Invasion	Perineural Invasion	Diabetes
S1	73	3.1	Moderate	Well/Moderate	2	3	18	0	0	1	1
S2	66	3.5	Moderate	Moderate	3	2	26	1 (SMV, 1 mm uncinate)	1	1	0
R1	80	3.8	Moderate	Moderate	3	4	25	0	1	1	0 (borderline)
R2	70	3.9	Poor	Moderate/Poor	3	1	17	1	1	1	0
R3	56	2.0 cm and 1.5 cm	Moderate	Moderate	3	3	18	0	1	1	0
R4	70	3	Moderate	Moderate	3	8	23	0	1	1	0
R5	48	3	Well, IPMN Associated	Moderate	3	2	37	Uncinate & retroperitoneal	?	1	0

Tumor	Disease Specific Survival	Adjuvant Tx?	Status
S1	15.5	Underwent portacath placement on 10/7/10 to begin chemotherapy	DEAD (Recurrance 11/22/10)
S2	9.9	Underwent portacath placement on 6/9/11 to begin chemotherapy	DEAD (Recurrance 3/16/11)
R1	26.8	Unknown	DEAD
R2	4.2	Cisplatin, Gemzar, Xeloda, Irinotecan & XRT	DEAD (Recurrance 12/4/09)
R3	7.3	Unknown	DEAD
R4	15.0	Unkown, supposed to see Med Onc in Orange County	DEAD
			DEAD (Recurrance to liver

Supp Table S4-1: Clinical data for patients from which xenografts were generated. (A) Identifiers are eliminated to maintain patient confidentiality. Important patient details regarding tumor differentiation, stage, burden, survival, therapeutic regimen, and other information is included. Follow-up data for patient R1 and R4 is not available due to treatment outside UCLA following surgery.

A.

	S1	S2		R1	R2	R3	R4	R5
EpCAM	79.25	92.20		97.95	75.13	95.80	96.35	87.13
CD24	52.2	82.25		65.55	72.87	10.48	60.65	77.17
CD44	46.35	93.70		32.675	76.93	29.97	13	80.87
CD133 (AC133)	20.4	0.65		12.4	56.07	0.26	8.475	14.30
c-MET	0.75	55.60		0.08	0.20	0.23	0.0	0.67
CXCR4	1.47	0.49		1.04	2.06	1.84	0.25	4.70
CD24+CD44+	18.9	76.50		29.9	53.20	5.24	10.29	49.77
EpCAM+CD44+	28.6	85.20		32.35	58.78	17.07	10.59	58.13
CD133+CXCR4+	0.65	0.04		0.64	0.34	0.0	0.16	1.63
EpCAM+CD24+CD44+	17.7	74.90		25.75		3.09		72.73
TWEAKR	19.15	55.00		2.98	19.53	3.00	11.57	19.07
CD138	24.85	0.74		13.8	14.05	7.79	5.73	1.25
uPAR	2.43	0.90		1.3	0.43	0.22	6.32	4.37
ALCAM	5.265	93.95		49.25	70.57	30.27	31.85	67.73
Her2	78.35	83.50		94.25		67.17	74.15	79.20
CD151	82.85	85.60		83.45	60.93	87.07	92.95	86.47
CD49f	81.85	94.75		98.4	83.17	92.97	95.1	88.00
Synd4	13.5	2.55		4.43	3.93	1.48	0.67	6.78

B.

Fold-Change: Gem/PBS	S1	p-value		R1	p-value	R2	p-value	R3	p-value	R4	p-value	R5	p-value
EpCAM	0.67	0.076		1.00	0.403	0.67	0.056	1.00	0.822	1.00	0.833	0.93	0.609
CD24	0.40	0.002		0.92	0.246	0.51	0.003	1.25	0.356	0.86	0.523	0.85	0.297
CD44	1.57	0.020		1.20	0.347	0.99	0.671	1.28	0.004	1.70	0.021	0.91	0.227
CD133	1.44	0.185		1.12	0.799	0.64	0.131	1.95	0.001	2.47	0.066	0.83	0.458
C-Met	2.04	0.134		0.47	0.127	1.85	0.344	2.48	0.059	-	-	1.29	0.563
CXCR4	1.54	0.036		0.54	0.288	0.87	0.668	0.94	0.708	1.78	0.396	0.72	0.430
CD24+CD44+	0.70	0.167		1.27	0.293	0.49	0.004	1.42	0.144	1.56	0.111	0.76	0.100
EpCAM+CD44+	0.85	0.149		1.23	0.402	0.69	0.003	1.18	0.180	1.65	0.170	0.84	0.290
CD133+CXCR4+	1.82	0.179		0.70	0.488	0.43	0.111	-	-	1.81	0.248	0.46	0.208
EpCAM+CD24+CD44+	0.52	0.193		1.35	0.257	-	-	1.65	0.037	-	-	0.81	0.095
TWEAKR	0.27	0.025		0.54	0.164	0.33	0.028	1.24	0.254	1.05	0.891	0.40	0.121
CD138	0.98	0.929		0.96	0.879	0.19	0.084	0.97	0.693	0.88	0.554	0.92	0.963
uPAR	1.80	0.244		1.01	0.927	0.26	0.027	1.00	1.000	0.16	0.230	0.91	0.604
ALCAM	1.75	0.008		1.02	0.873	0.51	0.006	1.19	0.011	1.06	0.885	0.88	0.185
Her2	0.53	0.005		0.99	0.584	-	-	0.86	0.038	1.11	0.492	0.94	0.727
CD151	0.60	0.009		0.94	0.589	0.86	0.212	1.01	0.738	1.04	0.453	0.89	0.250
CD49f	0.75	0.038		1.00	0.924	0.62	0.002	0.98	0.178	1.00	0.868	0.94	0.659
Synd4	0.84	0.473		1.20	0.677	0.19	0.005	1.10	0.720	0.52	0.286	0.50	0.109

Supp Table S4-2: Table of cell-surface marker expression values through FACS analysis before and after gemcitabine treatment. (A) Marker expression for each xenograft at baseline level represented as a percentage of total Lin-PDGFRβ- tumor cells. (B) Fold-Change ratio of marker expression after gemcitabine treatment for each xenograft ($\%_{Gemcitabine}/\%_{PBS}$). Student's t-test is used to calculate if change in marker expression is significant.

A.

Antibody	Company
EpCAM - FITC	Biolegend
EpCAM - APC	Biolegend
CD24 - APC	Biolegend
CD44 - PE.Cy7	Biolegend
CD133 - APC	Miltenyi Biotec
c-MET - PE	R&D Systems
CXCR4 - PE.Cy7	Biolegend
TWEAKR - PE	Biolegend
CD138 - PE	BD Bioscience
uPAR - APC	eBioscience
ALCAM - PE	R&D Systems
Her2 - APC	Biolegend
CD151 - PE	BD Bioscience
CD49f - PE	BD Bioscience
Synd4 - PE	BD Bioscience
humanPDGFRβ - PE	Biolegend
humanPDGFRβ - APC	Biolegend
mousePDGFRβ - PE	Biolegend
mousePDGFRβ - APC	Biolegend
CD31 - FITC	Biolegend
CD45 - FITC	Biolegend
Ter119 - FITC	Biolegend
CD31 - PE	Biolegend
CD45 - PE	Biolegend
Ter119 - PE	Biolegend
CD31 - APC	Biolegend
CD45 - APC	Biolegend
Ter119 - APC	Biolegend

Supp Table S4-3: Table of FACS antibodies. (A) A list of all the FACS antibodies used with specific fluorophore conjugates and manufacturers.

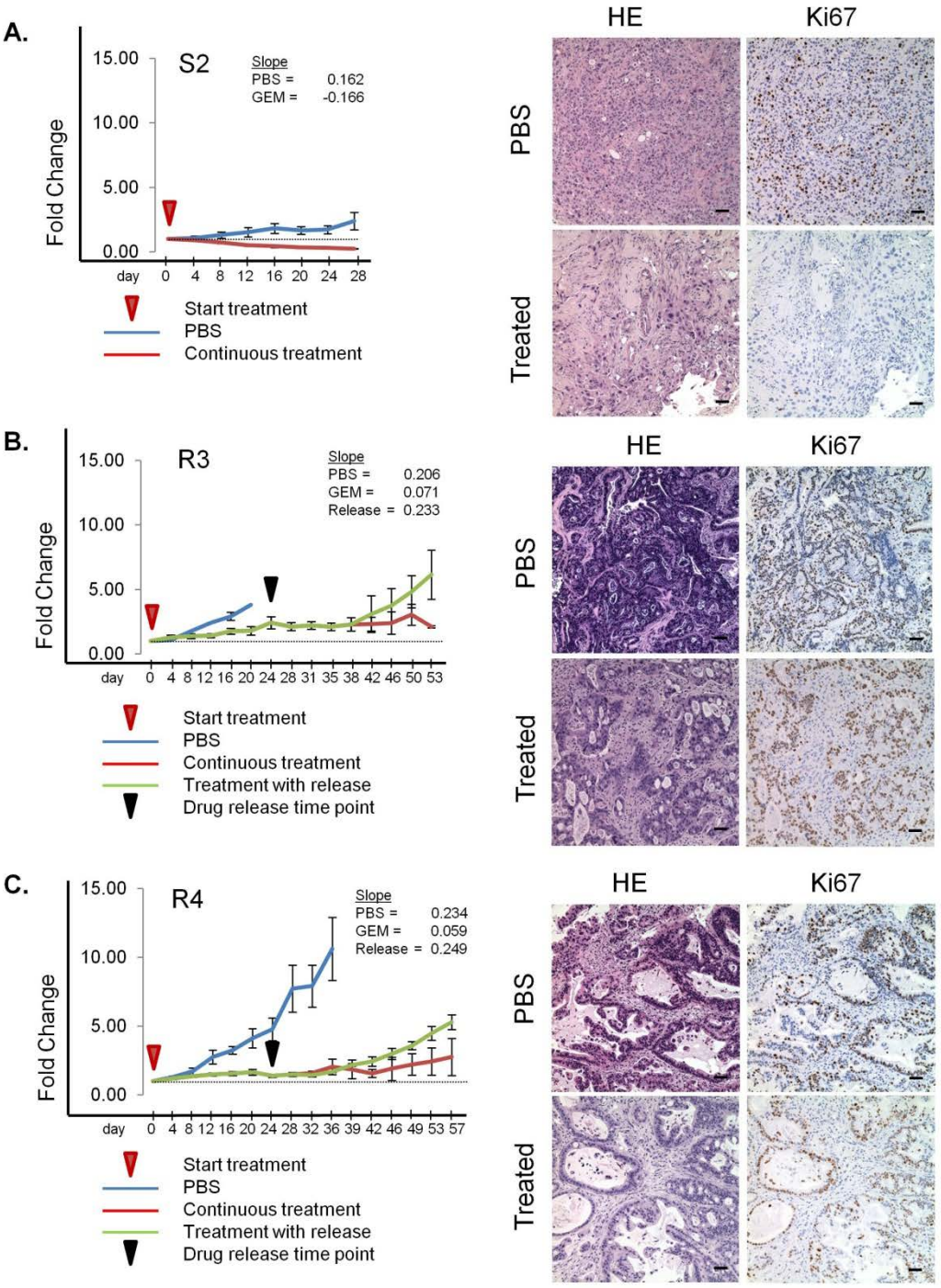

Supp Figure S4-1: Additional *in vivo* gemcitabine treatment results for select xenografts. (A-C) Graphs of *in vivo* tumor growth kinetics for three xenografts following gemcitabine treatment. Mice were treated with 100mg/kg gemcitabine i.p. starting day 0 (red arrow) twice weekly. Some mice were released from drug after 3-4 weeks (black arrow). Tumors were measured and plotted relative to day 0 tumor volume. Logarithmic tumor growth slopes are displayed for each treatment course. H&E and immunohistochemical staining for Ki67 were performed on PBS and gemcitabine treated tumors (scale: 50µm).

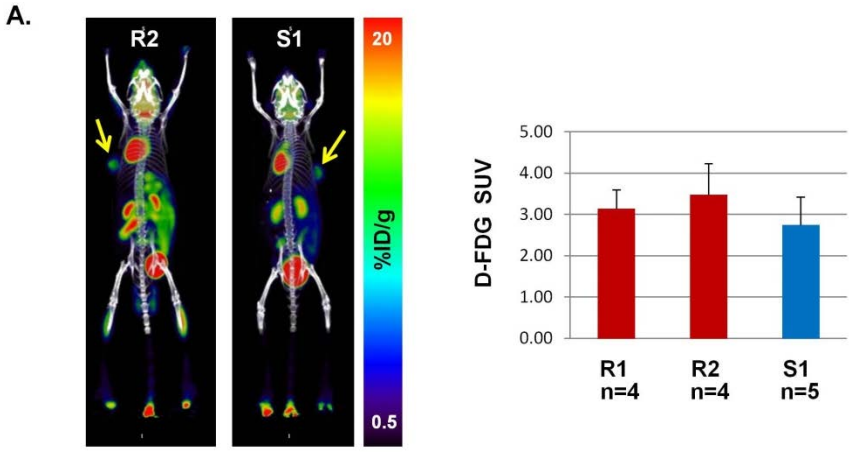

Supp Figure S4-2: ^{18F}FDG PET/CT scans show similar tumor metabolism and perfusion. (A) PET/CT scan images of tumor-bearing mice were performed 1hr after 200uCi of ^{18F}FDG probe was injected intravenously. Tumors are indicated by arrows and probe SUV quantitation is shown for three xenografts using liver as a control tissue.

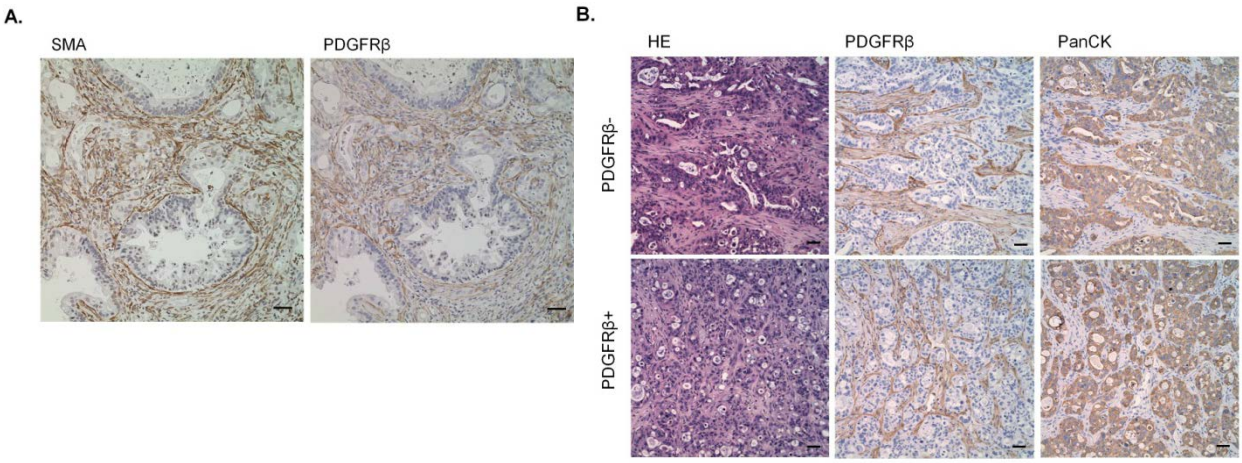

Supp Figure S4-3: PDGFRβ is a useful marker for cancer associated fibroblasts. (A) Immunohistochemical staining on consecutive human xenograft tissue sections indicate SMA and PDGFRβ are expressed very similarly on tumor stromal cells. (scale: 50μm). (B) H&E staining on tumors formed after FACS sorting and xenotransplantation of PDGFRβ- and PDGFRβ+ cells show a similar epithelial character. IHC validates that tumor cells are PanCK+ and that PDGFRβ is expressed on fibroblasts in both tumors, indicating tumors from the PDGFRβ+ fraction likely formed from contaminating PDGFRβ- cells (scale: 50μm).

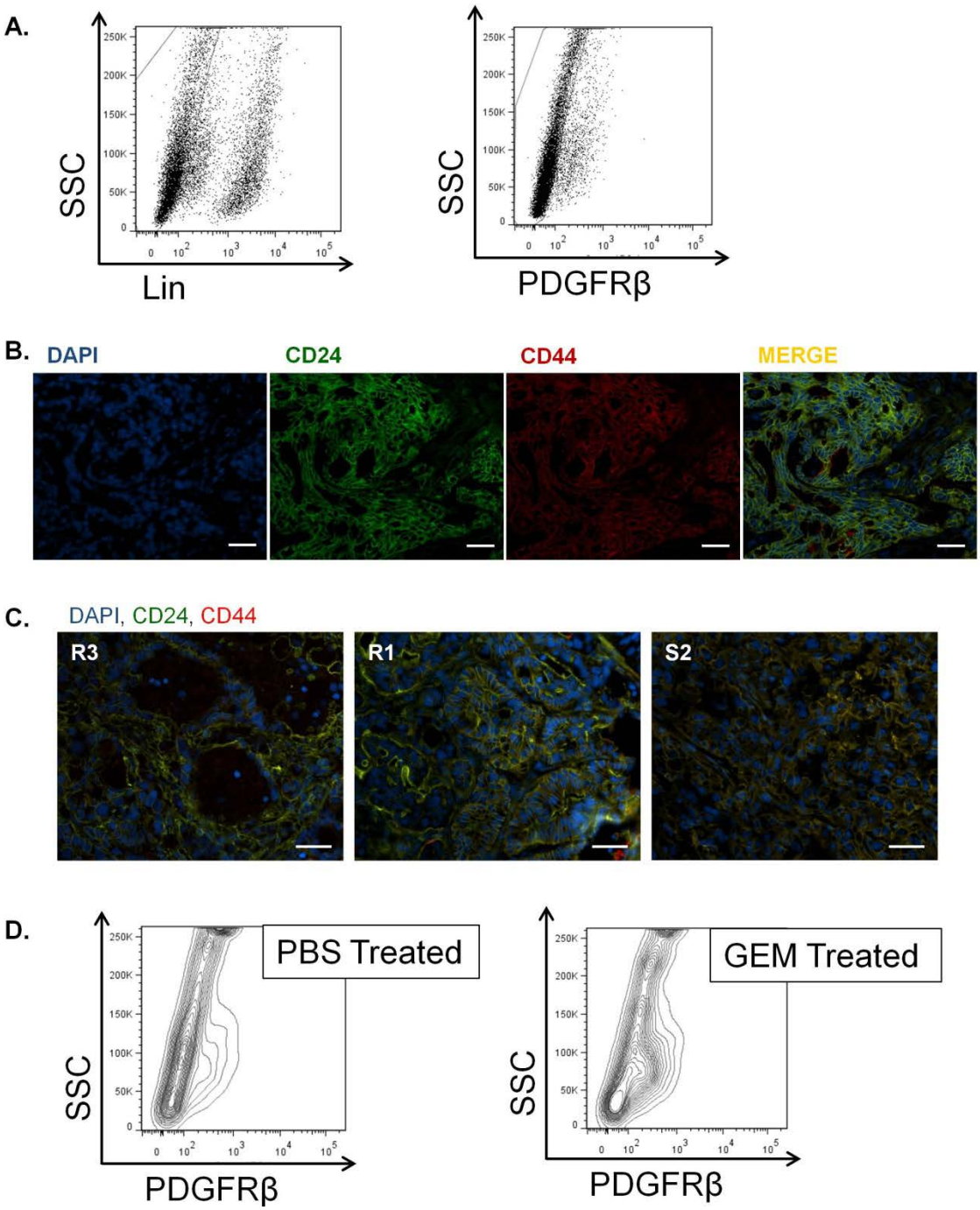

Supp Figure S4-4: Marker expression patterns are determined by FACS and immunofluorecsence. (A) For FACS analysis, murine cells were excluded through expression of a three antibody cocktail termed 'Lin' – CD45 (leukocyte), CD31 (endothelial), Ter119 (red blood cell). Additionally, fibroblast cells were excluded through an anti-human and anti-mouse PDGFRβ cocktail. (B-C) Immunofluorescent analysis of human xenografts with CD24 (green), CD44 (red), and (DAPI) shows these cancer stem cell markers are not confined to a small tumor population (scale: 50μm). (D) FACS blots showing the variability of expression of PDGFRβ after gemcitabine treatment.

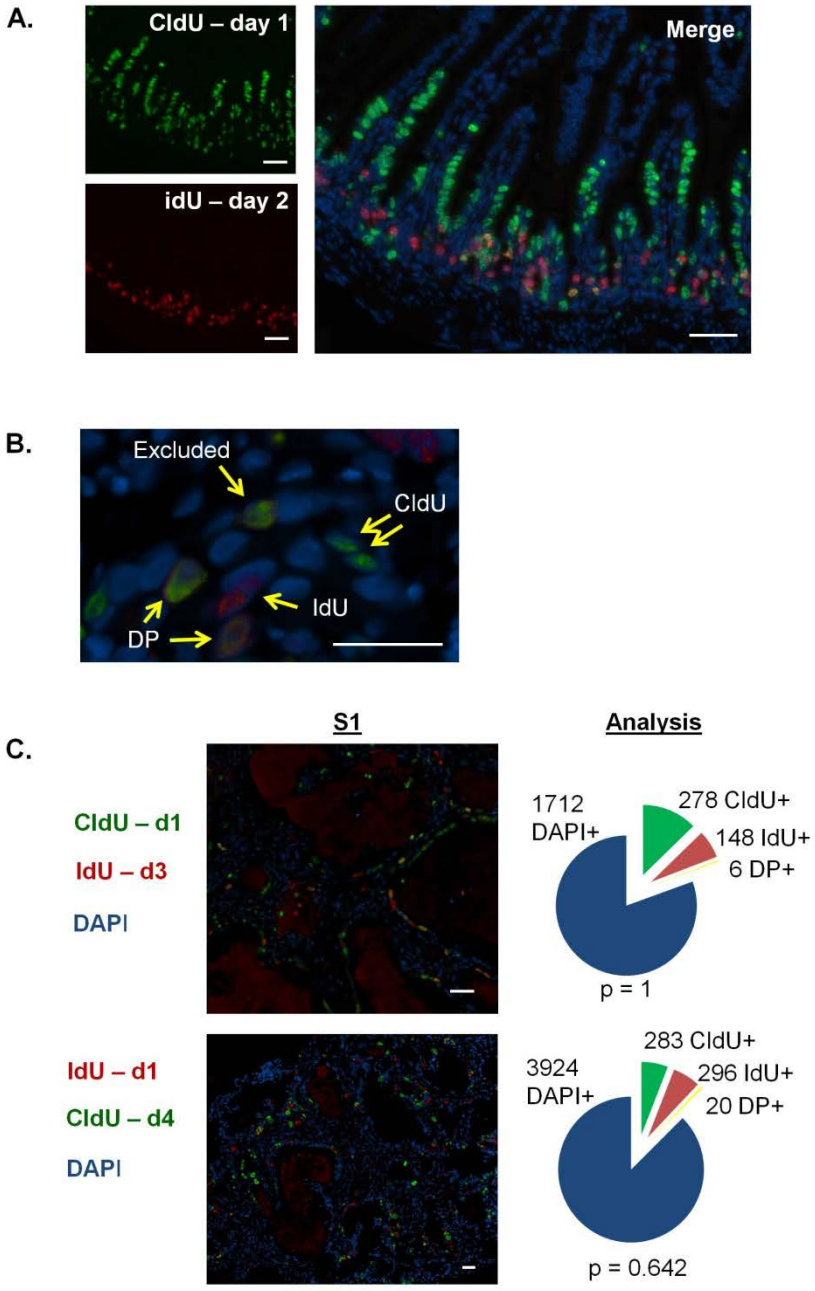

Supp Figure S4-5: Pulse and chase with CldU and IdU can effectively identify proliferating cells. (A) Mice were pulsed with CldU (green) and IdU (red) on consecutive days and intestines harvested 24hr after the last pulse. Immunofluorescent staining of intestines reveals many cells initially pulsed with CldU have migrated up the stalk, while newer IdU pulsed cells are in closer to the crypts. Double-labeled cells indicate stem/progenitor cells which continually proliferate and give rise to differentiated progeny (scale: 50μm). (B) Immunoflerescent staining of pulse-chase human xenograft tumors. Examples of single CldU+, IdU+, Double positive (DP), and Excluded cells are shown with arrowheads (scale: 50μm). (C) Immunofluorescent staining of xenografts with CldU (green), IdU (red), and DAPI (blue) (scale: 50μm). Quantitation of positive tumor cells are displayed in the pie charts, with no significant enrichment of double positive cells as calculated by Fisher Exact Test.

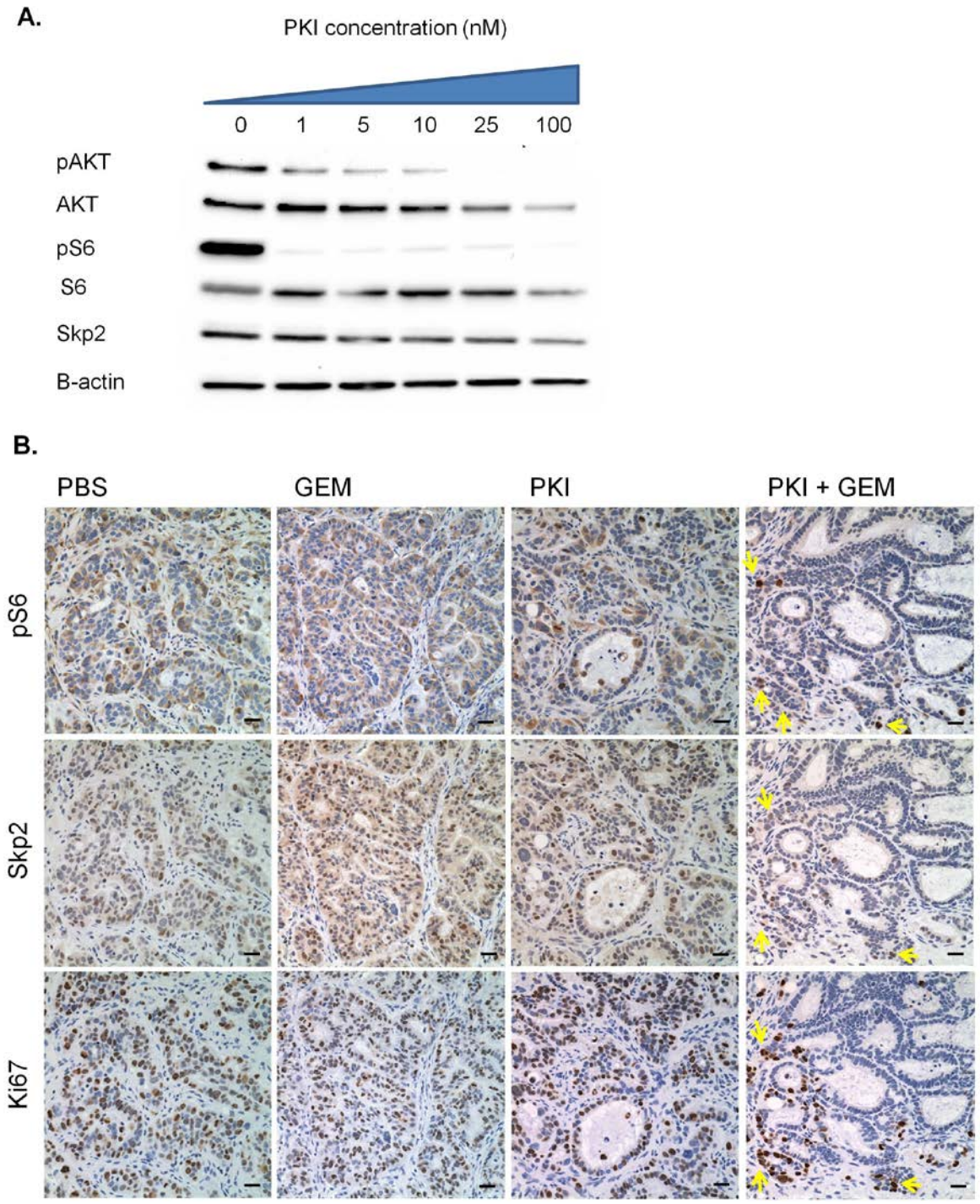

Supp Figure S4-6: PKI-587 can decrease pS6 and Skp2 levels *in vitro* and *in vivo*. (A) AsPC1 cells were cultured for 24 hours with an increasing concentration of PKI-587. Western blot analysis confirmed inhibition of the AKT and mTOR pathways, as well as inhibition of Skp2. (B) Immunohistochemical staining of xenografts after 16-day treatment with gemcitabine, PKI-587, or both *in vivo*. Dual treatment resulted in significant downregulation of pS6, Skp2, and Ki67. Interestingly, remaining Ki67+ cells tended to have high expression of Skp2 and pS6 (arrows) (scale: 50μm).

IV. Materials and Methods

Isolation and engraftment of primary PDAC. Human pancreatic ductal adenocarcinoma tissue was obtained via a research protocol that was approved by the UCLA Institutional Review Board. Informed written consent was obtained by all participants. A piece of cancer tissue was dissected away from the total surgically resected specimen following pancreatectomy. PDAC tissue specimens were brought immediately to the laboratory and minced into small fragments (1 mm^3) with razor blades in PBS, dipped into a 1:1 mix of Matrigel (Becton Dickinson) and DMEM:F12 (Invitrogen), and surgically implanted into the subcutaneous flanks of recipient NOD:SCID IL2γ knock-out (NSG) mice.

Single cell dissociation and xenotransplantation. Engrafted tumors were harvested and minced into small pieces, washed with PBS, then went through enzymatic digestion for 2.5-3 hr in 1 mg/mL Type IV collagenase (Invitrogen) at 37 °C with constant agitation. Digestion media was supplemented with 3mM $CaCl_2$, 0.1mg/mL DNAse I (Roche), Soybean Trypsin Inhibitor (Calbiochem), and 10mM HEPES (Invitrogen) in HBSS (Invitrogen). Cell suspensions were washed in DMEM:F12 media with 10% FBS containing DNAse I and Soybean Trypsin Inhibitor, then triturated through consecutive 18-gauge and 23-gauge needles and were passed through 40-μm filters. Cells were then xenotransplanted, FACS analyzed, or frozen for future study. For xenotransplantation, 1-5x10^6 single cells were mixed 1:1 into Matrigel/DMEM:F12 and implanted into subcutananeous flanks of NSG mice for *in vivo* drug studies.

Drug treatment protocol and measurements. Tumors were allowed to grow to approximately 4-5 mm in width when treatment commenced. Gemcitabine (Eli Lilly) was injected twice weekly for 3-4 weeks intraperitoneally at a dose of 100mg/kg, with PBS used for control treatment arm. After treatment period, some mice were released from drug and monitored up to 5 weeks. Tumor size was measured twice weekly with calipers utilizing length and width for volume assessments ($0.52*Length*Width^2$). For dual treatment, PKI-587 (Pfizer) was injected twice weekly intraperitoneally at a dose of 25mg/kg, diluted in 5% dextrose and 0.25% lactic acid vehicle. All animal experiments were performed following Institutional Approval for Appropriate Care and use of Laboratory animals by the UCLA Institutional Animal Care and Use Committee (Chancellor's Animal Research Committee).

FACS sorting and analysis. Dissociated tumor cells were suspended in HBSS/2% FBS and stained with antibodies for 15 min at 4 °C. Antibodies are listed in Supp Table 3. Cell sorting was performed using BD FACS Aria in the UCLA Jonsson Comprehensive Cancer Center and Center for AIDS Research Flow Cytometry Core Facility. FACS analysis was performed with BD FACS LSRII (BD Biosciences, San Jose, CA).

Immunohistochemistry and immunofluorescence analyses. Immunohistochemical analysis was performed on formalin-fixed, paraffin-embedded tissue. Antigen retrieval was performed by heating the slides at 95°C in citrate buffer (pH 6.0) for 15 minutes. Stains were visualized with Vectastain ABC Elite Kit (Vector Labs). Sections (4μm) were stained with hematoxylin and eosin (H&E) or with specific antibodies against Ki67 (1:500, Vector), PDGFRβ (1:100, Cell Signaling), Skp2 (1:100, Invitrogen), pS6 (1:100, Cell Signaling), PTEN (1:100, Cell Signaling),

SMA (1:1000, Sigma), and PanCK (1:1000, Sigma). Immunofluorescence was performed on frozen tissue after fixation with cold methanol for 10 minutes with the following antibodies: CD31 (1:500, BD), EpCAM (1:200, Abcam), CD44 (1:100, eBioscience), and CD24 (1:100, NeoMarkers). DAPI Anti-Fade reagent (Invitrogen) was used as a counterstain.

Ki67 index quantification. 8 regions were selected at 40x magnification for each xenograft sample with biological duplicates. Stromal cells were excluded from analysis. Tumor nuclei were counted manually using ImageJ software.

Western Blot analysis. Total protein was extracted with SDS buffer (50 mM Tris-HCl, pH 7.5, 150 mM NaCl, 1 mM EGTA, 1mM EDTA, 1% NP-40, 0.5% sodium deoxycholate, 1% sodium dodecyl sulfate) with freshly added phosphatase inhibitors (Sigma) and protease inhibitors (GE Healthcare). Protein concentrations were determined by BCA Protein Assay (Thermo Scientific). Protein was separated by 10-12% SDS/PAGE with a 5% stacking gel and transferred onto a nitrocellulose membrane (BioRad). The membrane was blocked in 5% skim milk or BSA, and subsequently incubated with primary antibodies against dCK (1:2000, Sigma), CDA (1:300, Sigma), b-actin (1:20000, Sigma), PTEN (1:1000, Cell Signaling), phospho-S6 (1:1000, Cell Signaling), S6 (1:1000, Cell Signaling), Skp2 (1:500, Invitrogen), p27 (1:500, Santa Cruz), phospho-AKT Ser473 (1:1000, Cell Signaling), AKT (1:1000, Cell Signaling), and γH2AX (1:1000, Cell Signaling) overnight at 4°C, followed by incubation with peroxidase-conjugated anti-mouse or anti-rabbit IgG and developed with ECL Prime reagent (GE Healthcare). Blots were developed and analyzed utilizing the ChemiDoc XRS+ platform with ImageLab software (BioRad).

RNA Isolation and qRT-PCR. Sorted cells were collected, spun down, and RNAs were extracted using TRIzol® Reagent (Invitrogen). RNAs were reverse transcribed into cDNA with SuperScript III First-Strand Synthesis System for qRT-PCR (Invitrogen), and quantitative PCR was done in the iQ thermal cycler (BioRad) using the iQSYBR Green Supermix (BioRad) in triplicate. Primers used were Ck19 (F5′- ATGGCCGAGCAGAACCGGAA-3′; R5′-CCATGAGCCGCTGGTACTCC-3′), EpCAM (F5′- CGCAGCTCAGGAAGAATGTG-3′; R5′-TGAAGTACACTGGCATTGACG-3′), Vimentin (F5'-TCTGGATTCACTCCCTCTGG -3'; R5'-GCAGAAAGGCACTTGAAAGC -3'), PDGFRβ (F5′- GTGAACGCAGTGCAGACTGT-3′; R5'- AGGTGTAGGTCCCCGAGTCT-3′), RPL13a (F5'-CATCGTGGCTAAACAGGTACTG-3'; R5'- GCACGACCTTGAGGGCAGCC-3').

Gene expression processing and analysis. The gene expression was investigated by Affymetrix HGU133 Plus 2 Array. The mRNA expression data from CEL files was normalized by using the Bioconductor *rma* package. Two-tail t-test was used for comparing expression between gemcitabine sensitive (n = 2) and resistant (n = 5) groups. For a gene represented by multiple probes, its representative probe was the one with the lowest p-value among the probes. A differentially expressed gene between two groups was identified based on (1) its t-test p-value <0.05 and (2) fold-change>1.5. Gene set enrichment analysis (GSEA) (Subramanian 2005) was used to identified altered pathways whose data base was downloaded from KEGG (http://www.kegg.jp/). Cluster 3.0 was used in hierarchical clustering analysis in which the expression profile of each probe/gene was first transformed to z-scores, and then samples were clustered by using average linkage method based on un-centered correlation coefficients as distance metric among samples.

DCK kinase assay. Analysis of dCK kinase activity was measured as described previously (Shu 2010). Proteins were either extracted from 50 mg tumor tissue or, by freeze-thawing in liquid nitrogen, from cell lines (10^6 cells). First, tumor tissue was minced with a scalpel on ice. Broken-down tissue was then resuspended in 400 µl dCK kinase lysis buffer containing 50 mM Tris-HCl (pH 7.6), 2 mM DTT, 20% glycerol, 0.5% Nonidet P40, and proteinase inhibitors. Proteins were extracted on ice using a ULTRA-TURRAX® T 10 (VWR LLC) tissue homogenizer. 2 µg of total protein extracts were incubated for 20 min with 1 µCi ^{3}H-FAC at 37^0C in a buffer containing 50 mM Tris-HCl (pH 7.6), 5 mM $MgCl_2$, 2 mM DTT, 10 mM NaF, 5 mM UTP and 1 mM thymidine. The reaction was quenched by adding ice-cold water and enzyme activity stopped by heat-inactivation for 2 min at 95 ^{0}C. Samples were spotted onto DE-81 filter discs (Whatman Inc), dried and washed three times in 4 mM ammonium formate and twice in EtOH. Dried filter discs were placed into scintillation vials and radiation analyzed using a Tri-Carb® 2100 liquid scintillation analyzer.

MicroPET/CT Imaging. Mice were kept warm under gas anesthesia (2% isoflurane) and injected with 200 µCi of 18F-labeled probes (i.v. for ^{18}F-FAC, i.p. for ^{18}F-FDG). 1 hr interval for uptake was allowed between probe administration and microPET/CT scanning. Data were acquired using a Preclinical Solutions microPET Focus 220 (Siemens) and a MicroCAT II CT instrument (Siemens). MicroPET data were acquired for 10 min and was reconstructed using statistical maximum a posteriori probability algorithms (MAP) into multiple frames (Qi 1998). The spatial resolution of PET is ~1.5 mm, 0.4 mm voxel size. CT images are at low dose 400 µm resolution acquisitions, with 200 µm voxel size. MicroPET and microCT images were co-registered using a previously described method (Chow 2006). 3D regions of interest (ROI) were

drawn using Osirix software. Color scale is proportional to tissue concentration with red being the highest and lower values in yellow, green & blue.

***In vitro* sphere assay.** Pancreatic tumor cells were grown as previously described (Li 2011). Briefly, tumor cells were dissociated to single cells, with 5,000 cells placed per 96 well low-attachment plate (Corning). Spheres were grown in DMEM:F12 media supplemented with N-2, B27, Glutamax, 20ng/mL EGF (Invitrogen), and 20ng/mL bFGF (R&D Systems). Prior to culture, tumor cells were separated from fibroblasts utilizing magnetic beads. Cells were incubated with APC conjugated anti-PDGFRβ, CD31, CD45, and Ter119 antibodies, washed, and mixed with anti-APC magnetic beads (Miltenyi Biotec). Cells were then run through MACS LD Separation columns (Miltenyi Biotec), and flow-through PDGFRβ- cells were used for sphere culture.

siRNA transfection. Skp2 custom siRNA oligonucleotides were obtained from Bioland: Skp2-1 (F5′- GGGAGUGACAAAGACUUUG-3′; R5′- CAAAGUCUUUGUCACUCCC-3′); Skp2-2 (F5′- GCAUGUACAGGUGGCUGUU-3′; R5′- AACAGCCACCUGUACAUGC-3′). FAM-labeled siRNA duplex was used as negative control. Cell lines were cultured in 6 or 24-well format. 3uL of HiPerFect Transfection Reagent (Qiagen) was added per 100uL of diluted siRNA and incubated at room temperature for 10 minutes. siRNA was then transferred to each well at a final concentration of 50nM.

Cell proliferation assay. $2*10^5$ cells were seeded in each 24-well plate one day prior to drug addition. On day 0, media was changed and either drug (Gemcitabine, PKI-587) or siRNA

(Skp2) was added to each well at appropriate concentrations and combinations in triplicate. After 72 hours, MTT was added to each well according to manufacturer's protocols (Molecular Probes). Plate absorbance was analyzed at 570nM using Benchmark Plus Microplate Spectrophotometer with Microplate Manager software (BioRad).

Pulse/Chase experiment. Both IdU and CldU were administered i.p. at 100mg/kg. Mice were sacrificed 24 hours after the last pulse, with tumors harvested, fixed in formalin, and prepared for immunohistochemical analysis as previously described (Tuttle 2010). Mouse anti-BrdU is specific for IdU (1:250, BD) and Rat anti-BrdU for CldU (1:250, Novus). Tissue sections were analyzed and counted with Ariol Wholeslide Scanner and Software. Fisher Exact Test was used for statistical analysis.

References

Adams JM and Strasser A (2008). Is Tumor Growth Sustained by Rare Cancer Stem Cells or Dominant Clones? Cancer Research, *68*: 4018-4021.

Akada M, Jurcevic T, Lattimore S, Mahon P, Lopes R, Sunamura M, Seiki M, Lemoine NR (2005). Intrinsic Chemoresistance to Gemcitabine is Associated with Decreased Expression of BNIP3 in Pancreatic Cancer. Clin Cancer Res, *8*: 3094-3101.

American Cancer Society (2013). Cancer Facts and Figures 2013. Atlanta: American Cancer Society

Bachem MG, Zhous S, Buck K, Schneiderhan W, Siech M (2008). Pancreatic stellate cells – role in pancreas cancer. Langerbecks Arch Surg, *393*: 891-900.

Barretina J, Caponigro F, Stransky N, Venkatesan K, Margolin A, Kim S, Wilson C, Lehar J, Kryukov G, Sonkin D, Reddy A, Liu M, Murray L, Berger MF, Monahan JE, Morais P et al, Porter J, Warmuth M, Finan P, Harris JL, Meyerson M, Golub T, Morrissey MP, Sellers W, Schlegel R, Garraway L (2012). The Cancer Cell Line Encyclopedia enables predictive modeling of anticancer drug sensitivity. Nature, *483*: 603-607.

Bashir T and Pagano M (2004). Don't Skip the G^1 Phase: How APC/C^{Cdh1} Keeps SCF^{Skp2} in Check. Cell Cycle, *3*: 850-852.

Bhagwandin VJ and Shay JW (2009). Pancreatic cancer stem cells: Fact or fiction? Biochimica et Biophysica Acta, *1792*: 248-259.

Biankin AV et al, International Cancer Genome Consortium (2012). Pancreatic cancer genomes reveal aberrations in axon guidance pathway genes. Nature, *491*: 399-405.

Burris H, Moore MJ, Andersen J, Green MR, Rothenberg ML, Modiano MR, Cripps MC, Portenay RK, Storniolo AM, Tarassoff P, Nelson R, Dorr FA, Stephens CD, Von Hoff DD (1997). Improvements in Survival and Clinical Benefit With Gemcitabine as First-Line Therapy for Patients With Advanced Pancreas Cacner: A Randomized Trial. J Clin Oncol *15*: 2403-2413.

Campbell PJ, Yachida S, Mudia LJ, Stephens PJ, Pleasance ED, Stebbings LA, Morsberger LA, Latimer C, McLaren S, Lin ML, McBride DJ, Varela I, Nik-Zainal SA, Leroy C, Jia M, Menzies A, Butler AP, Teague JW, Griffin C, Burton J, Swerdlow H, Quail M, Stratton MR, Iacobuzio-Donahue C, Futreal A (2010). The patterns and dynamics of genomic instability in metastatic pancreatic cancer. Nature, *467:* 1109-1113.

Chan CH, Lee SW, Wang J, Lin HK (2010). Regulation of Skp2 Expression and Activity and Its Role in Cancer Progression. Sci World Journal, *10*: 1001-1015.

Chan CH, Li CF, Yang WL, Gao Y, Lee SW, Feng Z, Huang HY, Tsai K, Flores LG, Shao Y, Hazle JD, Yu D, Wei W, Sarbassov D, Hung MC, Nakayama K, Lin HK (2012). The Skp2-SCF E3 Ligase Regulates Akt Ubiquitination, Glycolysis, Herceptin Sensitivity, and Tumorigenesis. Cell *149*: 1098-1111.

Chen J, Yu T, McKay R, Burns D, Kernie S, Parada L (2012). A restricted cell population propagates glioblastoma growth after chemotherapy. Nature, *488*: 522-526.

Chow PL, Stout DB, Komisopoulou E, Chatziioannou AF. A method of image registration for small animal, multi-modality imaging. Phys Med Biol, *51*: 379-390.

Collisson EA, Sadanandam A, Olson P, Gibb WJ, Truitt M, Gu S, Cooc J, Weinkle J, Kim GE, Jakkula L, Feiler HS, Ko AH, Olshen AB, Danenberg KL, Tempero MA, Spellman PT, Hanahan D, Gray JW (2010). Subtypes of pancreatic ductal adenocarcinoma and their differing responses to therapy. Nature Medicine, *4*: 500-503.

Conlon KC, Klimstra DS, Brennan MF (1996). Long-term survival after curative resection for pancreatic ducatal adenocarcinoma: clinicopathologic analysis of 5-year survivors. Ann Surg, *223*: 273-279.

Conroy T, Desseigne F, Ychou M, Bouche O, Fuimbaud R, Becouarn Y, Adenis A, Raoul JL, Fourgou-Bourgade S, Bachet JB, Akouz, F, Pere-Verge D, Delabaldo C, Assenat E, Chauffert B, Michel P, Montoto-Grillot C, Chem M, Ducreux M (2011). FOLFIRONOX versus Gemcitabine for Metastatic Pancreatic Cancer. NEJM, 364: 1817-1825.

Dalerba P, Cho RW, Clarke MF (2007). Cancer stem cells: models and concepts. Annu Rev Med, *58*: 267-284.

Dietel M, Johrens K, Laffert M, Hummel M, Blaker H, Muller BM, Lehmann A, Denkert C, Heppner FL, Koch A, Sers C, Anagnostopoulos I (2013). Predictive molecular pathology and its role in targeted cancer therapy: a review focusing on clinical relevance. Cancer Gene Ther,

Donahue TR, Tran LM, Hill R, Li Y, Kovochich A, Calvopin J, Patel S, Wu N, Hindoyan A, Farrel JJ, Li X, Dawson D, Wu H (2012). Integrative Survival-Based Molecular Profiling of Human Pancreatic Cancer. Clin Cancer Res, *18*: 1352-1363.

Duxbury MS, Ito H, Zinner MJ, Ashley SW, Whang EE (2004). RNA interference targeting the m2 subunit of ribonuncleotide reductase enhances pancreatic adenocarcinoma chemosensitivity to gemcitabine. Oncogene, 23: 1539-1548.

Eda H, Ura M, F-Ouchi K, Tanaka Y, Miwa M, and Ishitsuka H (1998). The antiproliferative activity of DMDC is modulated by inhibition of cytidine deaminase. Cancer Res, *58:* 1165-1169.

Einama T, Kagata Y, Tsuda H, Morita D, Ogata S, Ueda S, Takigawa T, Kawarabayashi N, Fukatsu K, Sugiura Y, Matsubara O, Hatsuse K (2006). High-level Skp2 Expression in Pancreatic Ductal Adenocarcinoma: Correlation with the Extent of Lymph Node Metastasis, higher Histological Grade, and Poorer Patient Outcome. Pancreas, *32*: 376-381.

Farrow B, Albo D, Berger D (2008). The Role of the Tumor Microenvironment in the Progression of Pancreatic Cancer. J Surg Res, *149*: 319-328.

Frank N, Schatton T, Frank M (2010). The therapeutic promise of the cancer stem cell concept. Jour Clin Invest, *120*: 41-50.

Frescas D and Pagano M (2008). Deregulated proteolysis by the F-box proteins SKP2 and β-TrCP: tipping the scales of cancer. Nat Rev Cancer, *8*: 438-449

Fujita H, Ohuchida K, Mizumoto K, Itaba S, Ito T, Nakata K, Yu J, Kayashima T, Souzaki R, Tajiri T, Manabe T, Ohtsuka T, Tanaka M (2010). Gene Expression Levels as Predictive Markers of Outcome in Pancreatic Cancer after Gemcitabine-Based Adjuvant Chemotherapy. Neoplasia, *12*: 807-817.

Fukunaga AK, Marsh S, Murry DJ, Hurley TD, McLeod HL (2004). Identification and analysis of single-nucleotide polymorphisms in the gemcitabine pharmacologic pathway. Pharmacogenomics Journal, *4*: 307-314.

Gao D, Inuzuka H, Tseng A, Chin R, Toker A, Wei W (2009). Phosphorylation by Akt1 promotes cytoplasmic localization of Skp2 and impairs APC-Cdh1-mediated Skp2 destruction. Nat Cell Bio *11*: 397-408.

Garcia-Manteiga J, Molina-Arcas M, casado FJ, Mazo A, Pastor-Anglada M (2003). Nucleoside tranporter profiles in human pancreatic cancer cells: rolf of hent1 in 2',2'-difluorodeoxycytidine-induced cytotoxicity. Clin Cancer Res, *9*: 5000-5008.

Garnett MJ, Edelman EJ, Heidorn S, Greenman CD, Dastur A, Lau KW, Greninger P, Thompson I, Luo X, Soares J, Liu Q, Iorio F, Surdez D, Chen L, Milano RJ, Bignell G, Tam AT et al, Engelman JA, Sharma SV, Delattre O, Saez-Rodriguez J, Gray NS, Settleman J, Futreal PA, Haber DA, Stratton MR, Ramaswamy S, McDermotte U, Benes CH (2012). Systematic identification of genomic markers of drug sensitivitiy. Nature, 483: 570-575.

Garrido-Laguna I, Uson M, Rajeshkumar, Tan AC, de Oliveira E, Karikari C, Villaroel MC, Salomon A, Taylor G, Sharma R, Hruban RH, Maitra A, Laheru D, Rubio-Viqueira B, Jimeno A, Hidalgo M (2011). Tumor engraftment in nude mice and enrichment in stroma-related gene pathways predicts poor survival and resistance to gemcitabine in patients with pancreatic cancer. Clin Cancer Res, *17*: 5793-5800.

Hafsi S, Pezzino FM, Candido S, Ligresti G, Spandidos DA, Soua Z, McCubrey JA, Travali S, Libra M (2012). Gene alterations in the PI3K/PTEN/AKT pathway as a mechanism of drug-resistance (review). Int J Oncol, *40*: 639-644.

Hanahan D and Weinberg RA (2011). Hallmarks of Cancer: The Next Generation. Cell, *144*: 646-674.

Heldin CH, Westermark B (1990). Signal Transduction by the receptors for platelet-derived growth factor. J Cell Sci, *96*: 193-196.

Hermann PC, Huber SL, Herrier T, Aicher A, Ellwart J, Guba M, Bruns CJ, Heeschen C (2007). Distinct Populations of Cancer Stem Cells Determine Tumor Growth and Metastatic Activity in Human Pancreatic Cancer. Cell Stem Cell, 1: 313-323.

Hill R, Li Y, Tran L, Dry S, Calvopina J, Garcia A, Kim C, Wang Y, Donahue T, Herschman HR, Wu H (2012). Cell intrinsic role of COX-2 in pancreatic cancer development. Mol Cancer Ther, *11*: 2127-2137.

Hong SP, Wen J, Bang S, Park S, Song, SY (2009). CD44-positive cells are responsible for gemcitabine resistance in pancreatic cancer cells. Int J Cancer, *125*: 2323-2331.

Hori Y, Fukumoto M, Kuroda Y (2008). Enrichment of Putative Pancreatic progenitor Cells from Mice by Sorting for Prominin1 (CD133) and Platelet-Derived Growth Factor Receptor β. Stem Cells, *26*: 2912-2920.

Huang H, Regan KM, Wang F, Wang D, Smith D, can Deursen J, Tindall DJ (2005). Skp2 inhibits FOXO1 in tumor suppression through ubiquitin-mediated degradation. PNAS, 102: 1649-1654.

Hu R and Aplin A (2008). Skp2 Regulates G2/M Progression in a p53-dependent Manner. Mol Bio Cell, *19*: 4602-4610.

Hung SW, Mody H, Govindarajan R (2012). Overcoming nucleoside analog chemoresistance of pancreatic cancer: A therapeutic challenge. Cancer Letters, *320:* 138-149.

Hwang RF, Moore T, Arumugam T, Ramachandran V, Amos K, Rivera A, Ji B, Evans D, Logsdon C (2008). Cancer-Associated Stromal Fibroblasts Promote Pancreatic Tumor Progression. Cancer Res, *68*: 918-926.

Jimeno A, Feldmann G, Suarez-Gauthier A, Rasheed Z, Solomon A, Zou GM, Rubio-Viqueiro B, Garcia E, Lopez-Rios F, Matsui W, Maitra A, Hidalgo M (2009). A direct pancreatic cancer xenograft model as a platform for cancer stem cell therapeutic development. Mol Cancer Ther, *8*: 310-314.

Jonason JH, Gavrilova N, Wu M, Zhang H, Sun H (2007). Regulation of SCF^{SKP2} Ubiquitin E3 Ligase Assembly and $p27^{KIP1}$ Proteolysis by the PTEN Pathway and Cyclin D1. Cell Cycle, 6: 951-961.

Jones S, Zhang X, Parsons D, Lin J, Leary R, Angenendt P, Mankoo P, Carter H, Kamiyama H, Jimeno A et al, Hruban RH, Karchin, Papadopoulos N, Parmigiani G, Vogelstein B, Velculescu V, Kinzler K (2008). Core Signaling Pathways in Human Pancreatic Cancers Revealed by Global Genomic Analyses. Science, 321: 1801-1806.

Kalia M (2013). Personalized oncology: Recent advances and future challenges. Metabolism, *62*: S11-14.

Kim MP, Fleming JB, Wang H, Abbruzzese JL, Choi W, Kopetz S, McConkey DJ, Evans, DB, Gallikc GE (2011). ALDH Activity Selectively Defines an Enhanced Tumor-Initiating Cell Population Relative to CD133 Expression in Human Pancreatic Adenocarcinoma. Plos One, *6*: e20636.

King SL, Dekaney CM (2013). Small intestinal stem cells. Curr Opin Gastroenterol, *29*: 140-45.

Kraman M, Bambrough PJ, Arnold JN, Roberts EW, Magiera L, Jones JO, Gopinathan A, Tuveson DA, Fearon DT (2010). Suppression of Antitumor Immunity by Stromal Cells Expressing Fibroblast Actiavation Protein-a. Science, *330*: 827-830.

Lee C, Dosch J, Simeone (2008). Pancreatic Cancer Stem Cells. J Clin Oncol, *26*: 2806-2812.

Lewis MT (2008). Faith, heresy and the cancer stem cell hypothesis. Future Oncol, *4*: 585-589.

Li C, Wu JJ, Hynes M, Dosch J, Sarkar B, Welling T, Magliano M, Simeone D (2011). c-Met is a Marker of Pancreatic Cancer Stem Cells and Therapeutic Target. Gastro *141*: 2218-2227.

Li C, Heidt DG, Dalerba P, Burant CF, Zhang L, Adsay V, Wicha M, Clarke M, Simeone D (2007). Identification of Pancreatic Cancer Stem Cells. Cancer Research, *67*: 1030-1037.

Lin HK, Wang G, Chen Z, Teruya-Feldstein J, Liu Y, Chan CH, Yang WL, Erdjument-Bromage H, Nakayama K, Nimer S, Tempst P, Pandolfi PP (2009). Phosphorylation-dependent regulation of cytosolic localization and oncogenic function of Skp2 by Akt/PKB. Nat Cell Bio *11*: 420-431.

Lobrich M and Jeggo PA (2007). The impact of a negligent G2/M checkpoint on genomic instability and cancer induction. Nat Rev Cancer, *7*: 861-869.

Lord C and Ashworth A (2012). The DNA damage response and cancer therapy. Nature, *481*: 287-294.

Mallon R, Feidberg LR, Lucas J, Chaudhary I, Dehnhardt C, Santos ED, Chen Z, dos Santos O, Ayral-Kaloustian S, Venkatesan A, Hollander I (2011). Antitumor Efficacy of PKI-587, a Highly Potent Dual PI3K/mTOR Kinase Inhibitor. Clin Can Research, *17*: 3193-3203.

Mantoni TS, Lunardi S, Al-Assar O, Masamune A, Brunner TB (2011). Pancreatic Stellate Cells Radioprotect Pancreatic Cancer Cells through β1-Integrin Signaling. Cancer Res, *71*: 3453-3458.

Mamillapalli R, Gavrilova N, Mihaylova VT, Tsvetkov L, Wu H, Zhang H, Sun H (2001). PTEN regulates the ubiquitin-dependent degradation of the CDK inhibitor $p27^{KIP1}$ through the ubiquitin E3 ligase SCF^{SKP2}. Current Biology, *11*: 263-267.

Mann K, Ward JM, Yew C, Kovochich A, Dawson D, Black MA, Bret BT, Sheetz TE, Dupuy AJ, Chang DK, Biankin AV, Waddell N, Kassahn KS, Grimmond SM, Rust AG, Adams DJ, Jenkins AN, Copeland NG (2012). Sleeping Beauty muragenesis reveals cooperating mutations and pathways in pancreatic adenocarcinoma. PNAS, *109:* 5934-5941.

Mimeault M, Hauke R, Mehta P, Batra S (2007). Recent advances in cancer stem/progenitor cell research: therapeutic implications for overcoming resistance to the most aggressive cancers. J Cell Mol Med, *11*: 981-1011.

Moore M, Goldstein D, Hamm J, Figer A, Hecht J, Gallinger S, Au H, Murawa P, Walde D, Wolff R, Campos D, Lim R, Ding K, Clark G, Voskoglou-Nomikos T, Ptaysnski M, Parulekar W (2007). Erlotinib Plus Gemcitabine Compared With Gemcitabine Alone in Patients With Advanced Pancreatic Cancer: A Phase III Trial of the National Cancer Institute of Canada Clinical Trials Group. Journal of Clinical Oncology, *25*: 1960-1966.

Morris JP, Wang SC, Hebrok M (2010). KRAS, Hedgehog, Wnt and the twisted developmental biology of pancreatic ductal adenocarcinoma. Nat Rev Cancer, *10*: 683-695.

Muerkoster S, Wegehenkel K, Arlt A, Witt M, Sipos B, Kruse ML, Sebens T, Kloppel G,Kalthoff H, Folsch UR, Schafer H (2004). Tumor Stroma Interactions Induce Chemoresistance in Pancreatic Ductal Carcinoma Cells Involving Increased Secretion and Paracrine Effects of Nitric Oxide and Interleukin-1β. Cancer Res, *64*: 1331-1337.

Nakayama K, Nagaharna H, Minarnishima Y, Miyake S, Ishida N, Hatakeyama S, Kitagawa M, Iernura S, Natsurne T, Nakayam K (2004). Skp2-Mediated Degradation of p27 Regulates Progression into Mitosis. Developmental Cell, *6*: 661-672.

Neesse A, Michl P, Frese K, Feig C, Cook N, Jacobetz M, Lolkema M, Bucholz M, Olive K, Gress T, Tuveson D (2011). Stromal biology and therapy in pancreatic cancer. Gut, *60*: 861-8.

O'Connell JT, Sugimoto H, Cooke VG, MacDonald BA, Mehta AI, LeBleu V, Dewar R, Rocha R, Brentani R, Resnick M, Neilson E, Zeisberg M, Kalluri R (2011). VEGF-A and Tenascin-C produced by S100A4+ stromal cells are important for metastatic colonization. PNAS, *108*: 16002-16007.

Oettle H, Post S, Neuhaus P, Gellert K, Langrehr J, Ridwelski K, Schramm H, Fahlke J, Zuelke C, Burkart C, Gutberlet K, Kettner E, Schmalenberg H, Weigang-Koehler K, Bechstein W, Niedergethmann M, Schmidt-Wolf I, Roll L, Doerken B, Riess H (2007). Adjuvant Chemotherapy With Gemcitabine vs Observation in Patients Undergoing Curative-Intent Resection of Pancreatic Cacner. JAMA, 297: 267-277.

Ohuchida K, Mizumoto K, Murakami M, Qian LW, Sato N, Nagai E, Matsumoto K, Nakamura T, Tanaka M (2004). Radiation to Stromal Fibroblasts Increases Invasiveness of Pancreatic Cancer Cells through Tumor-Stromal Interactions. Cancer Res, *64*: 3215-3222.

Olive K, Jacobetz MA, Davidson CJ, Gopinathan A, McIntyre D, Honess D, Madhu B, Goldgraben MA, Caldwell ME, Allard D, Frese KK, DeNicola G, et al, Hingorani SR, Huang P, Davies S, Plunkett W, Egorin M, Hruban RH, Whitebread N, McGovern K, Adams J, Iacobuzio-Donahue C, Friffiths J, Tuveson DA (2009). Inhibition of Hedgehog Signaling Enhances Delivery of Chemotherapy in a Mouse Model of Pancreatic Cancer. Science, *324*: 1457-1461.

O'Reilly EM (2010). Refinement of Adjuvant Therapy for Pancreatic Cancer. JAMA, *304*: 1124-1125.

Pei H, Li L, Fridley B, Jenkins GD, Kalari KR, Lingle W, Petersen G, Lou Z, Wang L (2009). FKBP51 Affects Cancer Cell Response to Chemotherapy by Negatively Regulating Akt. Cancer Cell, 16: 259-266.

Pour PM, Pandey KK, Batra S (2003). What is the origin of pancreatic adenocarcinoma? Molecular Cancer, *2*:13.

Provenzano PP, Cuevas C, Chang A, Goel VK, Von Hoff DD, Hingorani SR (2012). Enzymatic Targetinf of the Stroma Ablates Physical Barriers to Treatment of Pancreatic Ductal Adenocarcinoma. Cancer Cell, *21*: 418-429.

Qi J, Leahy RM, Cherry SR, Chatziioannou A, Farquhar TH (1998). High-resolution 3D Bayesian image reconstruction using the microPET small-animal scanner. Phys Med Biol, *43*: 1001-1013.

Quintana E, Shackleton M, Sabel MS, Fullen DR, Johnson TM, Morrison SJ (2008). Efficient tumour formation by single human melanoma cells. Nature, *456:* 593-598.

Radu CG, Shu CJ, Nair-Gill E, Shelly SM, Barrio JR, Satyamurthy N, Phelps ME, Witte ON (2008). Molecular imaging of lymphoid organs and immune activation by positron emission tomography with a new [^{18}F]-labeled 2'-deoxycytidine analog. Nat Med, *14*: 783-788.

Reichert M, Saur D, Hamacher R, Schmid RM, Schneider G (2007). Phosphoinositide-3-Kinase Signaling Controls S-Phase Kinase-Associated Protein 2 Transcription via E2F1 in Pancreatic Ductal Adenocarcinoma Cells. Cancer Research, *67*: 4149-4156.

Rosen JM and Jordan CT (2009). The Increasing Complexity of the Cancer Stem Cell Paradigm. Science, *324*: 1670-1673.

Schuler S, Diersch S, Hamacher R, Schmid R, Saur D, Schneider G (2011). SKP2 confers resistance of pancreatic cancer cells towards TRAIL-induced apoptosis. Int Jou Onc,*38*: 219-225.

Shim EH, Johnson L, Noh HL, Kim YJ, Sun H, Zeiss C, Zhang H (2003). Expression of the F-Box Protein SKP2 Induces Hyperplasia, Dysplasia, and Low-Grade Carcinoma in the Mouse Prostate. Cancer Research, 63: 1583-1588.

Shipitsin M and Polyak K (2008). The cancer stem cell hypothesis: in search of definitions, markers, and relevance. Laboratory Investigation, *88*: 459-463.

Shah AN, Summy JM, Zhang J, Park SI, Parikh NU, Gallick GE (2007). Development and characterization of gemcitabine-resistant pancreatic tumor cells. Ann Surg Oncol, *14*: 3629-37.

Shu CJ, Campbell DO, Lee JT, Tran AQ, Wengrod JC, Witte O, Phelps M, Satyamurthy N, Czernin J, Radu C (2010). Novel PET Probes Specific for Deoxycytidine Kinase. J Nuc Med, *51:* 1092-1098.

Stanger B and Dor Y (2006). Dissecting the Cellular Origins of Pancreatic Cancer. Cell Cycle, *5*: 43-46.

Stathis A and Moore M (2010). Advanced pancreatic carcinoma: current treatment and future challenges. Nat Rev Clin Oncol, *7*: 163-172.

Staub M and Eriksson S (2006). The role of deoxycytidine kinase in DNA synthesis and nucleoside analog synthesis. In: Peters GJ, ed. Cancer Drug Discovery and Development: Deoxynucleoside Analogs in Cancer Therapy. Humana Press Inc, 29-52.

Soucy T, Smith P, Milhollen M, Berger A, Gavin J, Adhikari S, Brownell J, Burke K, Cardin D, Critchley S, Cullis C, Doucette A, Garnsey J et al, Weatherhead GS, Yu J, Zhang J, Dick L, Claiborne C, Rolfe M, Bolen J, Langston S (2009). An inhibitor of NEDD8-activating enzyme as a new approach to treat cancer. Nature, *458*: 732-736.

Song MS, Carracedo A, Salmena L, Song SJ, Egia A, Malumbres M, Pandolfi PP (2011). Nuclear PTEN regulates the APC-CDH1 tumor suppressive complex in a phosphatase-independent manner. Cell, *144*: 187-199.

Subramanian A, Tamayo P, Mootha VK, Mukherjee S, Ebert BL, Gillette MA, Paulovich A, Pomeroy SL, Golub TR, Lander ES, Mesirov JP (2005). Gene set enrichment analysis: a knowledge-based approach for interpreting genome-wide expression profiles. PNAS, *102*: 15545-15550.

Sultana A, Cox T, Ghaneh P, Neoptolemos JP (2012). Adjuvant therapy for pancreatic cancer. Recent Results Cancer Res, *196*: 65-88.

Sun Y, Campisi J, Higano C, Beer TM, Porter P, Coleman I, True L, Nelson PS (2012). Treatment-induced damage to the tumor microenvironment promotes prostate cancer therapy resistance through WNT16B. Nat Med, *18*: 1359-68.

Tuttle A, Rankin M, Teta M, Sartori D, Stein G, Kim G, Virgilio C, Granger A, Zhou D, Long S, Schiffman A, Kushner J (2010). Immunofluorescent Detection of Two Thymidine Analogues (CldU and IdU) in Primary Tissue. J Vis Exp, *46*: e2166, DOI: 10.3791/2166.

Van Duijn PW and Trapman J (2006). PI3K/AKT Signaling Regulates $p27^{kip1}$ Expression Via Skp2 in PC3 and DU145 Prostate Cancer Cells, but is not a Major Factor in $p27^{kip1}$ Regulation in LNCap and PC346 Cells. The Prostate, *66*: 749-760.

Wang Z, Fukushima H, Inuzuka H, Wan L, Liu P, Gao D, Sarkar F, Wei W (2012). Skp2 is a promising therapeutic target in breast cancer. Frontiers in Oncology, *1(57)*: 1-10.

Wang Z, Li Y, Ahmad A, Banerjee S, Azmi AS, Kong D, Sarkar FH (2011). Pancreatic cancer: understanding and overcoming chemoresistance. Nat Rev Gastro Hep, 8: 27-33.

Whitehurst AW, Bodemann BO, Cardenas J, Ferguson D, Girard L, Peyton M, Minna JD, Michnoff C, Hao W, Roth M, Xie XJ, White M (2007). Synthetic lethal screen identification of chemosensitizer loci in cancer cells. Nature, *446*: 815-819.

Wu L, Grigoryan A, Li YHao B, Pagano M, Cardozo T (2012). Specific Small Molecule Inhibitors of Skp2-Mediated p27 Degradation. Chemistry & Biology, *19*: 1515-1524.

Wu J, Zhang X, Zhang L, Wu CY, Rezaeian AH, Chan CH, Li JM, Wang J, Gao Y, Han F, Jeong YS, Yuan X, Khanna KK, Jin J, Zeng YX, Lin HK (2012). Skp2 E3 Ligase Integrates ATM Activation and Homologous Recombination Repair by Ubiquitinating NBS1. Molecular Cell, *46:* 351-361.

Yachida S, Jones S, Bozic I, Antal T, Leary R, Fu B, Kamiyama M, Hruban R, Eshleman JR, Nowak MA, Velculescu V, Kinzler K, Vogelstein B, Iacobuzio-Donahue CA (2010). Distant metastasis occurs lated during the genetic evolution of pancreatic cancer. Nature, *467*: 1114-1117.

Zhang X, Tang N, Hadden T, Rishi A (2011). Akt, FoxO and regulation of apoptosis. Biochimica et Biophysica Acta, *1813*: 1978-1986.

Chapter 5:

Concluding Remarks

I. Summary

The ‘cancer stem cell’ hypothesis remains an intriguing yet controversial concept in tumor biology. We sought to further explore its relevance within the context of prostate and pancreatic cancer. Throughout this dissertation, we have made use of two major experimental model systems to address this question: 1) genetically engineered mouse models (GEMs); and 2) patient-derived tumor samples and xenografts. While GEMs can provide the natural initiation and evolution of cancers within a native environment with defined genetic perturbations, patient samples and xenografts provide the genetic variability which can better model the functional heterogeneity observed in the clinic (Richmond 2008). Combined utility of both systems was a powerful and invaluable tool to dissect and address our specific questions.

a. Prostate

There is a rich literature on the existence of stem/progenitors cells in the prostate, shown functionally through the repeated rounds of involution and regeneration following castration (Tsujimura 2002). Both basal and luminal cells have been implicated to have putative stem/progenitor activity previously (Wang 2009, Goldstein 2010, Choi 2012). We have shown that CD166 can further enrich prostate stem/progenitor cells, and that this cell type may exhibit a basal/luminal intermediate cell type. Moreover, this population exhibits tumor-initiating properties and is enriched in human CRPC. Genetic deletion of CD166, however, does not delay tumor initiation or progression in the $Pten^{L/L}$ background, indicating CD166 may not have a functional role.

Another finding revealed that while Lgr5 does not mark a stem cell compartment in prostatic epithelium, Lgr5+ cells can be found in the prostate-associated stroma. Although the

functional relevance of stromal Lgr5 expression will be the focus of future studies, it is tempting to speculate that Wnt ligand production from this specific stromal population may play a role in prostate cell maintenance and oncogenic transformation.

b. Pancreas

The existence of multipotent pancreatic stem cells in the adult pancreas has not been clearly elucidated (Yalniz 2005). While our analysis revealed several populations which exhibit some stem/progenitor qualities, such as expression in pancreatic spheres and upregulation upon pancreatic damage, functional evidence *in vivo* is lacking. Furthermore, while we identified several cell-surface proteins to be upregulated upon oncogenic transformation and associated with stem/progenitor qualities, their expression were inconsistent on human-derived tissues and were not restricted to a cancer stem cell population specifically. In addition, Lgr5 was not found to be expressed in benign or cancerous pancreatic tissue. Moreover, gemcitabine resistance and relapse of human pancreatic xenografts was determined irrespective of CSC content and function. Specific signal transduction pathways, including the Skp2-Ubiquitin and PTEN-PI3K pathway, were found to segregate gemcitabine 'Sensitive' and 'Relapseable' tumor cohorts. This suggested that combining potent PI3K pathway inhibitors with gemcitabine in patients with high Skp2 expression may be a novel therapeutic approach to increase clinical efficacy.

c. Implications and Future Directions

This dissertation sought to explore the relationship between prospective cancer stem cell populations with cancer initiation, progression, and chemoresistance. Intriguingly and unsurprisingly, we had mixed results that were largely dependent on cellular context. While the

prostate seems to be hierarchally organized both in benign and malignant backgrounds, pancreatic cells seem to have a more linear differentiation potential. The latter finding was completely unexpected given the established literature of identified cancer stem cell function in pancreatic cancer. Our results indicate that many more cells within the pancreatic tumor bulk have tumor-initiating ability than currently appreciated, and that tumor lines respond to chemotherapy based upon their specific mutational backgrounds, rather than intrinsic cancer stem cell potential. This finding has important clinical significance and speaks to the importance of testing hypotheses. A similar refinement to the cancer stem cell paradigm was observed in melanoma, where optimizing experimental protocols resulted in a complete shift in the interpretation of tumor initiation potential (Quintana 2008). However, several cancer types have been rigorously shown to harbor rare tumorigenic cells which are chemoresistant and predict poor prognosis, signaling the importance of identifying such cells (Eppert 2011, Chen 2012). Accordingly, we have clearly shown this population to be important in prostate tumor initiation and progression, both in a murine prostate cancer model as well as in human cancer tissues. The next step in this study will be to determine the nature of these prostate tumor-initiating cells, and to understand whether therapeutic elimination of these cells will destroy the tumor proper.

There are many purported surrogates of cancer stem cell populations currently utilized in the field. Disturbingly, many of these markers have not been sufficiently functionally tested and simply adapted for use. One must be very careful when defining CSCs in their experimental system, as well as validating its function prior to assigning any relevance to its use. Furthermore, the utility of the cancer stem cell paradigm has yet to be successfully therapeutically tested in the clinic. As this is an area of intense research, it will be interesting to see the results of upcoming clinical trials specifically targeting CSC populations.

II. References

Chen J, Yu T, McKay R, Burns D, Kernie S, Parada L (2012). A restricted cell population propagates glioblastoma growth after chemotherapy. Nature, *488*: 522-526.

Choi N, Zhang B, Zhang L, Ittmann M, Xin L (2012) Adult Murine Prostate Basal and Luminal Cells Are Self-Sustained Lineages that Can Both Serve as Targets for Prostate Cancer Initiation. Cancer Cell 21: 253-265.

Eppert K, Takenaka K, Lechman ER, Waldron L, Nilsson B, van Galen P, Metzeler KH, Poeppl A, Ling V, Beyene J, Canty AJ, Danska JS, Bohlander SK, Buske C, Minden MD, Golub TR, Jurisica I, Ebert BL, Dick JE (2011). Stem cell gene expression programs influence clinical outcome in human leukemia. Nat Med, *17*: 1086-1093.

Goldstein AS, Huang J, Guo C, Garraway IP, Witte ON (2010) Identification of a cell of origin for human prostate cancer. Science 329: 568-571.

Quintana E, Shackleton M, Sabel MS, Fullen DR, Johnson TM, Morrison SJ (2008). Efficient tumour formation by single human melanoma cells. Nature, *456:* 593-598.

Richmond A, Su Y (2008). Mouse xenograft models vs GEM models for human cancer therapeutics. Dis Model Mech, *1*: 78-82.

Tsujimura A, Koikawa Y, Salm S, Takao T, Coetzee S, et al. (2002) Proximal location of mouse prostate epithelial stem cells: a model of prostatic homeostasis. J Cell Biol, *157*: 1257-1265.

Wang X, Kruithof-de Julio M, Economides KD, Walker D, Yu H, et al. (2009) A luminal epithelial stem cell that is a cell of origin for prostate cancer. Nature 461: 495-500.

Yalniz M, Pour P (2005). Are There Any Stem Cells in the Pancreas? Pancreas, *31*: 108-118.